A CONCENTRATED SOLAR and PHOTOVOLTAIC THERMAL COOLED SYSTEM FOR DOMESTIC USE

by

NAMBUA ELIZABETH NTEKA
Student No.: 212120166

Thesis submitted in fulfilment of the requirements for the degree

Master of Engineering: Mechanical Engineering

in the Faculty of Engineering and Built Environment

at the Cape Peninsula University of Technology

Supervisor: Dr Kant Kanyarusoke

Bellville
July 2019

DECLARATION

I, Nambua Elizabeth Nteka, declare that the contents of this thesis represent my own unaided work, and that the thesis has not previously been submitted for academic examination towards any qualification. Furthermore, it represents my own opinions and not necessarily those of the Cape Peninsula University of Technology.

Signed

7/7/19

Date

ABSTRACT

Electric power shortage remains one of the biggest problems in Africa. Over 600 million people on the continent lack access to electricity. Researchers and engineers around the continent are looking at solar energy as a quick and environmental friendly solution to this crisis. Solar PV panels are considered to be the best way to generate electrical power from the sun's radiation. However, the conversion efficiency is known to be between 10-15%. This is not considered to be cost effective by many people. Over 80% of incident energy is dissipated as heat. Research shows that, PV panels lose efficiency due to overheating of the cells.

As a solution to the above, this research work presents a design that overcomes a big part of the downsides of using photovoltaic panels. A concentrated solar photovoltaic thermal cooled system (CSPVT) was developed. The system aimed to improve the efficiency of PV modules while also producing useful thermal energy simultaneously. The CSPVT consists of the following: a concentrating reflector, a PV panel, a water cooling system and a sun tracking mechanism. The cooling system is introduced to prevent overheating of the PV panel and to produce hot water for domestic use; the reflector is meant to increase the intensity of sunlight onto the panel so that more energy can be generated and/or collected from the system using the same PV surface; the tracking mechanism ensures that the panel and reflector surfaces are pointed to the sun at all times throughout the day.

The methodology used was a design, construct and test, supplemented by both MATLAB® programming and TRNSYS simulation for validation. The performance of the CSPVT was analysed under Cape Town meteorological conditions and compared to an identical non-modified PV panel. Experimental results showed an increase of at least 60.1% on electrical yield, coming from both concentration and tracking compared to the normal fixed PV panel. TRNSYS predicted an electricity yield increase of 40% and a combined electricity and thermal efficiency of 82% from the CSPVT. The actual overall efficiency of the normal PV panel was 11% compared to a combined 62.4% (14.5% electrical and 48% thermal) from the CSPVT.

The study showed that the CSPVT has a great potential in improving both the efficiency and the total energy yield of PV panels. A quick economic analysis also showed the system to be cost effective because of concurrent generation of electricity and useful thermal energy in a space that is less than half of what would have been necessary if two systems were used. As an improvement, the study recommends use of pumping in place of natural convection to control the cell temperatures better and improve the electric efficiency further.

Keywords: Concentrated photovoltaic, PV panel efficiency, solar tracking, TRNSYS

ACKNOWLEDGEMENTS

I wish to thank and express my sincere gratitude to:

- Dr Kant Kanyarusoke for the supervision and mentorship provided throughout this research work.

- The National Research Fund for supporting my research through its funding program.

The financial assistance of the National Research Foundation towards this research is acknowledged. Opinions expressed in this thesis and the conclusions arrived at, are those of the author, and are not necessarily to be attributed to the National Research Foundation.

DEDICATION

I would like to dedicate this work to my parents and siblings.

CONTENTS

LIST OF FIGURES

LIST OF TABLES

GLOSSARY

A	Surface area	m^2
A_a	Aperture area	m^2
A_r	Area of the receiver	m^2
C	Concentration ratio	-
C_d	Centre distance	mm
CPV	Concentrated photovoltaic- a term used to classify PV modules that used reflectors	-
d	Diameter	mm
E_{elec}	Electrical energy	Joules (J)
F	Fahrenheit, scale of temperature	-
F	Desired reaction force	N
FV	View factor	-
G_{gl}	Irradiance onto the panel	W/m^2
G_{in}	Irradiance into the panel	W/m^2
h_w	Enthalpy of water (or convection coefficient in equation 4.8)	kJ/kg or W/m^2K
I	Current	A
I_{sc}	Short circuit current	A
k	Thermal conductivity	W/m.K
K	K factor	-
L	Length	mm
m_{water}	Mass of water	kg/s
N	Speed	rpm
Nu	Nusselt Number	
P	Power	W
$Q_{collected}$	Energy collected	J
Ra	Rayleigh Number	
T	Torque	Nm
T_n	Number of teeth on larger sprocket	-
t_n	Number of teeth on smaller sprocket	-
U_L	Total heat loss	J
V	Voltage	V
V_{oc}	Open circuit voltage	V
β	Panel slope	Degrees
d	Thickness	m
e	Emissivity	

θ	Angle of incidence	Degrees
Θ_z	Solar zenith angle	Degrees
γ_s	Solar azimuth angle	Degrees
α_s	Solar altitude angle	Degrees
ρ	Density	kg/m^3
S	Stefan and Boltzmann constant	W/m^2K^4
ω	Solar hour	-
η_{elec}	Electrical efficiency	%
$\eta_{thermal}$	Thermal efficiency	%

CHAPTER ONE:
INTRODUCTION

1.1. **Background**

Since discovery of photo electricity in 1876, solar cells have been used to produce electrical power. However, the cost of production was extremely high at $300/watt (Victoria, 2017). As time went on, the cost of solar cells dropped tremendously to around $2.71- $3.57 per watt (Matasci, 2018) and eventually to a present quotation of $0.5 - $0.7 (R7-R10) per watt (Sustainable, 2019). These amounts are predicted to drop even further. Such prices have changed people's opinions on solar energy. PV panels are now seen as a good and cost effective way to provide green-energy at cheaper rates for regions without access to the power grid; regions where people rely on expensive, unreliable and/or even dangerous sources of energy.

According to the international energy agency, about 1 billion of the world's population lack access to electricity (Cozzi et al., 2018). More than a half of them are in sub-Sahara Africa (SSA) (Labordena, 2018). The African continent is known for its poor electricity grids. In Nigeria for example, many factories and households use diesel and/or petrol generators as power generation units (Akindele & Adejumobi, 2017). Also, the majority of people rely on candles, kerosene and paraffin lamps to light their homes (Solar Aid, n.d.). South Africa on the other hand, depends on coal as its main source of power production (Khumalo, 2019). Mpumalanga province for instance, is considered the world's largest NO_2 air pollution hotspot - according to Greenpeace environmental talk group (Meth, 2018). These statistics and many others, should move Africans to research and invest on solar power as a main source of energy production instead of relying on fossil fuels which pollute the environment.

Reducing the cost and increasing the overall efficiency of solar panels is one way to solve Africa's energy demand and reduce world's dependency on hydrocarbon fuels. SSA is known to have great weather conditions making it suitable for solar energy harnessing.

1.2. **Research Problem**

In the quest for green energy, solar energy has gained much attention. Solar energy engineering is a science of converting sunlight into electricity or other forms of useful energy. Different technologies are used to accomplish this aim. One of which is the use of solar PV panels. However, the generated electrical efficiency is low. A large amount of solar radiation absorbed into the panel is dissipated as heat transfer to the surroundings while some is reflected back. Blakers et al. (2013) shows that the upper limit of silicon solar cell efficiency is 25%, but most panels have an efficiency range of 10-15%.

Increasing the output power of PV panels has been comprehensively researched in the past few years. Bailie et al. believe that the cost of solar panels can be partially reduced by improving its efficiency (Mailoa et al. 2015). Farret and Simões show that high efficiency is obtainable depending on the quality of the PV cells (Farret & Simões 2006). Although this may be true, high quality panels tend to cost more. Hence, the need for further research on how to make the most out of available solar panels without compromising cost and/or space.

In all cases the electrical efficiency of PV panels is mainly affected by the following factors: temperature, panel's orientation towards the sun and the intensity of sunlight. Research shows that energy output of a panel decreases rapidly once the temperature of the cells reaches a value above the design temperature of typically 25°C (Ponce-Alcantara et al., 2014). Orientation to the sun is very important because it enables the panel to receive a big percentage of direct – or beam - radiation from the sun. Manuel, (2010) stated that "flat plate panels are less efficient because they are motionless and have no concentration of sunlight on them".

With that in mind, it can be noted that the power output of the panel generally increases with the amount of radiation it receives. Under normal and acceptable working conditions, the amount of current produced from a panel is directly proportional to the intensity of sun's radiation available. However, available sunlight itself cannot increase the efficiency of the panel. One crucial factor that needs much attention is the amount of sunlight being absorbed by the panel. Therefore, one possible action to resolve this issue is to use reflectors to concentrate incident radiation onto the panel. But this will raise the temperature of the cells which in turn, will cause efficiency drops, although actual power may be going up. In this research, these problems are addressed by using a sun-tracking concentrated solar photovoltaic thermal (CSPVT) system.

1.3. **Solution Specification**

A CSPVT system consists of four key elements – namely: i) the PV panel itself, which receives and converts solar energy to electric energy; ii) the concentrator, which may be a plane or a curved reflector. This receives additional solar energy and reflects it onto the PV panel; iii) the sun tracking system and its mounting, which keeps both reflector and panel facing the sun to maximise energy incidence; iv) the thermal cooling and heat recovery system which cools the panel, heats water or other fluid, and stores the recovered energy for use at a convenient time. The arrangement is sketched in Figure 1-1 which also shows the energy transfers. The total radiation reaching the panel, G_{panel}, is the sum of the radiation reflected from the parabolic reflector and that received directly from the sun to the panel. G_{in} is the total radiation entering the surface of the panel or glazing.

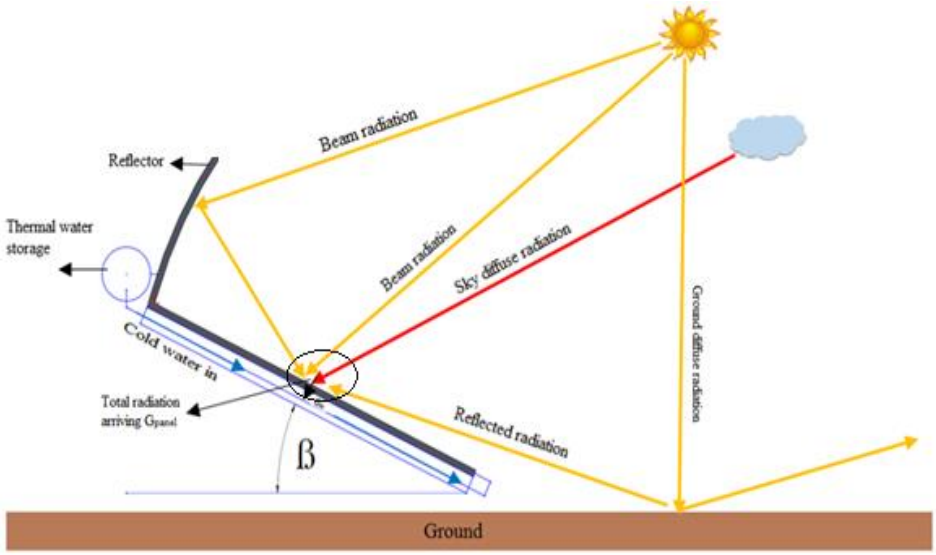

Figure 1-1: CSPVT Schematic (Nteka & Kanyarusoke, 2019a)

The reflector, as mentioned earlier, increases the temperature of the cell and can cause shading if its tilt relative to the noon sun is not designed properly. This would reduce electrical power generation and lower efficiency of the panel. To prevent the cells from overheating, liquid water is used as coolant which recovers thermal energy from the panel. To prevent shading and increase the yield of the panel, the system tracks the sun about a vertical axis. In that case, even low elevation morning and evening beam radiation is always captured by the system, albeit at lower incidence angles.

1.4. **Research objectives**

The overall objective of this research work was to design a home-sized system that can generate both electrical power and hot-water for domestic use. While that was the major objective, the following were the specific aims of the research:

1: Increase the electric energy yield from a domestic sized solar panel, well beyond what is achievable by a normal PVT system, thereby increasing photo cell productivity.

2: Increase the total energy yield from the PV panel by at least 100% without thermally damaging the cells, so that the overall energy efficiency of the system is safely maintained above 40%. A minor objective was to estimate the realistic costs of actions to achieve the above major objectives – and to determine whether those costs can be technically and economically justified.

1.5. **Research questions**

To provide desirable solution to the research problem on hand, the following questions were scrutinized:

👍 How much electric energy gain can relatively be made by tracking alone?

- How much electric energy can relatively be gained by reflection and consequential tracking and cooling?
- How much total energy (i.e. electric and thermal) can be gained relative to:
  (i) a normal fixed and tracking PV panel?
  (ii) a normal non tracking PVT without a concentrator?
  (iii) a tracking PVT without a concentrator?
- For each of the above cases, do energy yield gains mean electric and total efficiency gains?
- What are the implications on unit costs of energy, and what else could be done to improve overall performance?

1.6. **Research design and methodology**

Four approaches were used in addressing the above problems: Literature review, Design and Construction; Experimentation; and Analytical with computer simulations. The subsequent subsections summarise the steps.

1.6.1. **Literature review**

A literature survey was done to establish the current methods available to improve PV panel productivity. From the survey, limits of improvements were identified. The issue then, was to determine whether to use combinations of existing approaches in one set-up or to devise new ones to meet the research objectives.

1.6.2. **Design and Construction**

Different concepts were investigated, and based on simplicity and relative novelty, a decision was made to design and construct a sun tracking parabolic reflector – enhanced photovoltaic thermal system (CSPVT): hence, the title of this project. Geometric design through ray-tracing approaches and sun-earth relative motions through the year, were used to design a vertical axis sun tracking system that avoided reflector shading while maximising ray concentration onto the panel. A water heating subsystem which also acted as a panel cooling system was designed as part and parcel of the tracking assembly. This element - of a sun tracking tank, is one of the most important innovations of the project. Suffice to mention at this stage that the tracking design work involved time programming of a microcontroller.

1.6.3. **Testing and Experimentation**

The third approach was experimental. After system construction, the system was tested against suitable controls as required in answering the major questions highlighted in 1.4 above. The experiments were done on top of the roof of the Mechanical Engineering

department of CPUT, where a first class weather station and two identical 90 Wp PV mono-crystalline panels are installed from a previous research by Kanyarusoke, (2017).

In testing, solar radiation arriving on site was measured using the mentioned weather station and electric energy harvest was monitored by logging 15 minute PV generated voltages and currents in the weather station data logger. Thermal energy was monitored half hourly by direct readings of thermometers inserted at the bottom and top of the solar syphon tank. In addition, temperatures of the PV panel glazing and back plate were monitored to be able to give an indication of the cell temperatures through the King model as used in Kanyarusoke et al., (2012) and Kanyarusoke et al., (2016). This data was used to compute total energy yield, system energy efficiency and comparison was made with results from a standalone, non-tracking, and non-concentrating identical PV unit.

1.6.4. **TRNSYS Simulation and Economic evaluation**

To properly answer questions relating to comparison with an ordinary PVT system given in 1.4 above, first results from a previous project on PVTs are looked at. However, as the system size in that project was less than a quarter (Assembe, 2016) of the present one, it was necessary to use TRNSYS simulation to compare performances of similarly sized systems. Then, results are used in an engineering economics model to determine unit energy costs and whether the additional costs are justifiable. This covers the minor objective on 1.5.

1.7. **Delineation of the research**

- The solar system developed in this research is suitable for domestic use only and not for the industrial sector;
- The system is suitable for the middle income but not for the lowest income population;
- The heated water is not suitable for drinking;
- Detailed design was limited to 90Wp mono crystalline silicon panel under Cape Town weather conditions.

1.8. **Outcomes, results and contributions of the research**

The following are the outcomes of this work:

- A New system to co-generate electric power and provide hot water
- A Solar panel system with higher photocell productivity
- From an academic and intellectual property point of view, this work advances the technology of PVTs by introducing both tracking and concentration. One peer reviewed paper has been written, presented and published (Nteka and Kanyarusoke, 2019a) by

the time of submitting this dissertation. A second paper (Nteka and Kanyarusoke, 2019b) has been accepted for presentation and publication in an international journal.

1.9. Significance of the research

The outcomes of this research work can be of utmost advantage to middle income people in rural areas without access to electricity. In most of Africa, such people include government civil servants in rural government institutions, medium to large scale farmers, and even urban dwellers with rural homes as well. Use of the designed system or its larger versions can lead to improved health and hygiene, reduced rural night-lighting costs, reduced environmental pollution and degradation. Additionally, improved safety through reduced fire hazards is expected, just as an overall improvement of socio-economic productivity. In summary, this work makes some contribution in the area of energy and sustainability.

1.10. Outline of remainder of the dissertation

The remainder of the thesis follows the methodology approaches as follows: Chapters 2 and 3 give the literature review, and design and construction respectively. Experimentation procedures are described in chapter 4, with results and TRNSYS simulation being given and discussed in chapter 5. Chapter 6 closes the thesis with a brief on economics, conclusions and recommendations.

CHAPTER TWO
LITERATURE REVIEW

2.1. **Introduction**

This chapter reviews available literature on key issues in the study. The development and performance of the PV/T, the CPV and CPVT are reviewed.

2.2. **Solar Photovoltaic Panels**

A PV panel is an assembly of small semi-conductors called, solar cells. These cells are electronic devices designed to convert sunlight into electrical power. To date, solar PVs are the most used method to harness solar energy. There are different types of solar cells. Namely: crystalline-silicon, thin film, bio-hybrid solar cell… etc (Askari et al., 2015). The most common type is the crystalline-silicon cell. Silicon cells have highest efficiency rate when compared to other types of cells" (Blakers et al., 2013:1). Silicon cells have photo-electric properties; when exposed to solar radiation, they release electrons which produce electricity when allowed to move in an electric circuit. Thus, exposure of silicon cells to photons from the sun leads to a photo-electric effect (Salameh, 2014:33).

Solar cells are wired in: series, parallel or series-parallel combination to form a solar module. In most cases, these modules are then connected to form a PV panel or an array as illustrated in figure 2-1. This arrangement is required when more output power from the panels is needed.

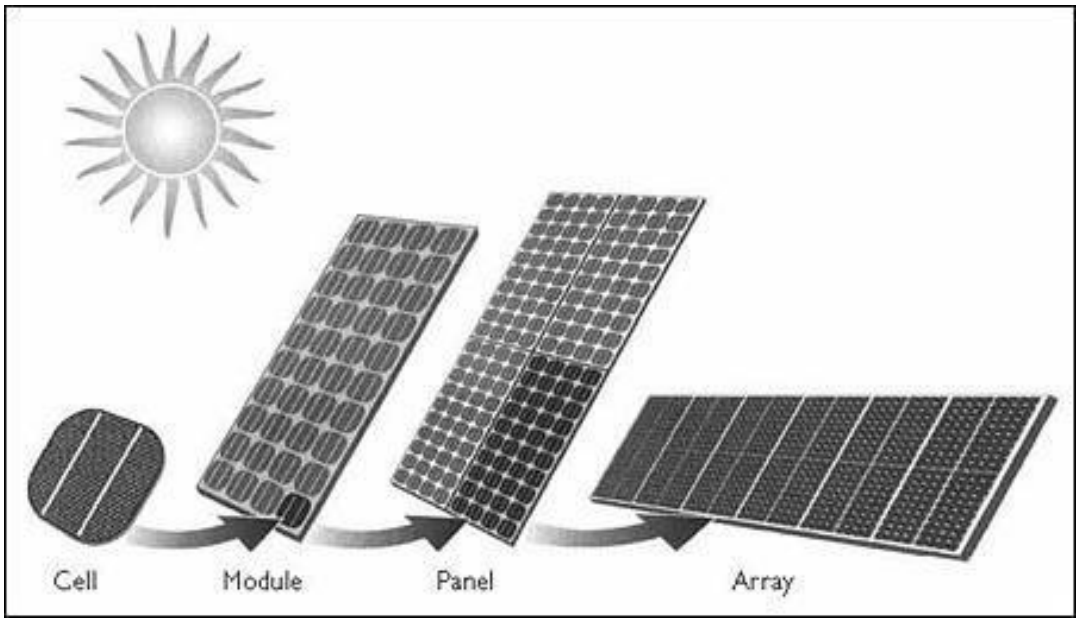

Figure 2-1: Building blocks of a solar panel. (Alkhalidi & Hussain Al Dulaimi, 2018)

2.3. **Effect of temperature on PV panels**

As mentioned above, solar cells are made of different materials. Every material has its own behaviour depending on the conditions surrounding it. This research focuses only on silicon cells, especially on the Mono-crystalline silicon solar panel. Mono-crystalline panels operate best when the temperature of the cells is kept within its optimum design range. As illustrated in figure 2-2, excessive heat reduces the efficiency of the panel and consequently damages the cells (Javed, 2014). Solar cell output is measured under STC (standard test conditions) which means that the temperature during testing represents the temperature during peak hours in certain locations. The temperature coefficients, which are the rates of change of current produced and voltage generated with temperature, are specified in the manufacturer's data sheet for each panel. So are the peak power (P_{max}) values at STC.

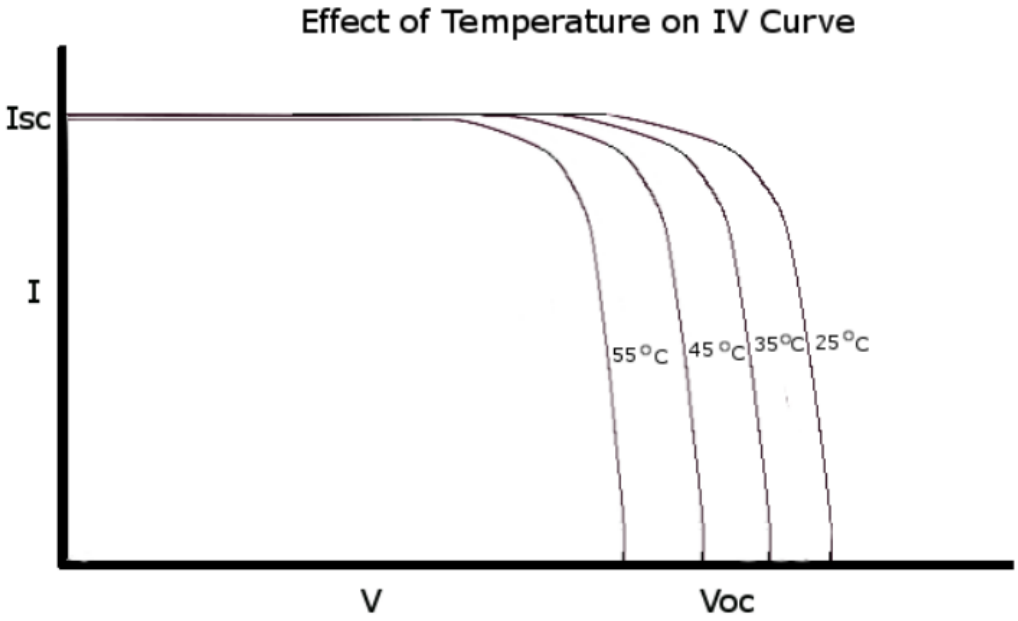

Figure 2-2: Effect of temperature on PV cell (Allan, 2015)

Charfi et al., (2018) and Rawat & Dhiran, (2017) research works show that when the temperature of the solar cells is stabilized at low levels the efficiency of the PV panel is improved significantly. During an experimental work, Dash & Gupta, (2015) noticed that Mono-crystalline silicon cells have an average temperature coefficient of -0.446%/^{o}C. Mar *et al*., (2015) show two studies conducted on a home PV panel in the United Kingdom and Nigeria. The studies revealed a drop of 1.1% of power output for every increase in ^{o}C once the panel reached the temperature of 42 - 44 ^{o}C.

2.4. **Historical and recent developments of Photo Voltaic Thermal (PV/T) systems**

PV/T systems were developed to solve the challenges of efficiency loss caused by the increase in temperature of solar cells. They were mainly developed to improve the overall efficiency of solar panels first by cooling the cells and secondly by making use of some of the

thermal energy generated. PV/T systems are a combination of two technologies as shown in figure 2-3: a) the solar PV (used for power generation) and b) the solar thermal collectors (used to heat a fluid, usually water or air). Solar thermal collectors convert solar radiation to thermal energy, which is often used to increase the temperature of a fluid. Thus, PV/Ts are used to produce both electrical and thermal energy simultaneously (Chow, 2007).

Figure 2-3: a) Photovoltaic panel at CPUT campus; b) Solar thermal collector at CPUT campus; c) Hybrid PV/T (TESZEUS, n.d.) .

2.4.1. **Types of Hybrid PV/T**

PV/T systems are categorized in two main areas: air, and liquid PV/T collectors. In PV/T air collectors, air is used to extract the thermal energy from the panel whilst in liquid collector, water is used (Kumar et al., 2015). The hot air extracted from the panel is used for various applications such as: to warm buildings and for space heating (Das et al., 2018). The present research considers only PV/T liquid collectors. An illustration of how a hybrid PV/T system is combined is shown in figure 2-4. The thermal system is simply adhered to the back of the PV panel. A water jacket figure 2-4 (a) or pipes figure 2-4 (b) are used to circulate the fluid. Cooling water enters the panel at point ‘d’, and leaves at point ‘a’ at higher temperature.

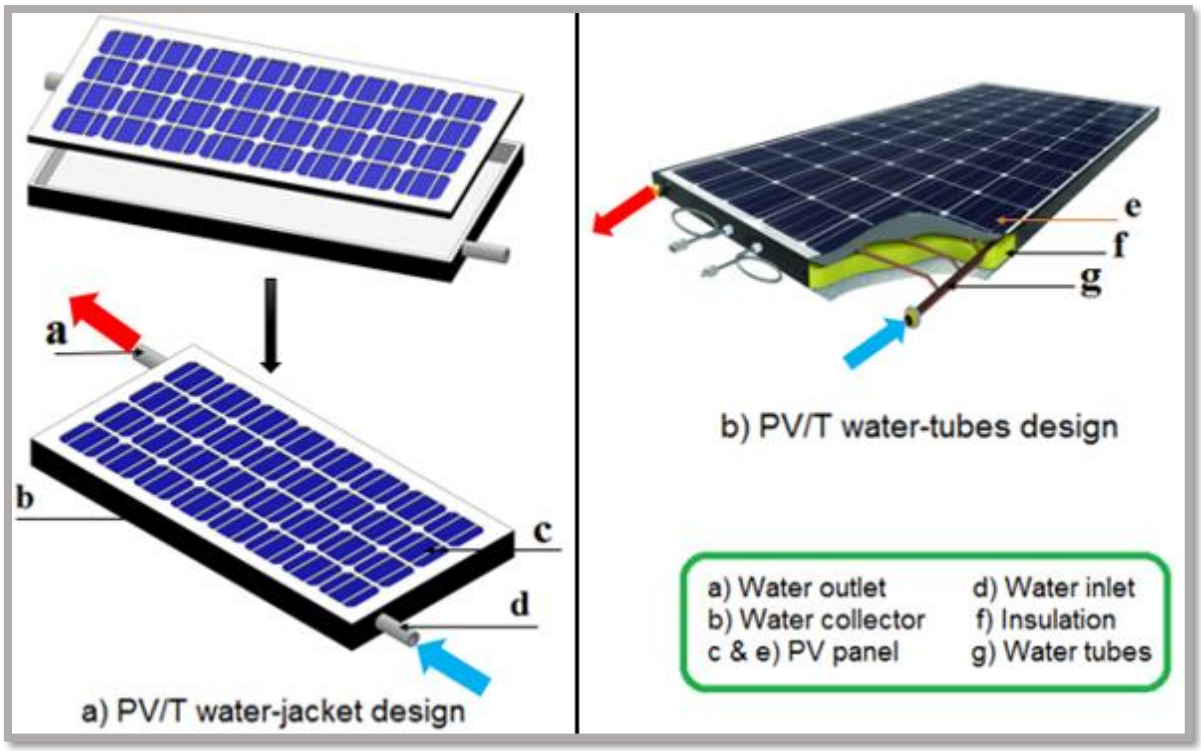

Figure 2-4: Different designs of hybrid PV/T (water collectors). a) PV/T water-jacket design; b) PV/T water-tubes/pipes design; Image source: (Barrett, 2017)

2.4.2. **Performance of a PV/T system**

Since the development of PV/T systems, numerous researches have been carried out to evaluate their performance. The results from different studies show a considerable improvement in the overall efficiency of PV panels. During numerical and experimental work, Bhattarai et al., (2012) found that PV/T systems work better than a conventional PV modules. Kumar et al. show that simultaneous cooling of the PV panel maintains its temperature at an acceptable level and consequently increases the efficiency (Kumar et al., 2015). Another study conducted on the possibility of developing hybrid PV/T solar system, showed that PV/T systems are a cost effective solution of increasing the efficiency of solar panels. During installation of solar panels, less area is required when using PV/Ts because of their higher output efficiencies (Dobrnjac et al., 2017).

A comparison study done in Cape Town by Assembe, (2016) reports 18.89% increase in electrical efficiency of a PV/T and a thermal efficiency of 61.65% from the cooling water. Although his results show an improved overall efficiency, more improvements are still possible. The research was conducted on a small scale 20W PV panel and no tracking was incorporated.

During an experimental investigation conducted in Konya, Turkey on PV/T systems, Ozgoren et al., (2013) reported 13.6% and 49% electrical and thermal efficiency of the PV panel with cooling system. The same system, on the other hand, showed a maximum electrical efficiency of 8% when the PV was operated without cooling. The research showed a

considerable improvement on PV efficiency. In addition, Dupeyrat et al., (2011) shows an overall efficiency above 87% (8.7% electrical efficiency and 79% thermal efficiency) on a PV/T system tested in Freiburg, Germany. These results prove a potential in PV/T systems. However, a PV/T only targets the heating of the cells, and does not look at other factors which potentially also affect the efficiency of PV panels.

Although the literature review shows a significant improvement on the overall efficiency of PV panels, a recent study on flat plate hybrid PV/T system indicates that PV/T can provide higher overall efficiencies and that they are more effective in areas with great solar radiation and high ambient temperature (Das et al., 2018). An economic analysis research based on simulations conducted in UAE, however, revealed that PV/T systems are not always cost-effective when compared to other solar energy technologies available depending on ambient temperatures of different countries and the economic factors in those countries (Kaya, 2013).

2.5. **Solar concentrators**

Solar concentrators are devices used to focus light on a smaller surface. In this research, we discuss solar concentrated photovoltaic (CPV). Contrary to traditional PV, CPVs use mirrors/reflectors to focus more light onto a small area where energy is needed (Mokri & Emziane, 2011). A contrast between PVs and CPVs is shown in figure 2-5. There are different types of concentrators namely: Fresnel lenses, reflectors, luminescent concentrators, parabolic and dish mirrors (Dricus, 2015). Figure 2-6 illustrates different types of solar concentrators.

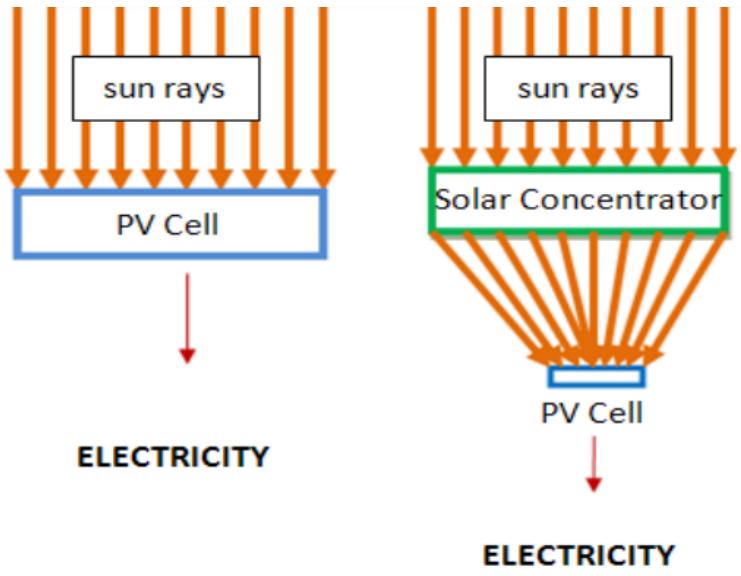

Figure 2-5: Electricity generation with and without solar concentrator. (Muhammad-sukki et al., 2001)

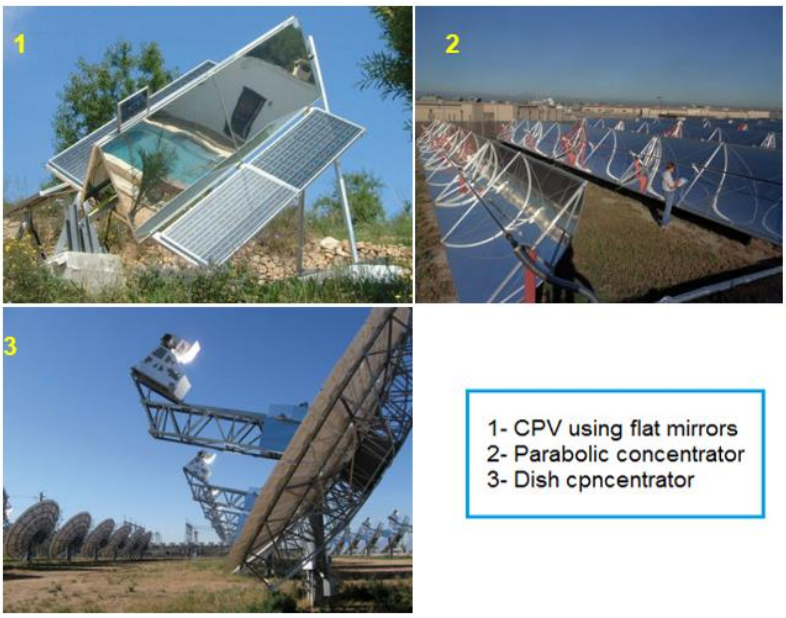

Figure 2-6: Different types of concentrators (Sheikh, 2018)

CPVs and concentrated collectors are both used in the energy industry to produce either electrical power or heat. Concentrating collector technology was developed some years ago for applications where a higher temperature is required as it increases the amount of sunlight a surface receives.

2.6. **History of concentrators**

Concentrators have been in existence for ages. “In 214-212 BC, Archimedes from ancient Greece, used a bronze shield illustrated in figure 2-7 to focus sunlight on a ship which is believed to have caught fire” (Lovegrove, 2012:4-5; Stein, 2012:4-5). Another source from Aalborg CSP (2015) shows that in 1973, Greek scientist Dr Loannis Sakkas used the same theory as Archimedes. He lined up 60 Greek sailors coated with mirrors to focus sunlight on a ship that was 200 ft. (60.96 m) away. Consequently, the ship caught fire within a few minutes.

Figure 2-7: Archimedes holding the bronze shield in 214-212 BC
(Darling, 2016)

Concentrators can help achieve concentration ratios from as low as a unit to values of the order of 10^5 (Duffie & Beckman, 2013:322). When used on PV systems, they are meant to reduce the number of PV cells used while increasing the power output. On thermal systems, concentrators are used to heat up a fluid (water, oil, etc.) to very high temperatures, which then produces steam that can be used to drive turbines to generate electrical power.

Concentration ratios greater than 1000 can be achieved for systems using high quality reflectors (Green Rhino Energy, 2016). A parabolic shaped reflector can concentrate sunlight 20 times or more. However, only about 0.1% of CPV systems are installed across the globe. The systems are still very unpopular and expensive. Flat plate collectors are still the most convenient ones to be used off-grid.

2.7. **Performance of CPV panels**

CPV panels are often reported to have a greater overall efficiency compared to analogous non-concentrating PV ones. In 2016, a group of postgraduate students from Peshawar, Pakistan, conducted a study on the efficiency of concentrated air-cooled PV panels. The team used rectangular concentrators to reflect light on a PV panel as shown in figure 2-8 (a). It was reported an increase of about 25% of the short circuit current (Bilal et al., 2016). In 2011, professor Joshua M. Pearce of the Michigan Technological University along with his team, did a research on the performance enhancement of solar panels using non-tracking planar concentrators as shown in figure 2-8 (b) (Andrews et al., 2015). The team was able to witness a 45% energy yield and a 30% increase in output efficiency of the panels.

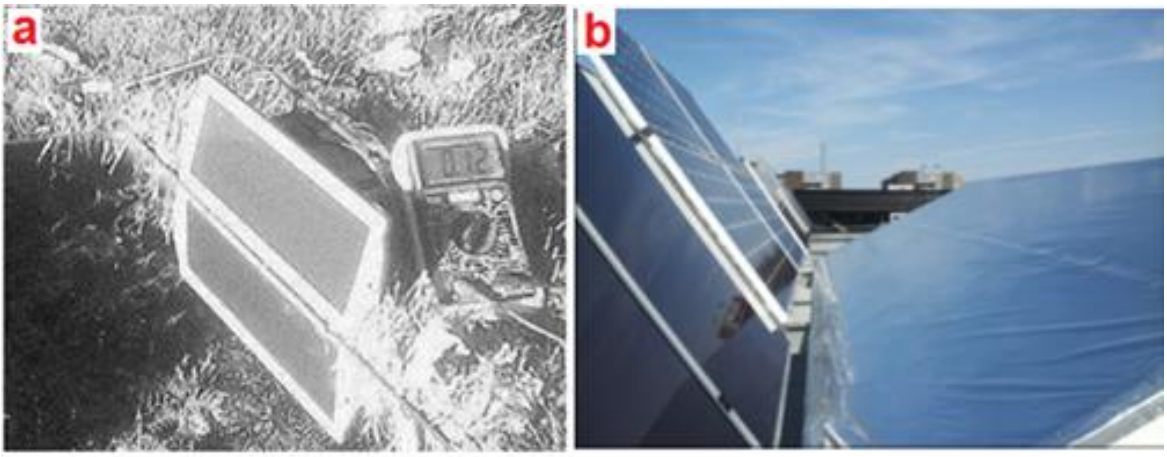

Figure 2-8: a) Bilal et al., (2016) and b) Andrews et al. (2015), experimental setup for solar concentrators

Sonneveld et al., (2011) used Fresnel lenses to increase the energy yield of a PV panel. The research showed 11% increase on electrical efficiency and an additional 56% of thermal yield was obtained. The thermal energy collected was enough to be stored and used on bad weather days. Further study by Baig et al., (2018) reveal that CPVs do increase the output power of a PV panel. During experimental analysis, they obtained an increase in power of 141%. However, they stated that concentrator technology can rapidly increase the temperature of the cells which is a downside effect to solar panels. Hence, it is important to add a cooling system when designing CPVs.

The CPV systems reported above, do not address all problems faced by PV panels. Therefore, more research is required.

2.8. **Concentrated Photovoltaic Thermal systems, CPVT**

A CPVT system combines two technologies: the CPV, and the PV/T. CPVTs generate electrical power as well as hot water from the dissipated heat. As mentioned previously, concentration of light onto PV panels causes cell temperatures to rise beyond design values. Unlike in CPVs, the excess heat from the panel is not wasted in CPVT systems. It is utilized to heat a fluid. Water is used as a heat transfer fluid to cool the panel and to absorb the thermal energy from the panel. There are several designs of concentrating collectors, but in this research, focus was on CPVT with a reflective surface to focus light onto a traditional solar PV panel.

Different research showed that solar panels perform better when getting enough sunlight. Hence, the use of concentrators was introduced. Since its development, concentrators have been combined with PV/T systems to boost PV cells output efficiency. That combination is done by using reflective surfaces to focus light onto the PV/T. Concentrators increase the amount and intensity of solar radiation received by the panel. One study showed that the use of reflectors can also reduce the heat loss and the cost of power generation (Oorjan Cleantech, 2018).

Further research on CPVT systems, showed that, concentrating PV systems (CPVT) offer greater overall efficiency when compared to traditional PV and PV/T systems. CPVT systems can generate a thermal and electrical efficiency of about 70% and 25% respectively depending on the design specifications and materials used for construction of the systems (Daneshazarian et al., 2018). The same research reported that there is still room for improvement and innovation when considering CPVT. Another review on concentrating photovoltaics showed that the overall efficiency of CPVT was dependent on many factors. When designing the CPVT, it is crucial to note each and every step of the design and manufacturing meticulously as the components chosen will have great impact on the output efficiency of the system (Azarian et al., 2017).

2.8.1. **Performance of CPVT**

Papadopoulos et al. found that the incorporation of a cooling system on PV panels can increase the overall efficiency by exploiting the excess heat (Papadopoulos et al., 2017). A MSc. student at Anna University in Chennai, India, developed a prototype called V-trough solar collector. The system provides both electricity and water. To yield higher efficiency it uses two rectangular reflectors attached on the panel in the form of a 'V' as seen in figure 2-9. The reflectors are used to channel solar radiation to the panel. To prevent overheating, a pipe mounted beneath the panel circulates cold water causing a cooling effect on the cells and providing hot water. The water cooling system allows the panel to deliver very high efficiencies. The energy yield of this panel was increased by 45%. Nevertheless, the system does not have a tracking mechanism which prevents it from achieving even higher energy yields throughout the day (Nivas, n.d.).

Figure 2-9: Prototype of a V-through solar collector created at Anna University, Chennai. Source: V-trough solar collector, (Nivas, n.d.)

Ceylan et al. performed an efficiency comparison study between concentrated and non-concentrated PV/T (Ceylan et al., 2016). To improve energy yield, the concentrators used in the experiment had a concentration ratio of approximately two. An increase of 11% of the overall efficiency and a maximum temperature difference of 37 ^{o}C at the back of the panel were reported. Additional research conducted by Azarian et al., (2017) from the faculty of New Sciences and technology, University of Tehran, Iran, concluded that CPVT systems are considered to be the most efficient solar collectors. They use less PV cells, yet deliver great output and water at high temperatures.

2.9. **Solar concentrator tracking mechanism**

In relation to tracking system, the most efficient solar photovoltaic system turns and faces the sun throughout the day using either a single or dual axis tracking mechanism. Solar tracking is a mechanized system used to follow the sun's position. CPVT technology is more efficient when using a tracking mechanism. Tracking ensures that the system is receiving more solar radiation throughout - hence increasing their energy yield and output efficiencies.

Figure 2-10 illustrates the basics of some of the solar tracking systems used. Single axis (a): rotating 180^0 east-west; Dual axis (b & c): rotating 360^0 both east-west and north-south across the sky. Single axis tracking can be either vertical or horizontal facing the sun east in the mornings and west in the afternoon. On the other hand, the dual axis rotates in both directions ensuring that the receiver gets enough sun radiation all day long. Depending on the position of the revolute axes, dual axis is either polar (b) or azimuthal (c). The azimuthal tracker rotates the system around a vertical axis while the polar tracker rotates around a fixed polar axis (Alexandru & Pozna, 2010).

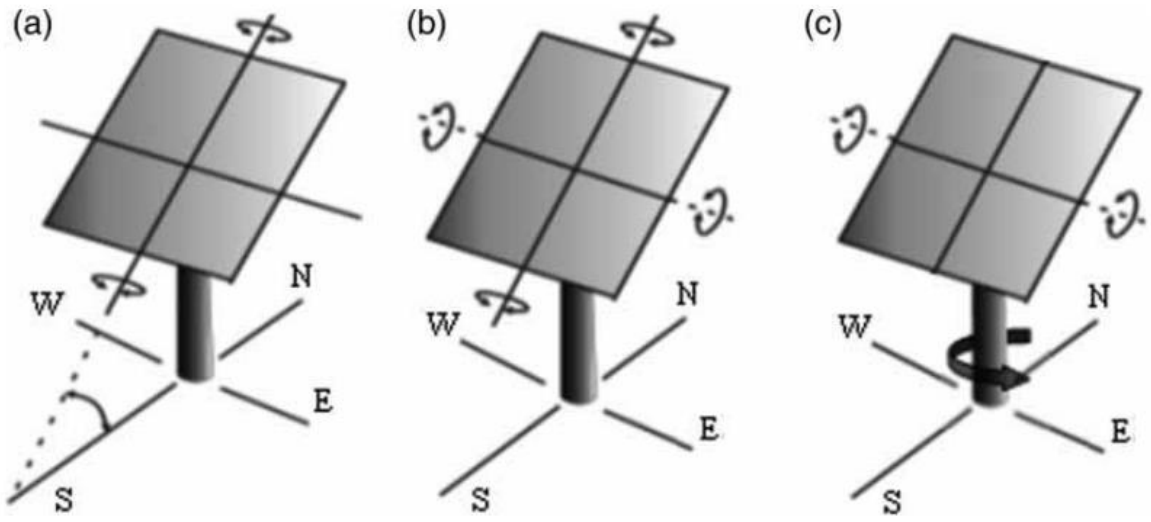

Figure 2-10: Basic types of solar tracking system(Alexandru & Pozna, 2010:799)

Tracking mechanisms help in minimizing the incident angle between the sun radiation and the surface (receiver), which in turn, aids in increasing the energy yield. Zipp suggested that all concentrated solar systems should have a tracking mechanism for better output efficiency (Zipp, 2013). The type of solar tracker to use depends on the system design, size of the system, electrical rates, geographical location, weather, etc.

2.10. **Tilt angle**

Another important factor to consider when trying to increase the energy yield from solar panels is the tilt angle ß, shown in figure 3-8. The angle at which the panel is inclined towards the sun is dependent on the geographical location of the installation. Kamanga et al. proposed that the optimum tilt angle for a fixed panel in Zomba, Malawi should be 25° facing direct north (Kamanga et al., 2014). While Handoyo & Ichsani (2013) suggested an angle between 0 – 40° with seasonal change for Surabaya, Indonesia. Moreover, Kanyarusoke et al., (2016) suggests that the best inclination angle for a PV panel installed in Cape Town would be 30°. Highlighted in figure 2-11 are different recommended slopes for various locations.

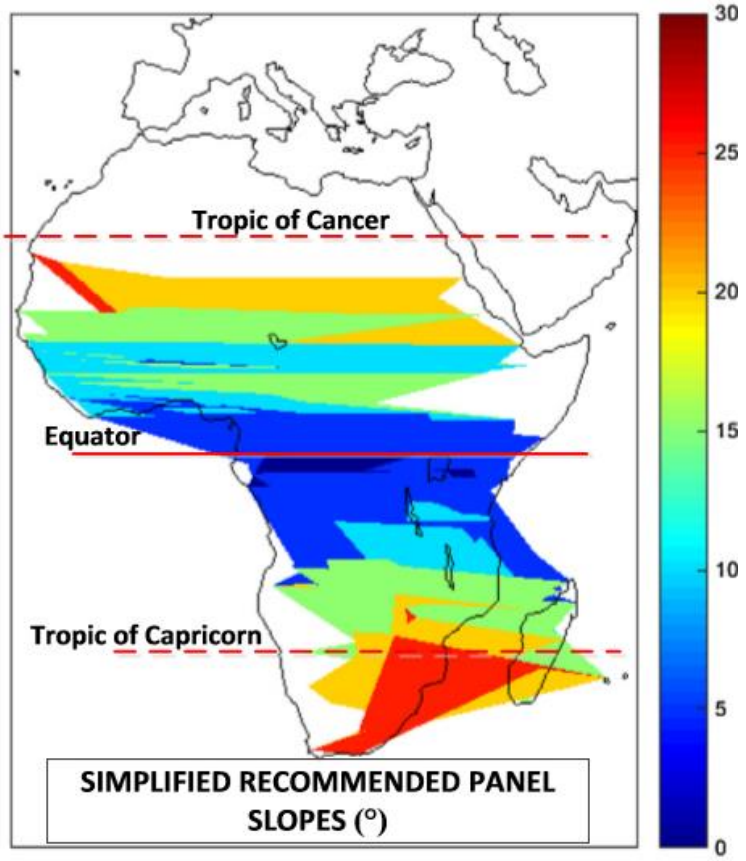

Figure 2-11: Simplified recommended panel slopes (Kanyarusoke et al., 2016:248)

2.11. **Conclusion**

This chapter highlighted some of the research work done on the efficiency of PV panels. We have seen the PV/T, the CPV and CPV/T. Each of the above does not completely address the issues causing the inefficiency of solar panels. There is still a huge gap in each of the researches cited above. The PV/T, although proven efficient, it does not track nor does it have a concentration of sunlight on it. In addition, most PV/Ts use pipes/tubes to circulate the cooling water as seen in figure 2-4b. Although reported efficient, tubes can reduce the cooling effect due to the clearance between them and the back plate of the PV panels. The CPV, on the other hand, only concentrates and does not include cooling or tracking. Most CPVT do not include a tracking mechanism.

In light of the above, it is important to develop a system that can target the main factors causing the inefficiency of PV panels. Therefore, this research work addresses all the above by presenting a PV panel with a concentrator, water cooling system and tracking. The concentrator will increase the intensity and the amount of solar radiation onto the panel, while the tracking mechanisms will ensure that the panel faces the sun at all times throughout the day. Finally, the water cooling system is added to keep the temperature of the cells at an acceptable range. The Assembe research mentioned in 2.3.2 used a small unit PV/T. In the present research, a domestic scale sized PV panel is used. The next chapter gives details on the design and development of the CSPVT system.

CHAPTER THREE
DESIGN OF THE CSPVT

3.1. **Introduction**

This chapter describes the design of the CSPVT. The materials selection, components and methods used to construct and assemble the system are given.

3.2. **CSPVT design components**

The design and construction of the thermal system was done in simple steps. Components were selected taking into account various factors such as: corrosion resistance, strength, cost, manufacturability, availability, weather, weight, etc. Table 3-1 gives all materials and components used.

Table 3-1: Design components of the CSPVT

Component	Specifications/Dimensions	Quantity
CSPVT		
90 Wp Photovoltaic panel	Mono-crystalline silicon panel (1200×544×25)mm	1
Galvanized steel	Food safe steel (0.5mm ×2400mm×1200mm)	1
Glue	Bostik gasket maker (black) 90ml	3
Flexible PVC water pipe	16mm x 2000mm pipe (rated 140F)	1
Reflective surface	500mm×1200mm, Stainless steel	1
Water Tank		
PVC pipe	160mm×1000mm	1
PVC plate	500mm×500mm	1
Aluminium sheet	1000mm×500mm×1mm	1
Insulation	Isotherm 75mm thermal insulation (1.2m×1m)	1
Rig		
Flat bar	Mild steel (MS) 50mm x 3000 mm	1
Square tubing	MS 31.7mm x 31.7mm x 3000mm x 1.6 mm	1
	MS 38mm x 38mm x 3000mm x 1.6 mm	1
Pipe	MS 36mm øx 4000mm	1
Sheet metal	MS 2500 x 2500 x 2 mm	1
Round bar	MS 31ø x1000 mm	1
Gloss spray	Colour black	4

Tracking Mechanism		
DC Motor	24V stepper motor, 1.89Nm	1
Gear box	N/A	1
Motor driver	Stepper motor driver	1
Microcontroller	Arduino Uno	1
Bread board	-	1
DC Batteries	12V	2
Voltage step down board	-	1
Bearings	30mm 4-bolt flange bearing UCF 206-30mm	2
Chain	06B	1
Pinion sprocket	06B 12 teeth	1
Output sprocket	06B 48 teeth	1
Jumper cables	Arduino Uno jumper cables	-
Cables	Electrical cables	2

The 90 Wp solar panel was used because in the first place, a pair of identical ones was already available on site. Consequently, every other aspect of the design was based on the size and specifications of the afore-mentioned PV panel.
The following are additional manufacturer' specifications of the PV panel used: V_{oc}=22.4 V; I_{sc}= 5.50 A; V_{mp}=18.4 V; I_{mp}=4.90 A; manufactured by Set solar, Cape Town.

3.3. **Materials selection**

Several materials were considered while designing the system. Due to factors mentioned above, galvanized steel was used to construct the PV/T. Aluminium was first considered before making the final decision. However, aluminium sheet can leach and alter the quality of the water. In addition to that, Aluminium is more expensive than steel. On the other hand, galvanized steel is the type of steel that has been hot-dipped in zinc which makes it corrosion resistant, long lasting and chemically non-reactive. It is important to get "food safe" or "food grade" steel as the water will be used in homes though not necessarily for drinking purposes (bathroom, toilets, in the kitchen for dish washing, etc.).

The rig structure was entirely made of mild steel. Other materials considered were stainless steel and wood. Wood is light and inexpensive compared to mild steel. But it requires a special coating to protect it from the weather elements, which adds to the cost. Stainless steel has higher corrosion resistance, higher ductility, higher cryogenic toughness and needs less maintenance compared to mild steel. However, it is more expensive to purchase and more expensive to weld.

On the other hand, beside its low corrosion resistance property, mild steel has high ductility due to its low carbon content. It is also low cost, easy to weld, and is more readily available compared to other metals. Hence, it was the preferred choice for the rig structure.

The tank was made out of general purpose Poly Vinyl Chloride (PVC). PVC is the most commonly used type of material when manufacturing plastic tanks. They are chemically stable, acid resistant and strong. Though a thermoplastic, the grade used can withstand temperatures up to 80°C under zero-gauge pressure – which was the case in this work. The other material considered was CPVC. CPVC is a thermoplastic similar to PVC but stronger as it withstands temperatures higher than PVC. During its manufacturing, it undergoes an extra chlorination process which makes it suitable for hot water transportation and/or storage. However, It costs more than the PVC. Since cooling water is not meant to reach temperatures above 80°C, PVC was considered a better option in this case.

The reflective surface was made of stainless steel. Other materials considered are shown in Table 3-2. Aluminium reflectors are light and corrosion resistant. Silver, acrylic and glass mirrors are more expensive compared to steel and aluminium. Nevertheless, glass and acrylic have good corrosion resistance similar to aluminium. In terms of reflective performance, aluminium and stainless steel are similar. Glass mirror has the best reflective properties and would perform better compared to others but is too costly. Hence stainless steel was chosen for the experiments.

Table 3-2: Material properties for reflecting surfaces as in Reddy et al., (2014). The table has been corrected by the author of the present research due to some errors on density in the original source.

Material	Material properties		
	Density (kg/m^3)	T.C (W/m.k)	Temp (ºC)
Stainless steel	7930	16.2	115
Glass mirror	2500	1.05	120
Polished Aluminium	2700	215	110
Silver mirror film	2100	1.15	100
Acrylic mirror	2400	1.10	85

3.4. **Conception of the PV/T**

The concept of the PV/T was decided upon after taking into account available designs. As mentioned in chapter 2, there are two main ways to collect dissipated heat from the PV panel. The water jacket and the water-piping system as described in Figure 2-4. On the piping system or water-tube, the fluid runs through the pipes mounted underneath the PV panel to cool it down as illustrated in the caption in figure 3-1. While for the water jacket, a sheet of metal/aluminium is adhered to the back of the panel (leaving a gap) so that the fluid is directly in contact with the panel's back sheet. The water-piping system offers great

advantage over the water jacket when it comes to leakage. It also protects the electronic part of the panel from the cooling water. However, it's more expensive to manufacture and/or to purchase. On the other hand, the water jacket is quite easy to make and assemble. Hence, it was selected for this experimental work.

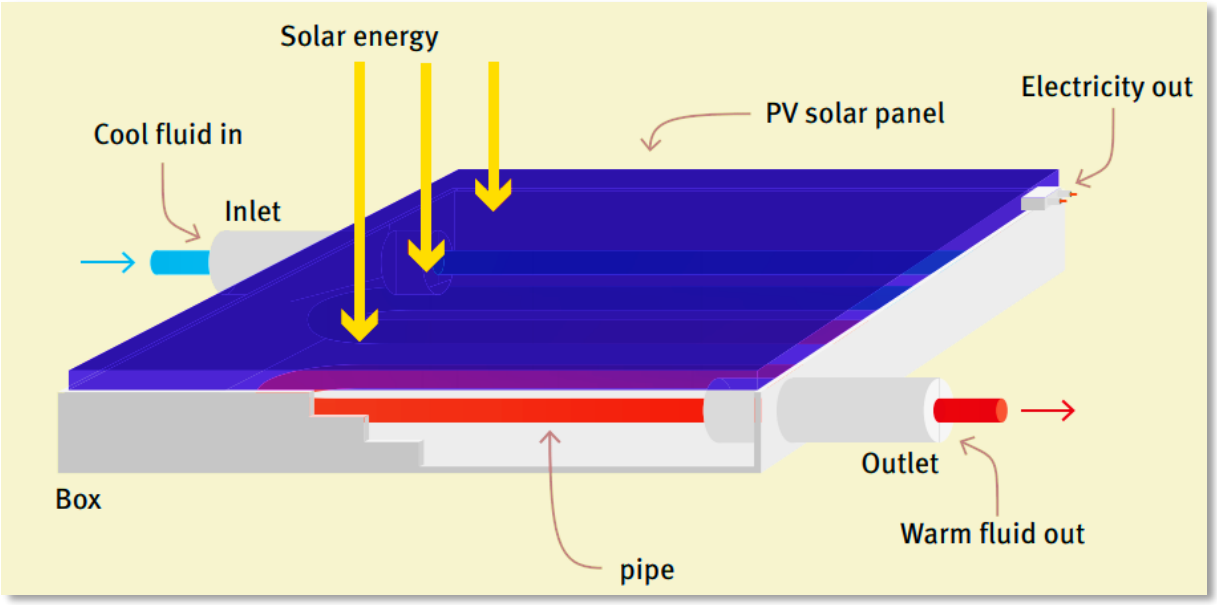

Figure 3-1: PV/T with piping system. (Ramos et al., 2017:13)

The PV/T system was assembled as seen in Figure 3.3 below. A galvanised steel tray, seen in figure 3-2, was joined to the panel leaving a 15 mm gap between the PV panel back sheet and the steel sheet for water circulation. The cut-out piece from the galvanised steel plate highlighted in figure 3-3 is meant to protect the electronic part of the panel from the cooling water. The water inlet and outlet pipes were both 16 mm in diameter. The hot water pipe was 300 mm long while the cold water pipe was 1000 mm. An insulator was added to the PV/T collector to prevent heat loss.

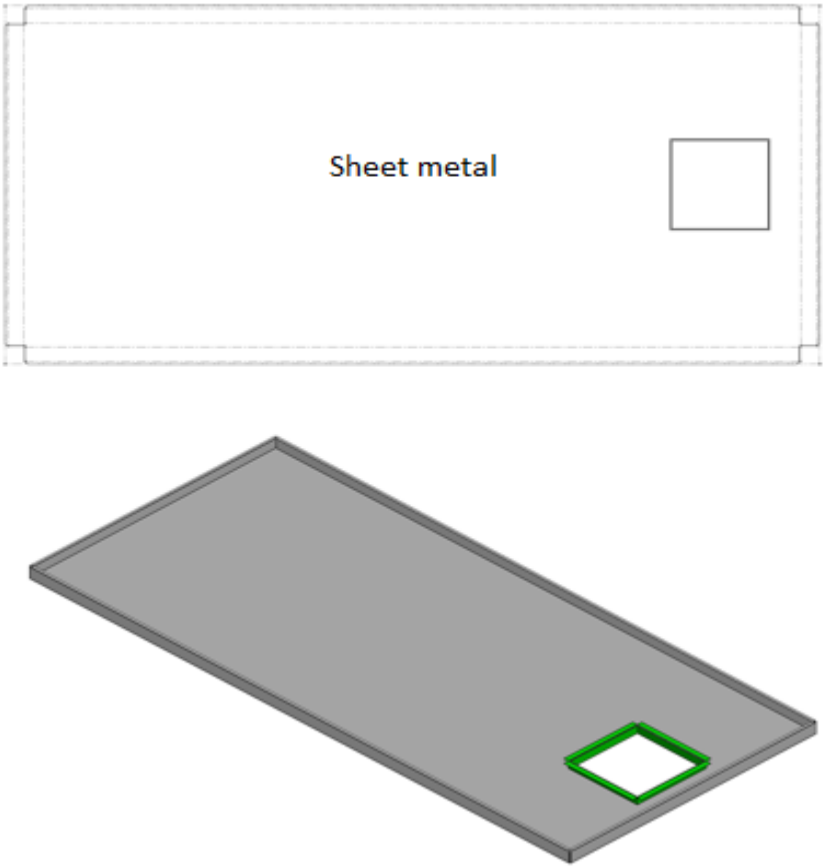

Figure 3-2: 2D and 3D diagram of the PV/T water container

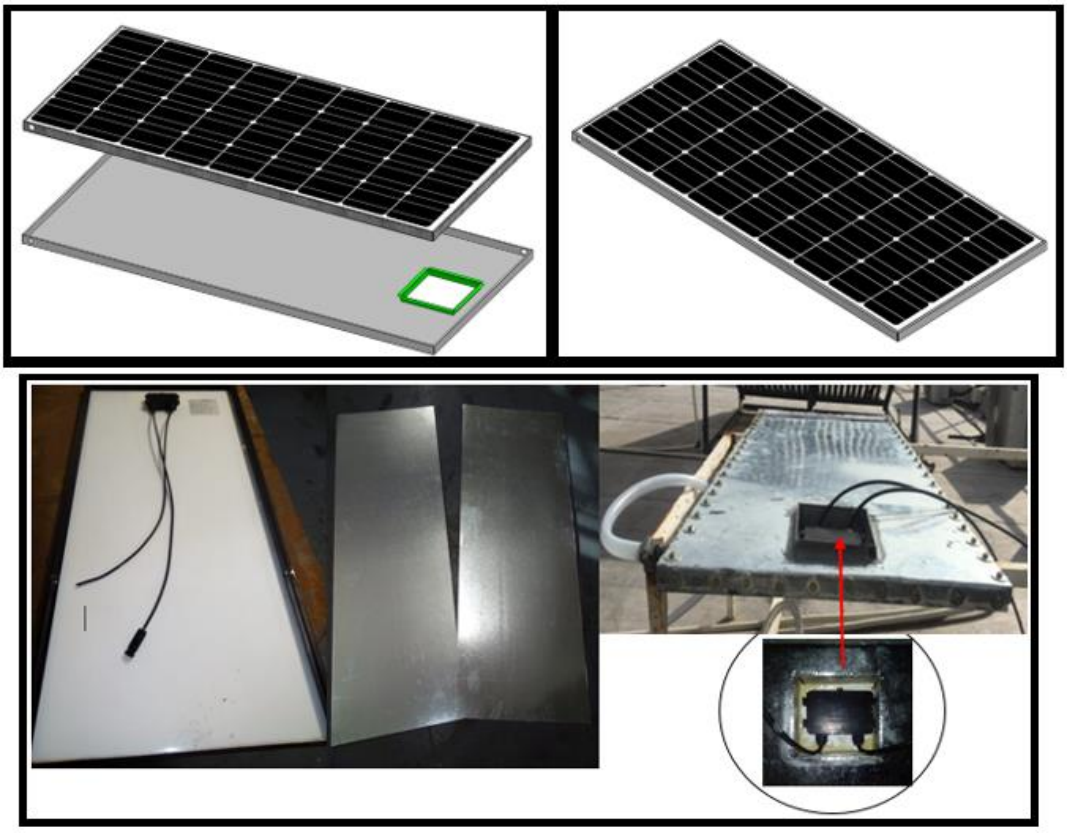

Figure 3-3: PV/T assembly

3.5. **Water reservoir**

The reservoir/tank construction and assembly was done as pictured in figure 3-4. Two plates Ø160 mm were welded on both ends of a meter - long pipe to form a closed cylinder. The capacity of the reservoir was calculated taking into account the estimated amount of dissipated heat and the required water temperature. For this research, the tank was limited of 20 litters of water. To prevent heat loss, the tank is insulated as illustrated below in “before” and “after” pictures. Detailed 3D CAD drawings and assembly are shown in appendix A7.

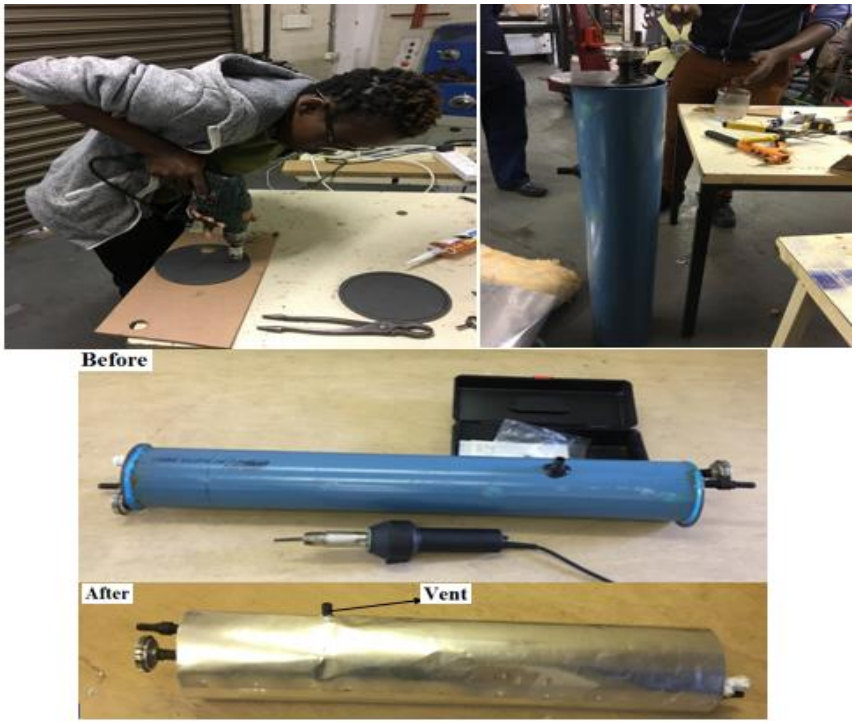

Figure 3-4: Tank assembly

3.6. **Design and construction of the rig structure**

The basic concept of the support structure was first drafted and then modelled in SOLIDWORKS for better understanding of structural integrity and to check for possible problems that might arise from structure construction. 3D modelling also aided in determining the exact measurement of angles at which the structure would be welded. The rectangular tubing was welded together with cross struts to provide extra stability and support as seen from the 3D concept model in Figure 3-5. The outer dimensions allow for an optimal square platform on which the structure is based giving the design a satisfactory safety factor. The rig will be able to withstand all harsh weather conditions including heavy wind. The structure does not require a permanent fixture to secure it to the ground. Its weight keeps the whole system steady.

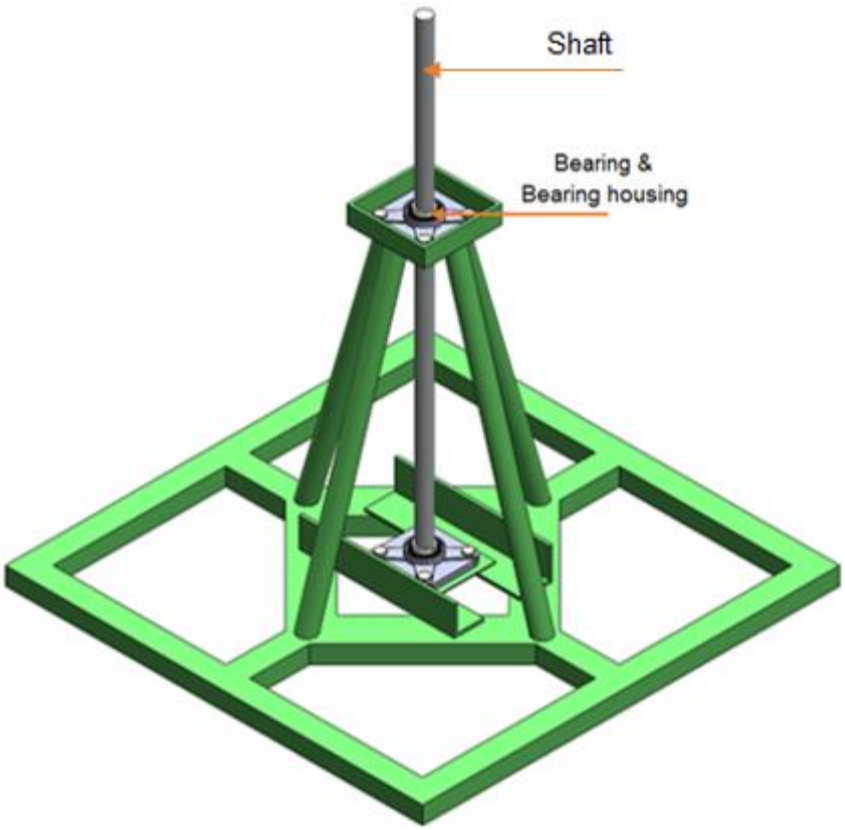

Figure 3-5: 3D Model of the rig base

The dimensions of the shaft were: 32×1000 mm. The two bearings mounted on it were 700 mm apart. The four pillars for extra support of the structure were 36×700 mm each. While the square base was 800 × 800 mm. Full assembly of the rig is shown in figure 3-6. All parts used to construct the rig were recycled from different companies' off-cuts. The parts were simply shaped and welded together to form the desired structure. Details of rig structure are presented in the appendix A6.

Figure 3-6: Full assembly of the rig

The panel's tilt angle (ß) is adjustable (depending on the season and location of the sun) using the tilt angle adjuster (member 4) shown in figure 3-7. As the tilt angle of the panel changes, the parabolic reflector must be adjusted accordingly. The parabola is able to shift in accordance with the movement of the sun and the panel as seasons change. The structure was constructed in a way that enables the reflector to move back or forward using member 3; up and down using member 2. The reflector is able to tilt about its own axis using member 1.

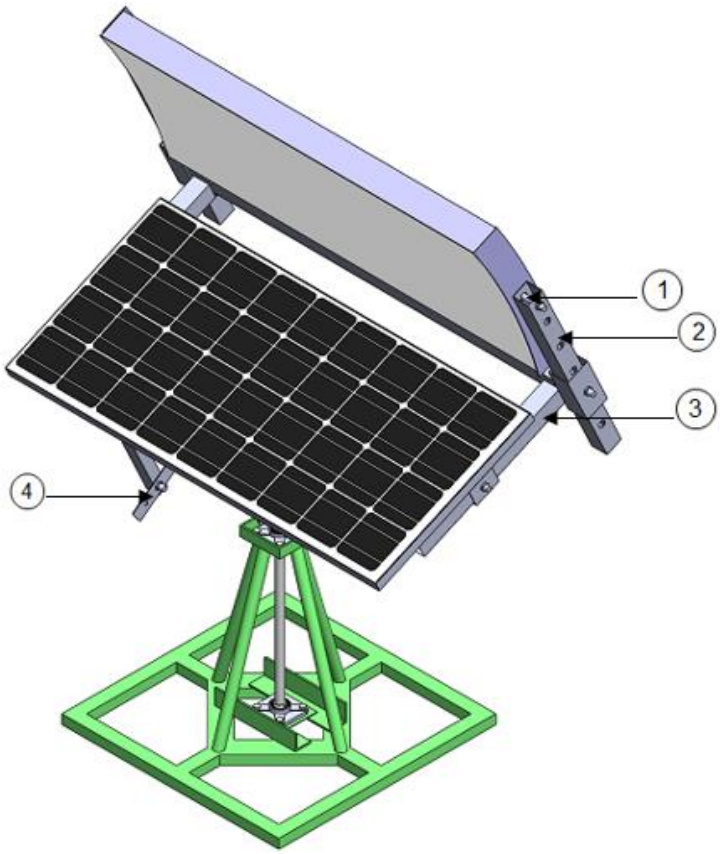

Figure 3-7: Full 3D model of the rig

3.7. **Design and construction of the reflective component**

During this research work, various projects and designs on PV/T and CPVT were compared. Most researchers use rectangular reflectors when designing concentrated photovoltaic. For this research work, the author used a parabolic reflector.

Many factors were taken into account when designing the parabolic reflector. The dimensions of the reflector used were determined taking into account the altitude angle represented in figure 3-8 and the dimensions of the receiver. Elevation or altitude angle(α_s) is the angular height of the sun measured from the horizontal as seen in figure 3-8. This angle varies throughout the day. The altitude angle of the parabola refers to the beam pointing direction and is calculated using equation 4-13. The average altitude was used to approximate the rim angle of the parabola. The rim angle and the aperture diameter, define the depth of the parabola and its focal length shown in figure 3-9. A small altitude angle within the same aperture gives a flatter parabola i.e. increases its focal length. The overall dimensions of the reflector used, are shown in table 3-2.

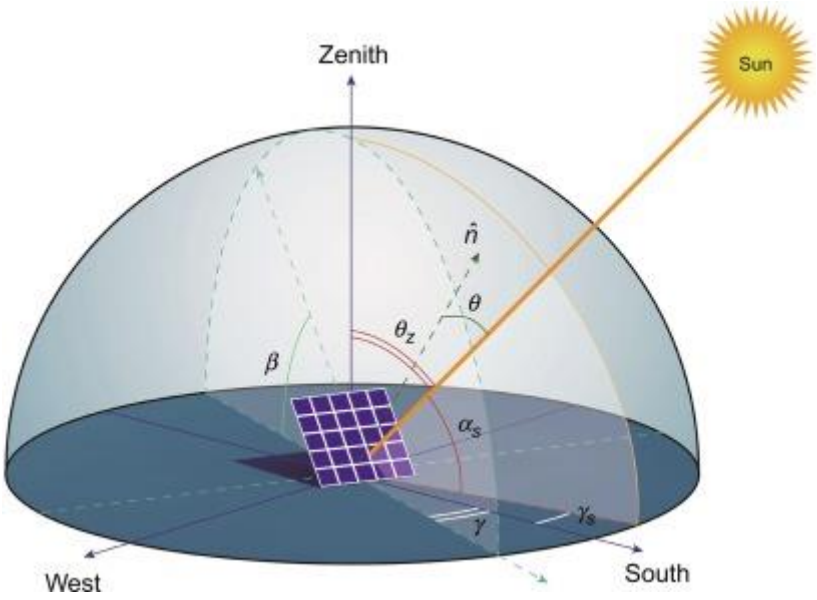

Figure 3-8: Solar PV panel characteristics angles. (Rosa-Clot & Tina, 2018)
θ_z, solar zenith; α_s, altitude angle; β, PV panel slope; γ_s, solar azimuth angle.

The geometry of the parabola is detailed in the figures below.

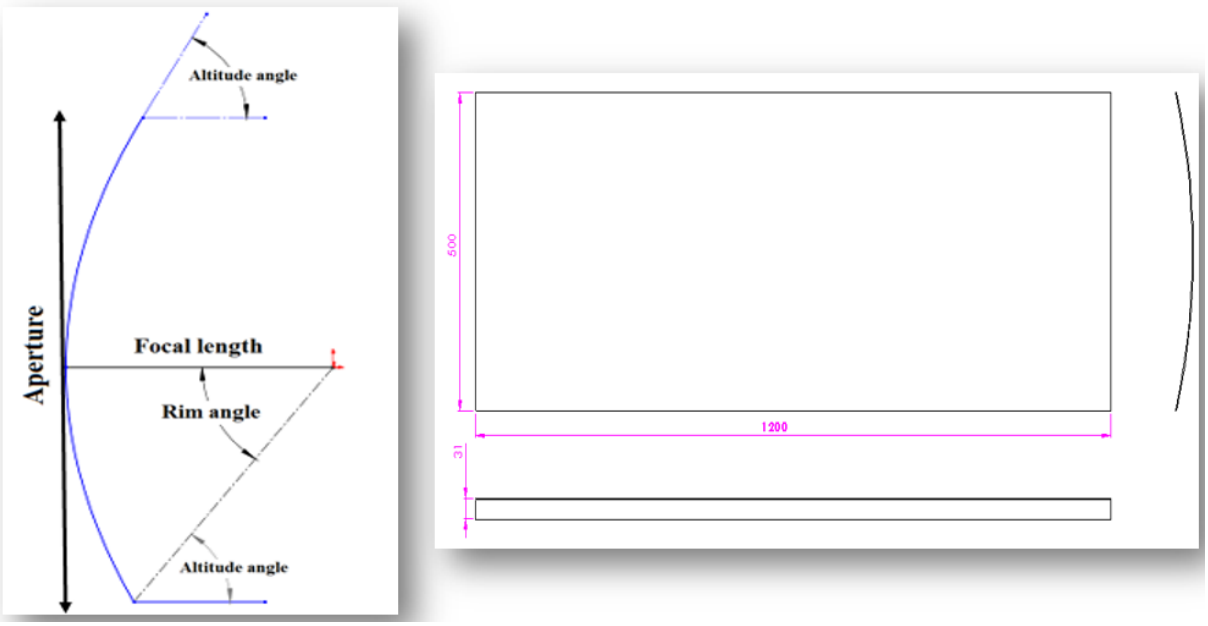

Figure 3-9: Parabola geometry

Table 3-2: Dimensions of the solar parabolic reflector

Parabolic trough dimensions	
Aperture width	500mm
Depth	31mm
Length	1200mm
Focal distance	504mm
Rim angle	34º
Thickness	1mm

3.8. **Design of the tracking mechanism**

There are two major types of solar tracking systems: the single axis, and the dual axis. Single axis solar trackers generally move from east to west while in dual axis, they track the sun to keep the incidence angle at zero all the time. Although the dual axis seems to be more effective than the single axis, it was not selected in this design due to the complexity of its construction and cost. The rig structure incorporates a water tank which rotates with the whole system. Therefore, dual axis was not selected. The final design of the tracker was made based on cost, availability of materials and durability. An automatic single axis solar tracking mechanism was designed. The design consists of a shaft, bearings, sprockets and a chain, DC stepper motor, motor driver, an Arduino micro-controller and a DC power supply. Given in figure 3-10 is the block diagram of the tracking system. Figure 3-11 shows the programming stage of the Arduino Uno controller.

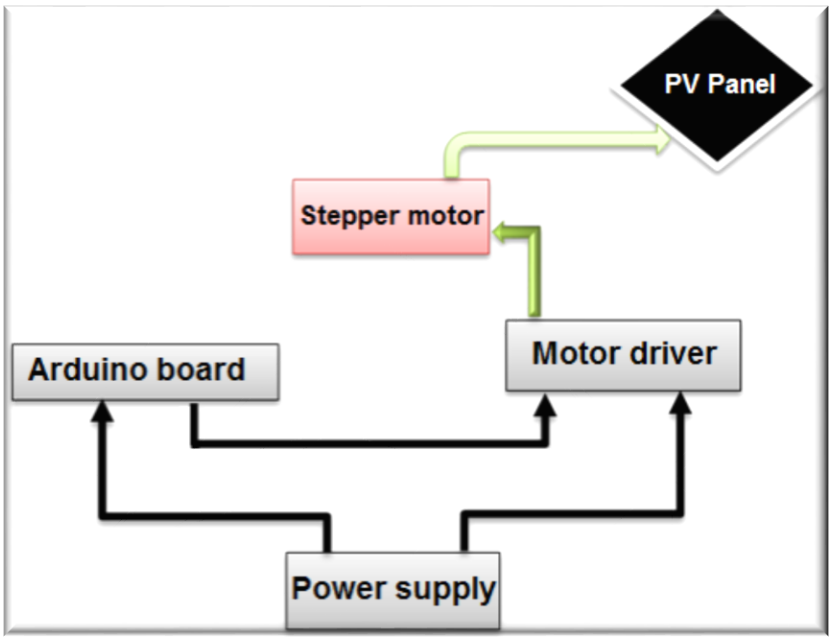

Figure 3-10: Solar tracker block diagram

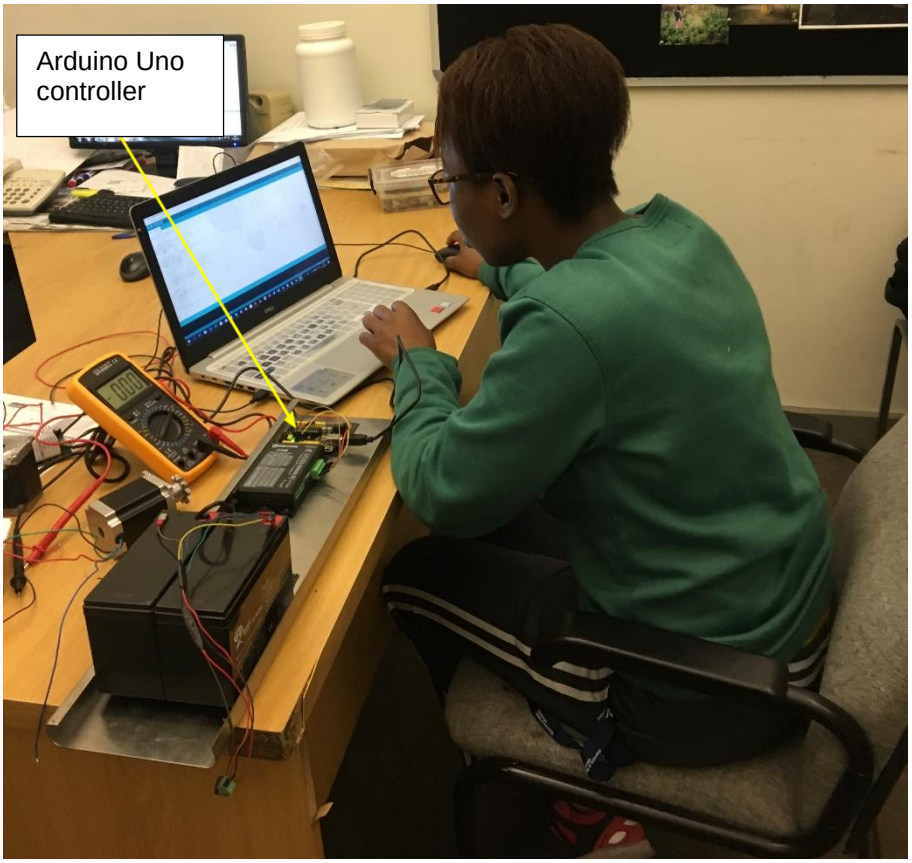

Figure 3-11: Motor and Arduino set-up

Many solar tracking systems make use of light-dependant-resistors (LDR). LDRs are small devices controlled by light. In solar tracking systems, those devices are used to sense the direction of the sun and send the signal to the motor driver to rotate it accordingly. This project, however, did not use LDRs. Rather, a stepper motor and an Arduino Uno to track the sun's location were used as highlighted above. Stepper motors are DC motors that rotate in steps. Motor selection was an integral part of the tracking system as the whole system would be fully dependant on it.

According to Duffie & Beckman, (2013) the earth rotates around the sun 15 degrees every hour. Consequently, the motor was programmed to enable the output chain drive sprocket make 12 steps, 12 hours per day. Each step being 15^0 at every top of hour from 7 am to 7pm. A sample video of the solar tracker prototype is given in the appendix A9. The programming code used is attached in the appendix A4.

3.9. **Bearing selection**

A bearing is a device used in mechanical systems to support relative motion between moving parts. For this research, 30mm UCF 4-hole flange bearings were used. To select the type and size of the bearing, the following was considered: expected life of the system; speed; static, dynamic and axial load. The two bearings selected are frictionless, and thus, less power is required to rotate the system. UCF bearings are sturdy, simple to install and have excellent strength. The bearings were placed accordingly as shown from the 3D model in

figure 3-5. The bearings selected were used to enable the motion along the shaft and also overcome the radial force.

Advantages of UCF bearings:

- Reliability
- Increased Life span
- Cleaner and neater look
- Power saving
- Reduced possibilities of fire hazards
- Increased production
- Power saving and Lubrication

The bearings were designed to run for 60 million revolutions. Using equation (3-6), the basic dynamic load rating (C kN) was calculated. The dynamic load should always be greater than the desired reaction force (C_{10} > F). In that case the bearings will be strong enough to support the weight of the system.

Life Equation

$$C_{10} = F \times L^{\frac{1}{k}} \tag{3-1}$$

3.10. **Sprockets and chain selection**

Sprockets are toothed wheels used to transmit rotary or linear motion between two shafts using a chain. They are mostly used in bicycles, cars, tracks or other machineries. As illustrated in figure 3-12, a single strand roller chain was used to transmit power between two parallel shafts separated by a fairly long distance. The type of prime mover is a DC electric motor which will be in operation daily during sun hours. A guideline for the selection procedure of Fenner chains found at (Fenner, n.d.) was used. The parameters relevant for chain selection are as follows:

- Service factor
- Design power
- Chain pitch
- Speed ratio
- Sprocket sizes
- Power rating
- Chain length

Chain length can be obtained from equation.

$$L = \frac{2C}{P} + \frac{T_n + t_n}{2} + \frac{KP}{C} \quad (3\text{-}2)$$

The chain drive was used in the design as it would be more effective for the following reasons:

- Chains have perfect velocity ratio as they do not slip;
- It occupies less space and can be used for any distance, long or short;
- It gives less load on the shafts;
- It offers long lifespan;
- Its power transmission is higher than belts or rope;
- It can operate under any atmospheric condition;
- Its transmission efficiency is fairly high when compared to belts.

However, chains require accurate mounting as their velocity can fluctuate when not stretched adequately. They also require careful maintenance for better efficiency.

Figure 3-12: CSPVT solar tracker: chain and sprocket arrangement

3.10.1. Calculations involved in chain and sprocket design

In figure 3-13 is the chain and sprocket diagram.

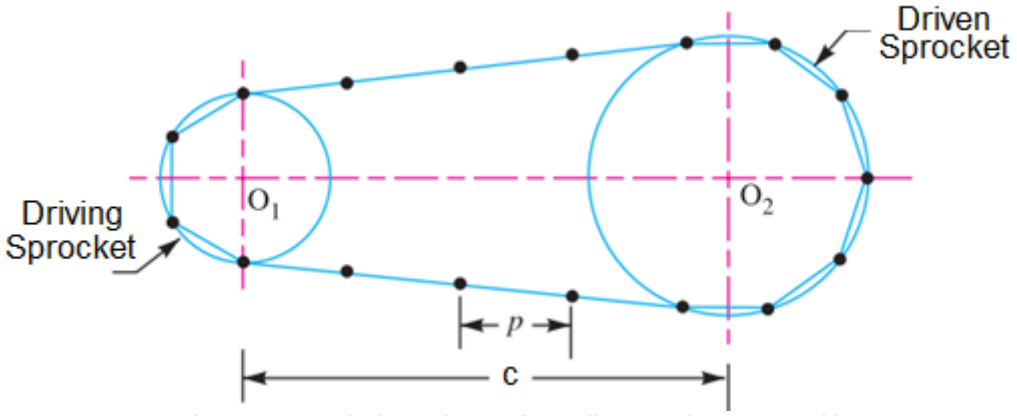

Figure 3-13: Chain and sprockets diagram (Fenner, n.d.)

Centre to centre distance between the sprockets is found from equation (3-3). The velocity ratio is found from equation (3-4).

$$C_d = \frac{p}{4}\left[K - \frac{t_n + T_n}{2} + \sqrt{\left(K - \frac{t_n + T_n}{2}\right)^2 - 8\left(\frac{T_n - t_n}{2\pi}\right)^2}\right] \quad (3\text{-}3)$$

$$VR = \frac{N_1}{N_2} = \frac{T_n}{t_n} \quad (3\text{-}4)$$

3.11. **Motor selection**

The selection of the motor was one important part of the solar tracking system as the design's rotary motion would be fully dependent on the motor selection. Of different types of motors used in solar tracking system, table 3-3 show a comparison between the three available.

Table 3-3: Different types of motors used in solar tracking system:

DC motor types	Description	Advantages	Disadvantages
Permanent magnet brush Dc motors (PMDC).	PMDC are a type of brushed DC motors whose poles are made of permanent magnets. Its working principle is similar to that of any DC motor	• It offers linear torque speed • Simple in construction • Cheaper and economical • Easily controllable • High power	• Is quite difficult achieving a speed control in this type of motor • Requires period maintenance and replacement of brushes

Brushless DC motors (BLDC)	BLDC are synchronous motors powered by DC current.	• They offer exceptional speed and torque when compared to brushed motors • High efficiency • Maintenance-free • Low energy consumption • Long operating life span	• Expensive to construct • They require a speed controller which can cost more than the motor
Stepper motors (STP)	Stepper motor is a brushless DC electric motor that divides a full rotation into a number of equal steps (EMworks, 2018). Stepper Motors are operated by digital pulses reaching the stator. This causes it to rotate discrete steps in proportion to number of pulses.	• They offer low speed • Highly reliable and flexible • Great low speed torque • It moves with precision • Excellent repeatability • They are overload safe • Pulses can be easily controlled • They can offer full torque at rest • Longer life span • Step angle accuracy of 3-5% of one step	• It does not give feedback on missed steps • Not easy to operate at very high speed

After a thorough analysis of the above, a stepper motor was chosen. The CSPVT was designed to make 15° angle every-hour from 7am to 7 pm. As mentioned in the previous section, LDRs will not be used in this solar tracking system. Therefore, the CSPVT had to be designed to track the installation's relative position to the sun accurately. It is known that the earth rotates about its axis everyday making an angle of 360º which is 15º every hour. Hence the system was designed to adjust to that. Stepper motors are great for applications where low speed and precision are required as they rotate through a specific angle with each step it makes. The step angle error of stepper motors is non-accumulative. Its accuracy is a function of mechanical precision of its parts and assembly. Table 3-4 highlights some of the specifications of the motor used.

Table 3-4: Stepper motor specifications

Electrical specification		Physical specifications	
Motor type	Bipolar stepper	Frame size	60×60 mm
Step angle	0.09 °	Motor length	78 mm
Holding torque without gearbox	1.89 Nm	Gearbox length	40 mm
Rated current	2.8A	Shaft diameter	Ø8 mm
Phase resistance	1.13 Ω	Shaft length	28 mm
Voltage	3.2 V	D-cut length	25 mm
Gear box specifications		Lead length	500 mm
Gearbox type	Spur	Weight	1.68 kg
Gear ratio	20	Number of leads	4
efficiency	70%		
Backlash at no load	$\leq 3°$		
Maximum permissible torque	5 Nm		

The torque provided by the motor and shaft was calculated using equations (3-5). The torque required is determined from equation (3-6).

$$T_{provided\ at\ shaft} = T_{provided\ at\ Motor} \times Gear\ reduction \tag{3-5}$$

$$T_{required} = F \times r \tag{3-6}$$

3.12. **Motor programming and coding**

The motor was coupled to an Arduino microcontroller. The Arduino board was programmed with the correct driver so it can send the right signal to the motor. In figure 3-14, the motor may be seen unattached whilst in the initial stages of design. The code used is attached in the appendix A4.

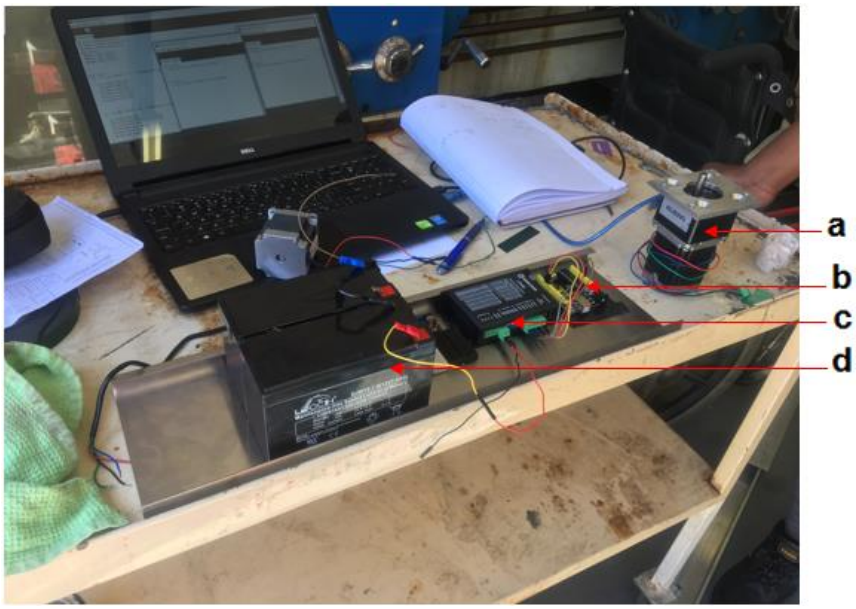

Figure 3-14: Motor and Arduino set-up. a) Stepper motor;
b) Arduino Microcontroller; c) Motor driver; d) DC batteries

3.13. **Motor cover**

The next step in design was catering for the conditions to which the structure would be exposed to. Hence, all elements needed to be protected from rain and dust. The design may be seen in figure 3-15.

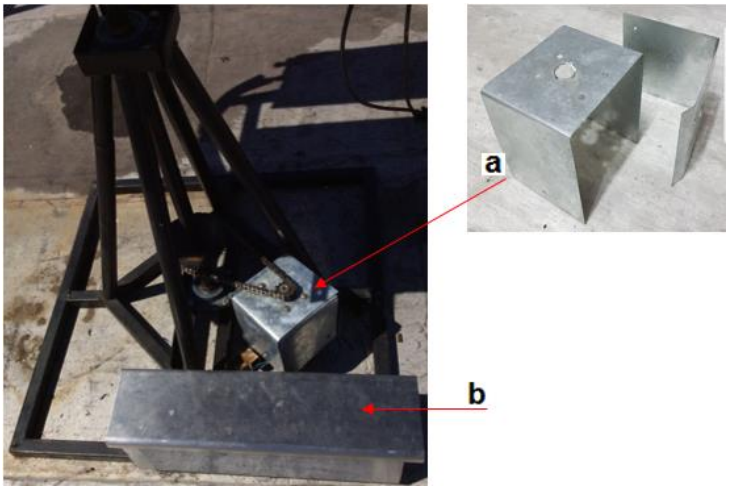

Figure 3-15: Tracking components cover.
a) Motor cover; b) Electronic components cover

3.14. **Assembly**

The final assembly of the CSPVT is shown in figure 3-16. Detailed structure assembly can be found in the appendix A6.

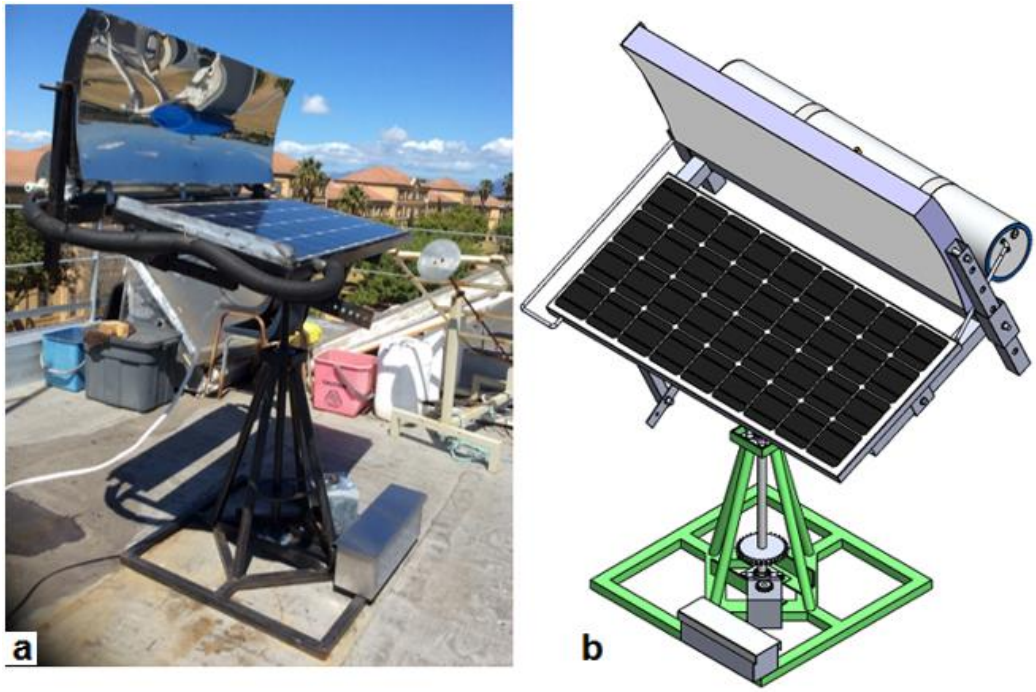

Figure 3-16: CSPVT
a) CSPVT prototype installed at Mechanical Eng. Roof
b) CSPVT 3D model

3.15. **Conclusion**

This chapter focused on design and construction of the CSPVT. The components and materials used as well as the manufacturing/assembly methods were described. The proceeding chapter, will discuss the experimentation and set-up used in analysing the designed system.

CHAPTER FOUR

EXPERIMENTAL SETUP AND METHODOLOGY

4.1. Introduction

This chapter details all the steps taken to conduct the experiments as well as the methodology.

4.2. Zone conditions

The experimental work for this research was conducted at Bellville-Cape Town in a period of 10 days during the months of September-October 2018. Table 4-1 shows the weather overview at Bellville during the experimental period.

Cape Town coordinates: Latitude and longitude of Cape Town: 33.9249° S, 18.4241° E

Table 4-1: Weather overview (extracted from the Campbell R-1000 data logger)

Months	Avg. Temp	Avg. humidity	Avg. daily sunshine	Max. wind speed	Avg. pressure
Sep.	24°C	77%	7h	7.2 m/s	1019 mbar
Oct.	26°C	65%	9h	7.7 m/s	1018 mbar
Avg. wind speed during experimental days					2.76m/s
Avg. ambient temperature during experimental days					28.6ºC

4.3. Experimental setup

The PV modules used in this experiment were both facing true north. The semi-fixed PV was inclined at an angle of 30° to the horizontal whereas the CSPVT at 25° with the horizontal. The schematic of the experimental rig prototype is shown in the figure 4-1. The rig was assembled on top of the Mechanical Engineering building of CPUT. Solar radiation arriving on site was measured using an existing weather station (shown in figure 4-5). Primary data of results obtained from the logger can be found in the appendix A2.

Electric energy harvest was monitored by logging 15 minute PV generated voltages and currents in the weather station data logger. The thermal energy was monitored half hourly by direct readings of thermometers inserted at the bottom and top of the solar syphon tank. In addition, temperatures of the PV panel glazing and back plate were monitored to be able to give an indication of the cell temperatures through the King model. This data was used to compute total energy yield, system energy efficiency and comparison was made with results from a standalone, non-concentrating identical PV unit.

To cross check the Voltage and current values recorded by the data logger, a digital multi-meter and a clamp on multi-meter (shown in figure 4-3) were used. The systems were connected as in figure 4-2. The panel and a DC battery were connected to the charge

controller. Then from the charge controller there was a load of 50W DC bulb to discharge some of the power as seen from figure 4-1 (d). Appendix A8 shows some photos taken during the experiments.

Figure 4-1: Experimental set-up prototype
a) Weather station; b) Semi-fixed PV; c) CSPVT; d) DC bulb
e) DC battery; f) Charge Controller

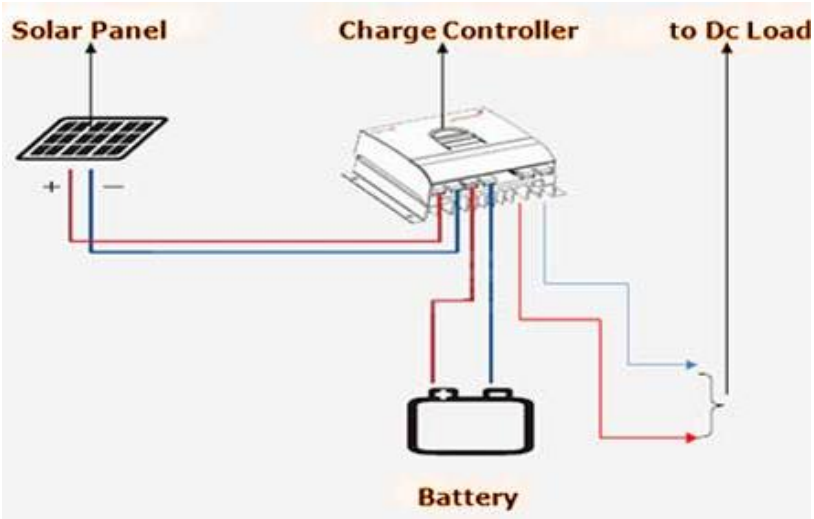

Figure 4-2: Charge controller in a circuit

4.4. Instrumentation and Equipment

- The CSPVT and the semi-fixed PV
- A digital multi-meter to measure the voltage displayed in figure 4-3
- Lutron CM-9930 clamp multi-meter to measure the current

- A 20A, 12V solar charge controller to limit the rate at which electric current was added to or drawn from the batteries. Its diagram is shown in figure 4-2
- Set Solar 12V, 102Ah batteries
- G178 12V, 50W bulbs displayed in figure 4-1
- Thermometers to measure the water temperatures in and out of the PV panel displayed in figure 4-4
- TP02A K-type thermocouples to measure the temperatures on top and the back of the panel
- Kipp & Zonen CMP06 pyranometer with a Campbell Scientific Africa weather station with a CR1000 data logger shown in figure 4-5 to record daily solar beam and diffuse radiation
- A 03101 R.M young three cup anemometer to measure the wind speed

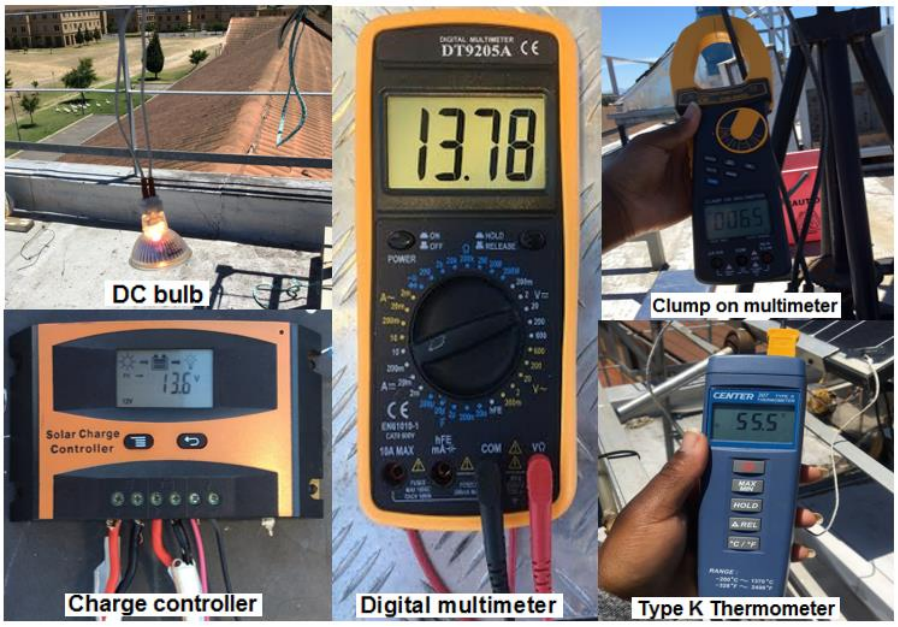

Figure 4-3: Display of different test tools used during the experimental work

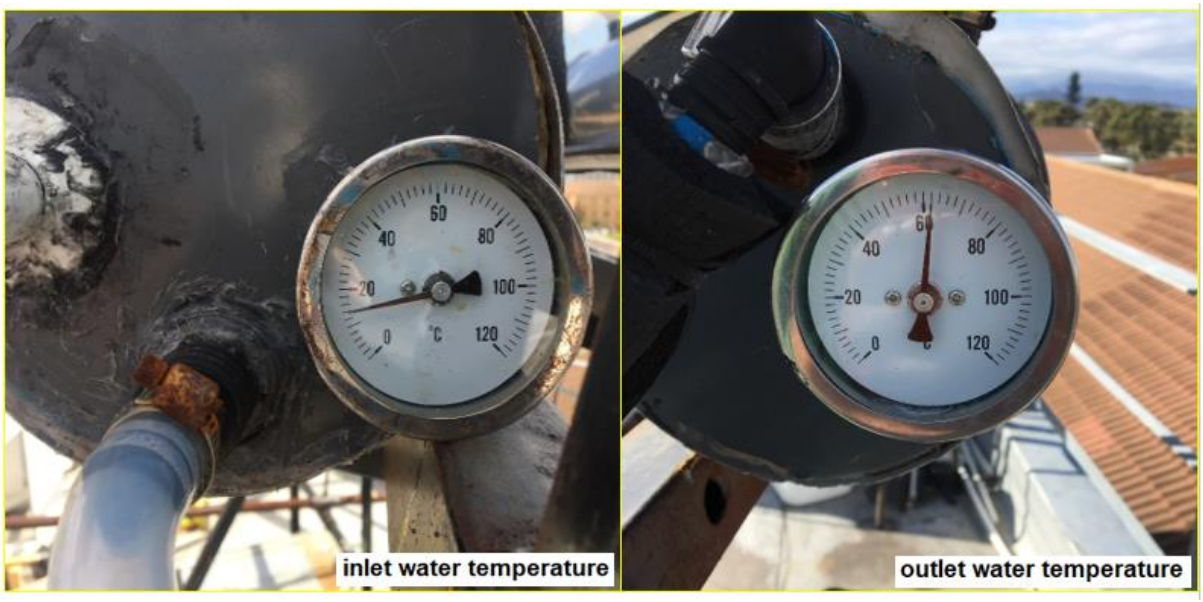

Figure 4-4: Thermometers used to record the inlet and outlet water temperature

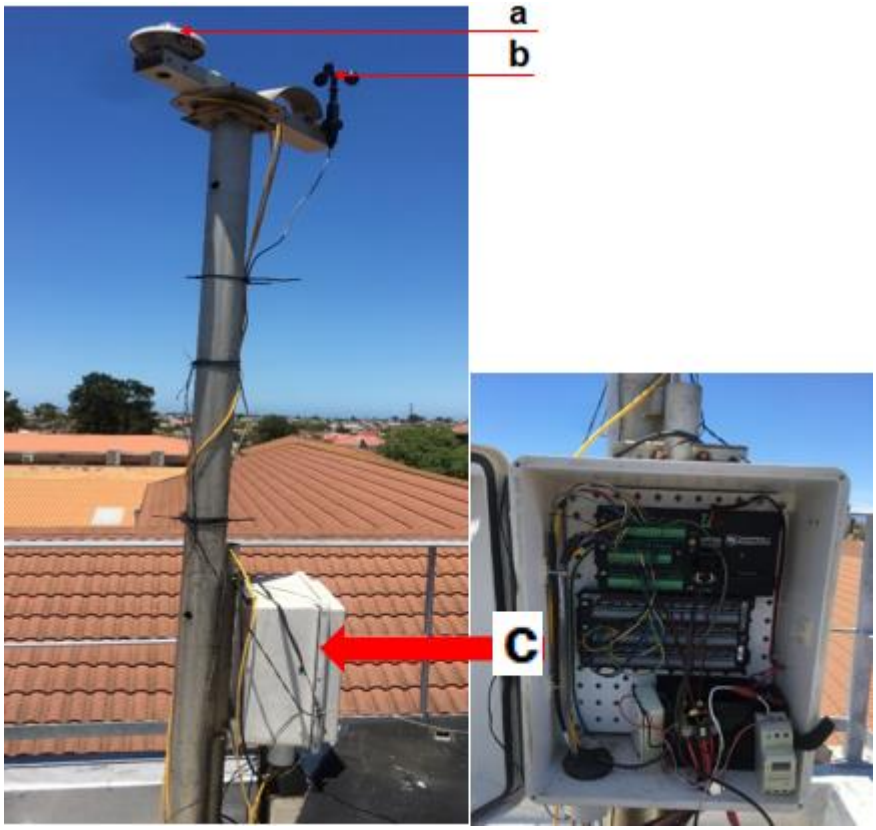

Figure 4-5: Campbell Scientific Africa weather station used for the experiments
a) Kipp & Zonen CMP06 pyranometer; b) Three cups anemometer; c) Data logger

4.5. Measured data

All data was measured and recorded every 15 minutes except for the water temperature which was measured half-hourly. The following parameters were measured and recorded:

- Total and diffuse radiation
- Wind speed

- Ambient temperature
- PV glazing temperature
- Temperature at the back of the panel (T_b)
- Inlet and outlet temperature of water (T_{in} and T_{out})
- Voltage, V
- Current, I

4.6. Calculated data

The following equations were used to calculate the efficiency of the CSPVT and the energy gain:

- **Electrical efficiency, η_{elec}:**

$$\eta_{\text{elec}} = \frac{E_{elec}}{A \int_{day} G_{gl} dt} \tag{4-1}$$

$$E_{elec} = \int_{day} VIdt \tag{4-2}$$

- **Thermal efficiency, $\eta_{thermal}$:**

$$\eta_{thermal} = \frac{Q_{collected}}{A \int_{day} G_{gl} dt - E_{elec}} \tag{4-3}$$

$$Q_{collected} = m_{water}(h_{max} - h_{in}) \tag{4-4}$$

- **CSPVT efficiency, η_{total}:**

$$\eta_{total} = \frac{Q_{collected} + E_{elec}}{A \int_{day} G_{gl}\, dt} \tag{4-5}$$

- **Optical efficiency, η:**

$$\eta = \frac{\mathrm{G_{in}}}{\mathrm{G_{gl}}} \tag{4-6}$$

- **Solar radiation, G_{gl} and G_{in}**

Total irradiance denoted G_{gl}, is defined as the amount of solar radiation reaching the glazing surface of the panel or collector. While G_{in} is a portion of G_{gl} going through the glazing with the rest being reflected off the glazing surface, or being absorbed to simply warm up the

glazing. The fraction G_{in}/G_{gl} is the optical efficiency and is given in figure 5-9. Both G_{gl} and G_{in} are calculated as described by Duffie & Beckman, (Duffie & Beckman, 2013). Matlab was used to ease the calculations. The programming code is given in appendix A5.

Concentrating collector view factor

View factor also termed the geometrical factor, is a fraction of the solar radiation leaving surface A_i that is intersected by surface A_j and is determined by using equation (4-7). The view factor only depends on the geometrical configuration of the system. It was necessary to calculate the view factor so as to determine the amount of radiation from the reflector getting onto the panel.

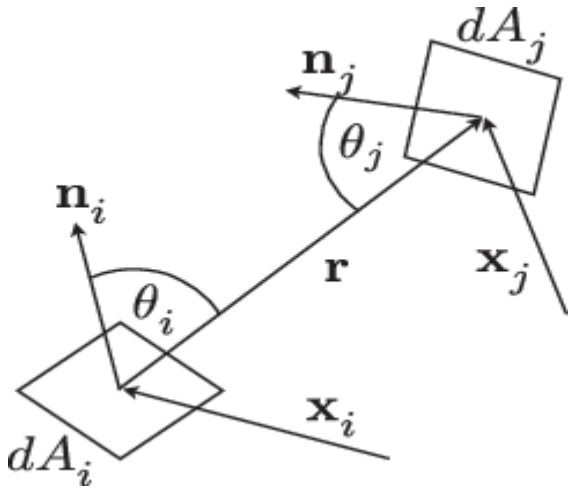

Figure 4-6: Geometry for view factor (Kramer et al., 2015:3)

$$FV = \frac{1}{A_i}\int_{A_i}\left(\int_{A_j}\frac{\cos\Theta_i \cos\Theta_j}{\pi r_{12}^2}dA_j\right)dA_i \tag{4-7}$$

Heat loss of the PV/T

The heat loss from the PV/T was determined using equation 4-8 (modified Duffie and Beckman equation).

$$U_L = \left[\frac{Nu \times k_a}{L_1} + \left\{\frac{\sigma}{\frac{1}{\varepsilon_p}+\frac{1}{\varepsilon_g}-1}\right\}\left(T_p^2+T_g^2\right)\left(T_p+T_g\right)\right]^{-1} + \left(h_w + \sigma\varepsilon_g\frac{\left(T_g^4-T_a^4\right)}{\left(T_g-T_a\right)}\right)^{-1} + \frac{\delta_g}{k_g}+\frac{L_1}{k_1} \tag{4-8}$$

$$N_u = 1 + 1.44\left[1 - \frac{1708(\sin 1.8\beta)^{1.6}}{Ra\cos\beta}\right]\left[1 - \frac{1708}{Ra\cos\beta}\right] + \left[\left(\frac{Ra\cos\beta}{5830}\right)^{\frac{1}{3}} - 1\right] \quad (4\text{-}9)$$

4.7. Angles calculated

The caption in figure 4-7, represents the solar angles considered for this experimental work.

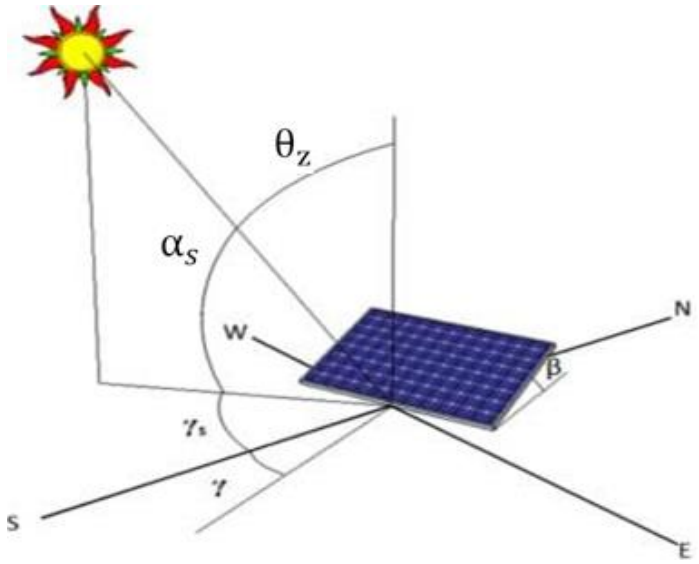

Figure 4-7: Solar angles, image source:
https://www.teachengineering.org/lessons/view/cub_pveff_lesson01

Angle of incidence, Θ

$$cos\theta = sin\delta\cos\beta - \sin\delta\cos\varphi\sin\beta\cos\gamma + \cos\delta\cos\varphi\cos\beta\cos\omega + \cos\delta\sin\varphi\sin\beta\cos\gamma\cos\omega + \cos\delta\sin\beta\sin\gamma\sin\omega \quad (4\text{-}10)$$

Azimuth angle, γ_s

$$\gamma_s = sign(\omega)\left|cos^{-1}\left(\frac{cos\theta_z sin\emptyset - sin\delta}{sin\theta_z cos\emptyset}\right)\right| \quad (4\text{-}11)$$

Zenith angle, Θ_Z

$$cos\theta_Z = cos\emptyset cos\delta\cos\omega + \sin\emptyset\sin\delta \quad (4\text{-}12)$$

Altitude angle

$$\alpha_s = sin^{-1}[sin\delta sin\emptyset + cos\delta cos\emptyset cos\omega] \quad (4\text{-}13)$$

Solar hour

$$\omega = 15(t - 12) \quad (4\text{-}14)$$

4.8. Parabolic reflector

The concentration ratio of the parabola was calculated using equation 4-15, as in Duffie & Beckman, (2013): where A_a is the rectangular area of aperture of the reflector and A_r is the area of the receiver (in this case the receiver was the PV panel)

$$C = \frac{A_a}{A_r} \tag{4-15}$$

4.9. Conclusion

This section discussed the methodology, equipment and equations used to analyse the performance of the CSPVT. The results obtained from the experiments and analysis of the same, are presented and discussed in the subsequent chapter.

CHAPTER FIVE
RESULTS AND DISCUSSION

5.1. Introduction

This chapter reports and discusses the experimental results of the CSPVT as well as of the conventional PV (semi-fixed PV unit). Comparison of their performance is analysed in detail. Graphical results are displayed in this chapter while the numerical ones are attached in the appendix A1. All 2D graphs were drawn using Excel while the 3D graphs were drawn using Matlab software. At the end, the experimental results are compared with those from TRNSYS simulation.

5.1.1. Weather condition

The meteorological conditions during the testing period are shown in Figures 5-1 to 5-3. Figure 5-1 shows the variation in ambient temperature (T_{amb}) for the duration of the experiments. The T_{amb} range was between 5°C and 40.8°C. Figure 5-2 displays the trend in wind speed, which ranged between 0 m/s and a maximum of 6.7 m/s on 22nd September. Figure 5-3 shows the solar radiation available during the experimental period. The maximum solar radiation logged was 996W/m^2 on 20th September 2018. The patterns seen from figures 5-1 and 5-3 indicate how T_{amb} and irradiance changes throughout the day. They usually reach their maximum values between 12pm-2pm. As it can be noted, the weather was quite good for the operation of the PV panel. Hence, the results obtained were satisfactory.

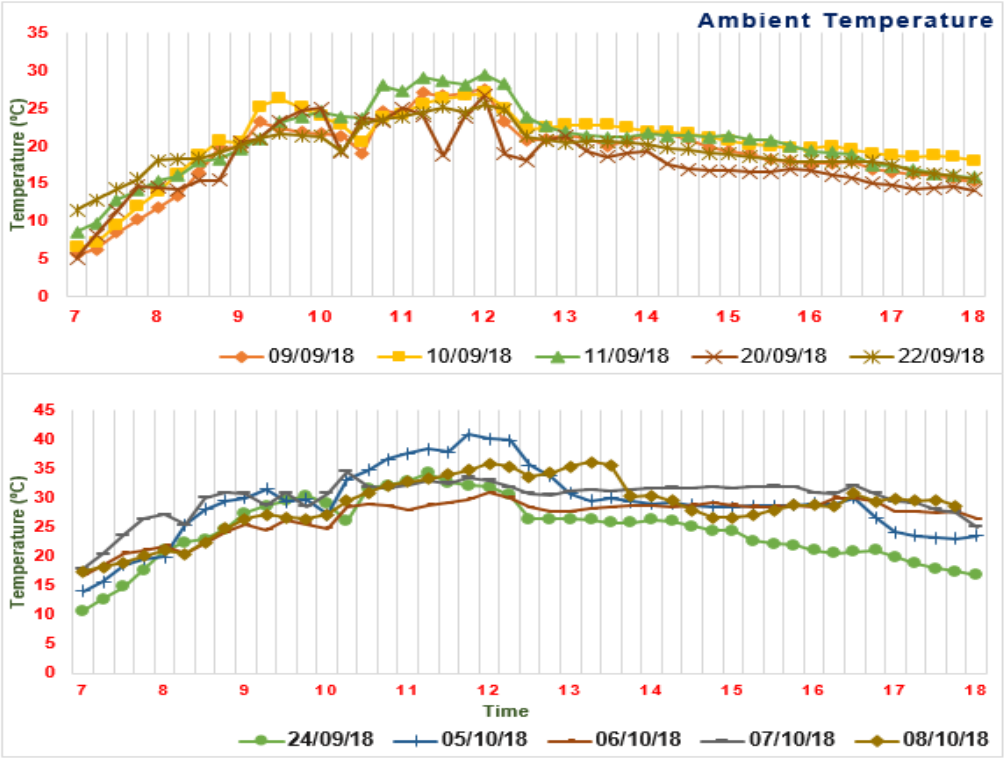

Figure 5-1: Variation of ambient temperature over the course of the experimentations

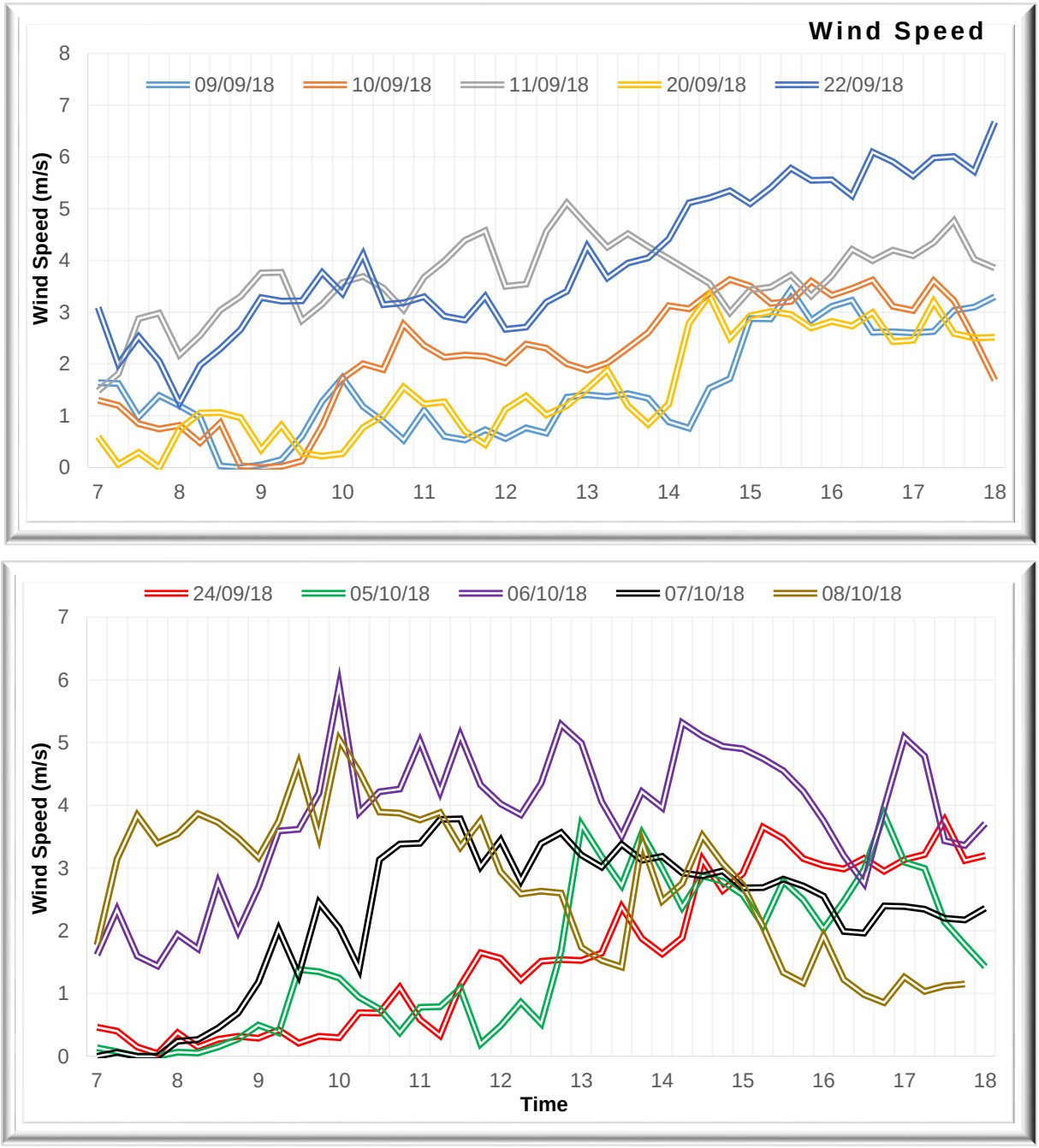

Figure 5-2: Variation of wind speed over the course of the experimentations

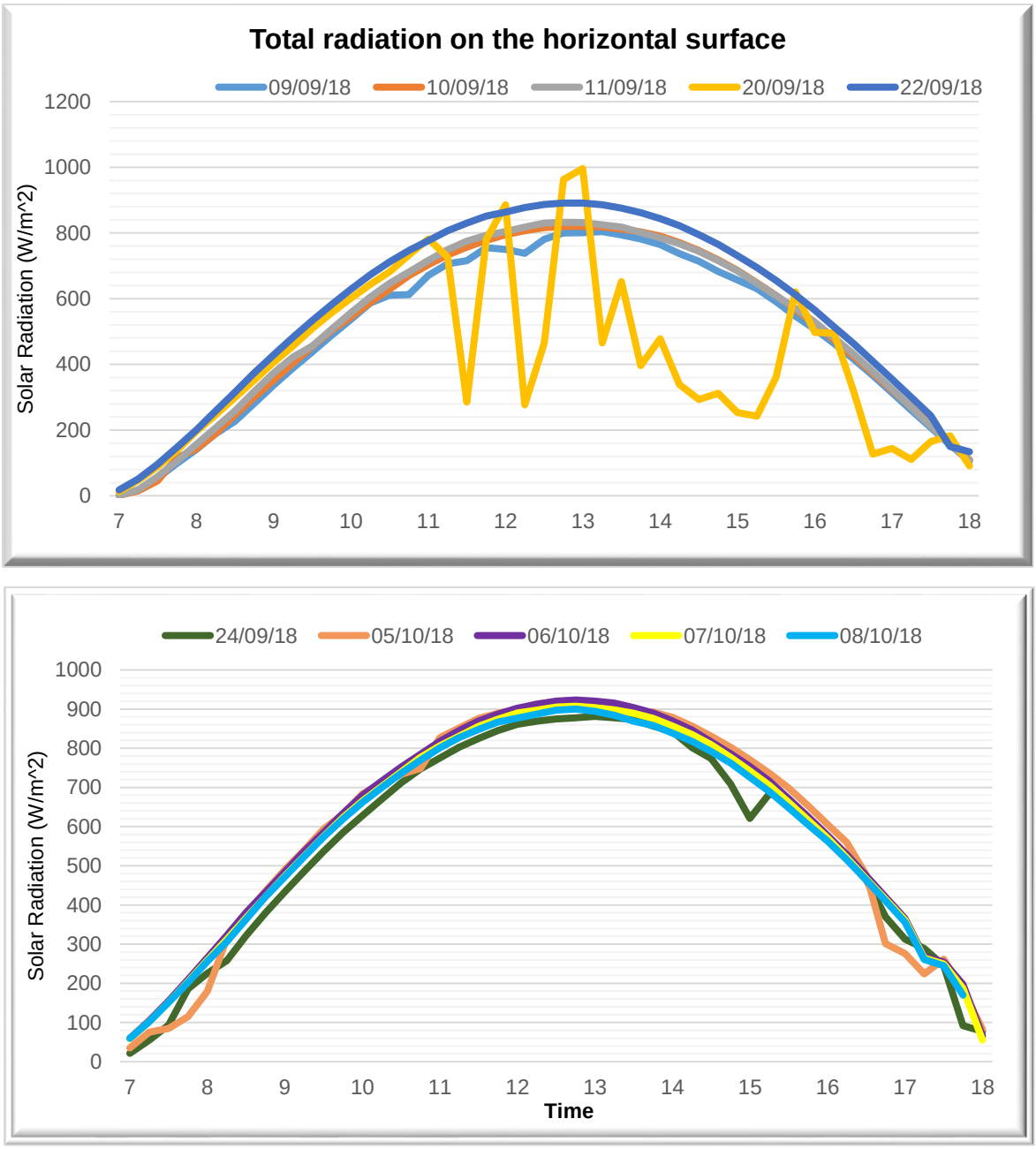

Figure 5-3: Pattern variation of the solar radiation over the experimental period

5.2. **Solar radiation G_{gl} on the inclined surface**

Figures 5-4 and 5-5 display the amount of total irradiance on both units: the CSPVT and conventional PV (semi-fixed unit), while figure 5-6 shows the total measured diffuse radiation per square meter. Total irradiance is defined as the amount of solar radiation reaching each square metre of a glazing surface of the panel or collector. The 3D representations below clearly indicate higher solar irradiance on the CSPVT compared to the convectional PV.

As explained in 4.6, the irradiance was converted to joules to estimate the energy available for both panels. That being said, the total energy incident on the CSPVT was 278.75 MJ. That was 64.4% higher than on the conventional PV which was only 169.56 MJ.

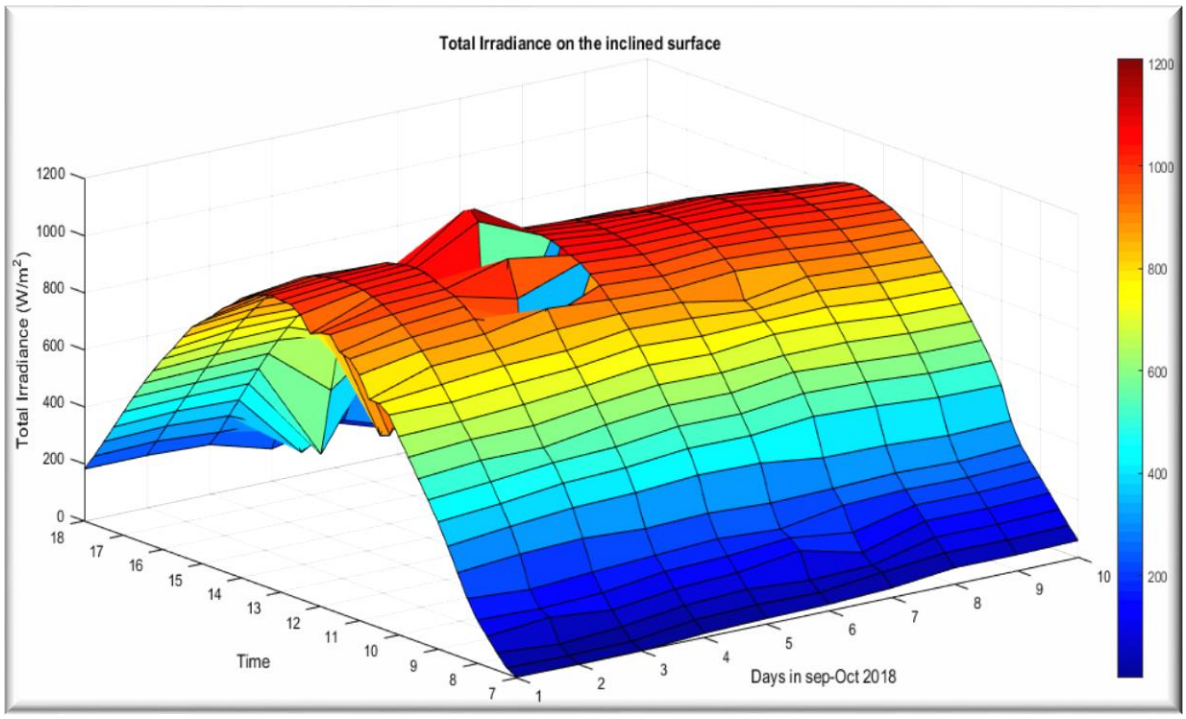

Figure 5-4: Representation of total solar irradiance on the conventional PV

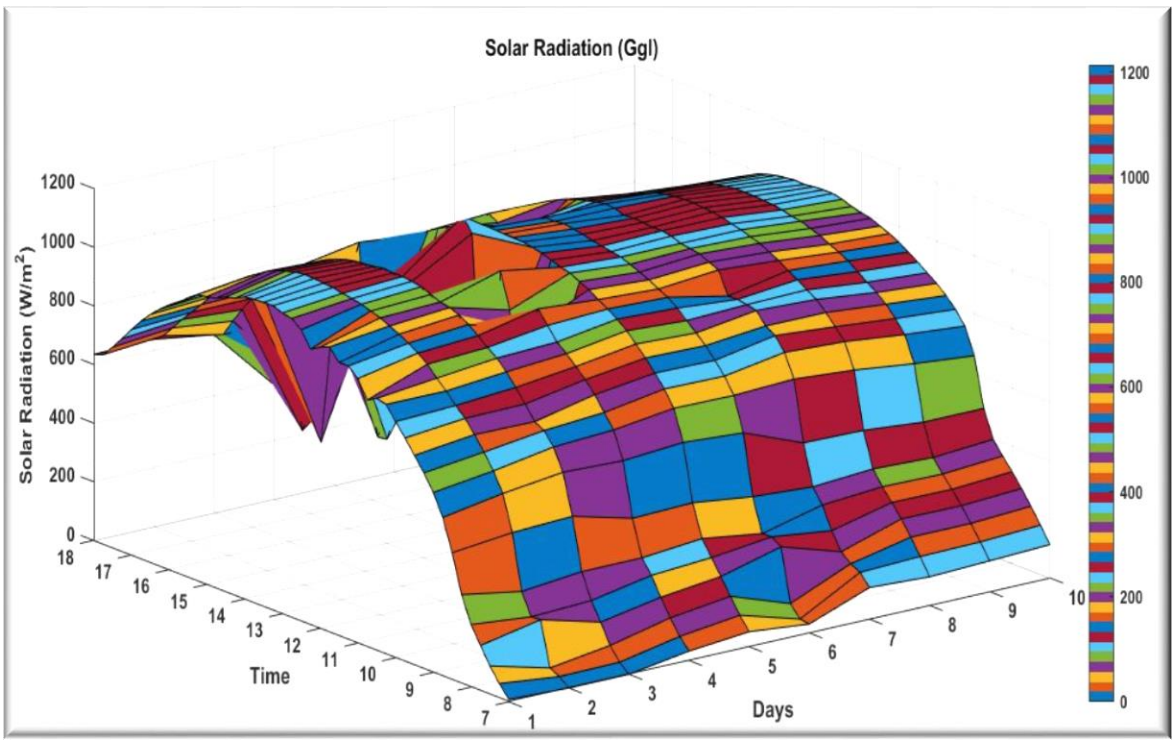

Figure 5-5: Representation of total solar irradiance on the CSPVT

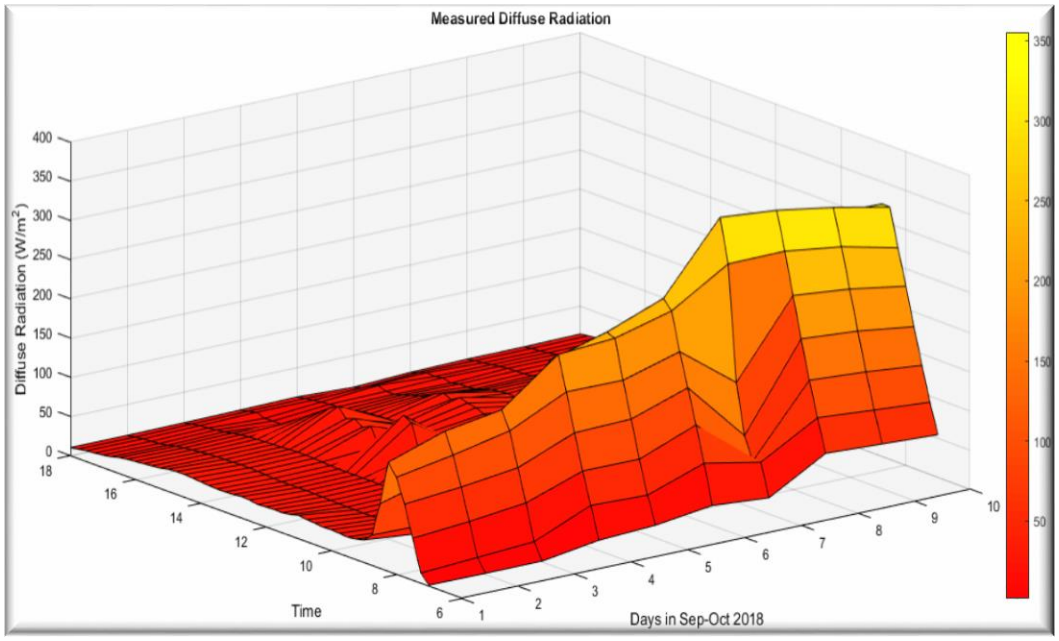

Figure 5-6: Representation of measured diffuse radiation

5.3. **Solar radiation into the glazing, G_{in}**

In engineering and science nothing operates at 100% efficiency. That theory applies to PV panels as well. Not all radiation reaching the glazing surface of the panel is transmitted through the glazing. Only a fraction of it goes in, and that is labelled G_{in} in this report. To make sense out of this, figure 5-9 represents the optical efficiency of both units. The optical efficiency being the fraction of G_{gl} transmitted into the panel in percentage form. The fractions of G_{gl} captured in terms of power per square meter, are represented in figures 5-7 and 5-8. The range of G_{in} on the CSPVT was between zero to 1193 W/m^2 while that for the semi-fixed panel was between zero and 603W/m^2. That is about half of the radiation absorbed by the improved PV unit. In terms of optical efficiency, the CSPVT had an average of 72% efficiency while its counterpart had an efficiency of 52%. It is clear that improvements were being noticed at this point as more energy was being absorbed by the CSPVT when compared to the normal PV.

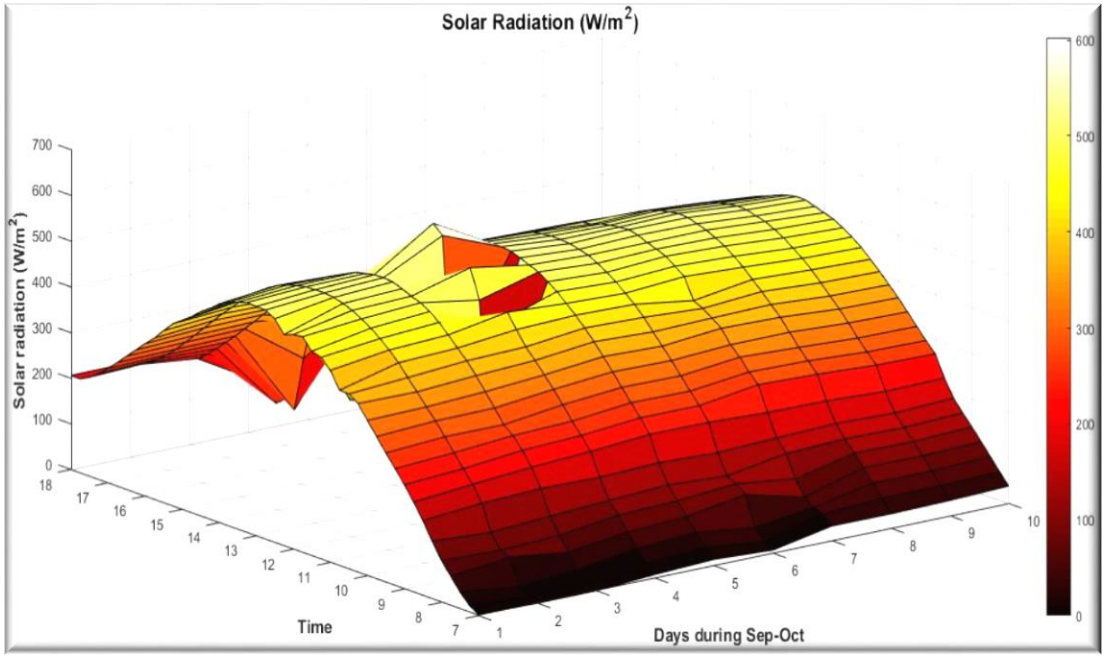

Figure 5-7: Total radiation G_{in} for the conventional PV panel

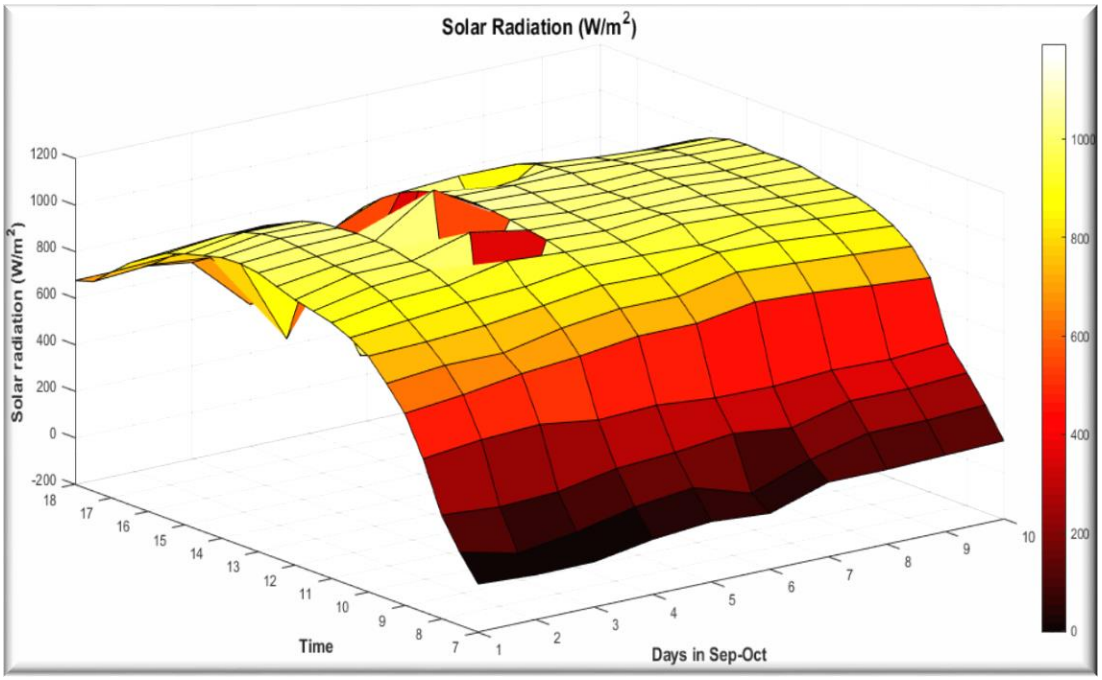

Figure 5-8: Total radiation G_{in} for the CSPVT

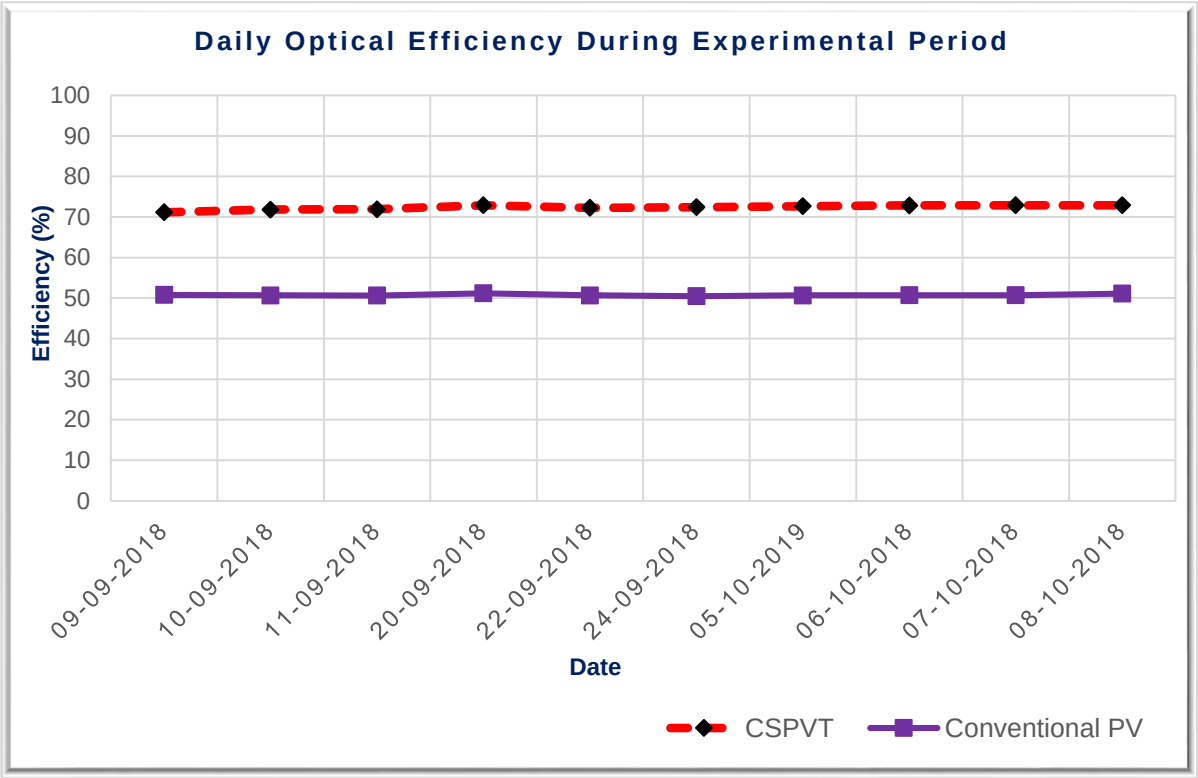

Figure 5-9: Optical efficiency for the CSPVT and the semi-fixed PV

5.4. **Electrical performance of the panels**

The electrical performance of both PV units is depicted in figure 5-10. A comparison between incident energy and the collected one in terms of useful electricity is clearly detailed. The total electrical energy collected in MJ was 18.3 from the conventional PV and 29.3 from the CSPVT respectively. Numerical data collected is attached in the appendices A1-A5. It is clear that the CSPVT collected an additional 11MJ of energy, which indicates 60.1% improvement over the semi-fixed unit. Kanyarusoke & Gryzagoridis, (2016) report a 34.1% gain from tracking alone, without concentration. It would appear therefore that concentration and cooling add about 26 percentage points, which is a significant increase.

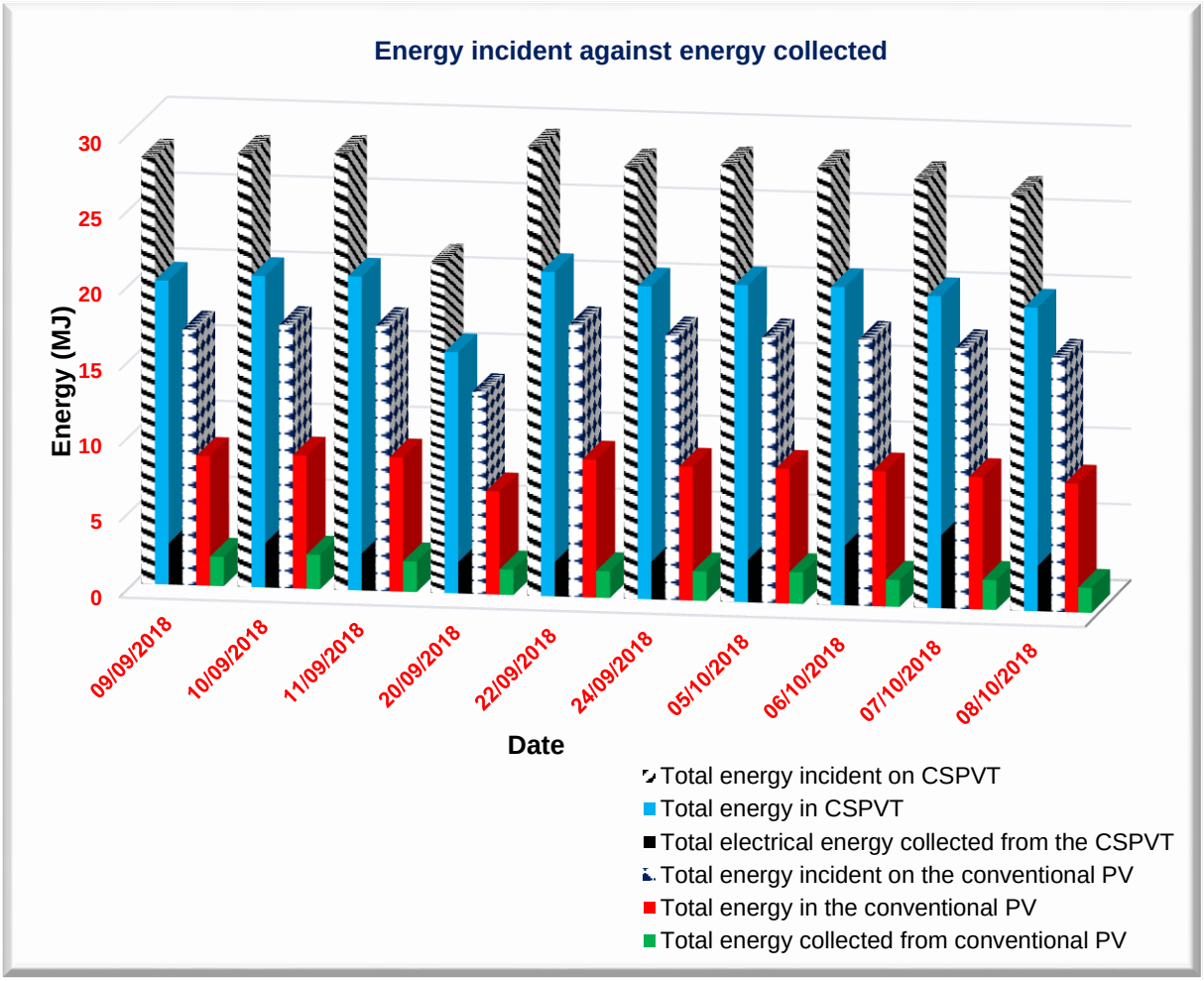

Figure 5-10: Daily incident irradiance and the total-daily energy collected

5.5. **Discussion**

5.5.1. **Energy output**

The energy produced by the panels on a daily basis, is shown in figure 5-11. During the experimental period, the conventional PV was able to produce a total of 5.08kWh of electrical energy while the CSPVT produced a total of 8.134 kWh. The power produced was given in Watts, which was converted to kWh to enable the estimation of their daily performance in terms of energy. This step was necessary to give us an idea of how much the CSPVT generated in terms of electrical power when compared to its counterpart.

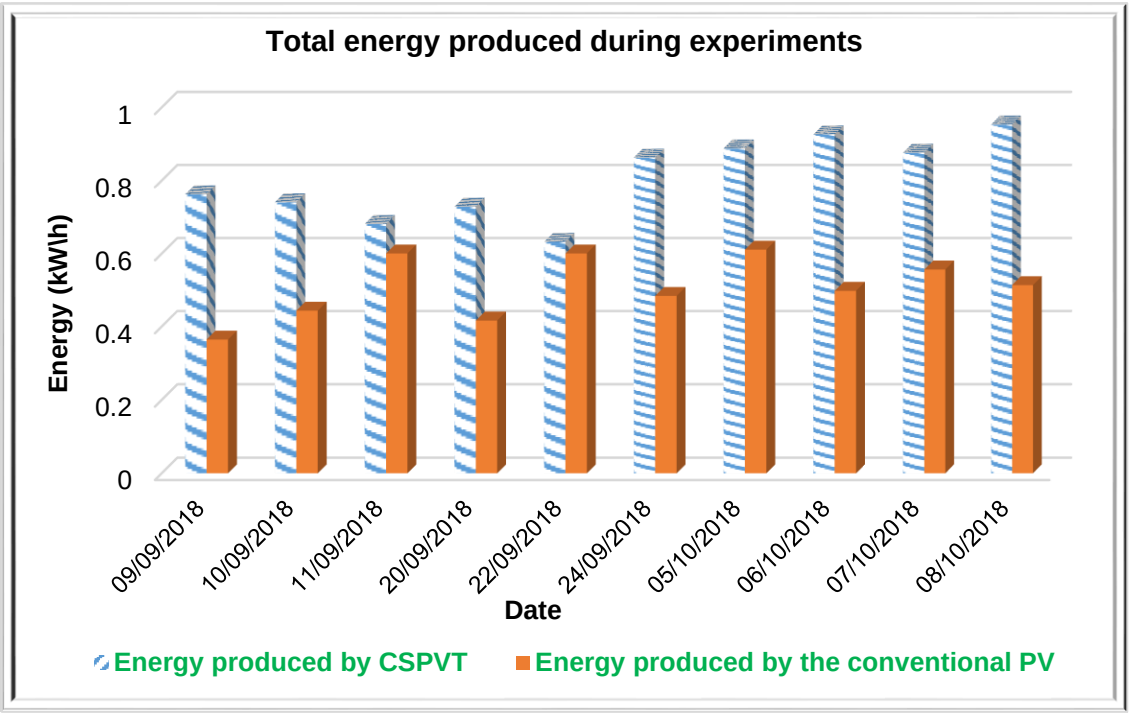

Figure 5-11: Daily electrical energy produced by the panels

5.5.2. **Performance of CSPVT**

The performance of CSPVT is determined by the thermal and electrical efficiency of the same. Given in figure 5-12, is the representation of the total energy collected from the CSPVT. The total energy collected ($E_{eletrical}$ and $E_{thermal}$) was 125.62 MJ. Total G_{in} calculated was 201.75 MJ. It is clear that the CSPVT was able to utilize 62.4% of the total energy, Gin. Figure 5-13 and 5-14 summarizes the overall performance of both systems tested during the trial period. The conventional PV utilized about 11% of the solar radiation available. Which means that over 88% of the energy was wasted.

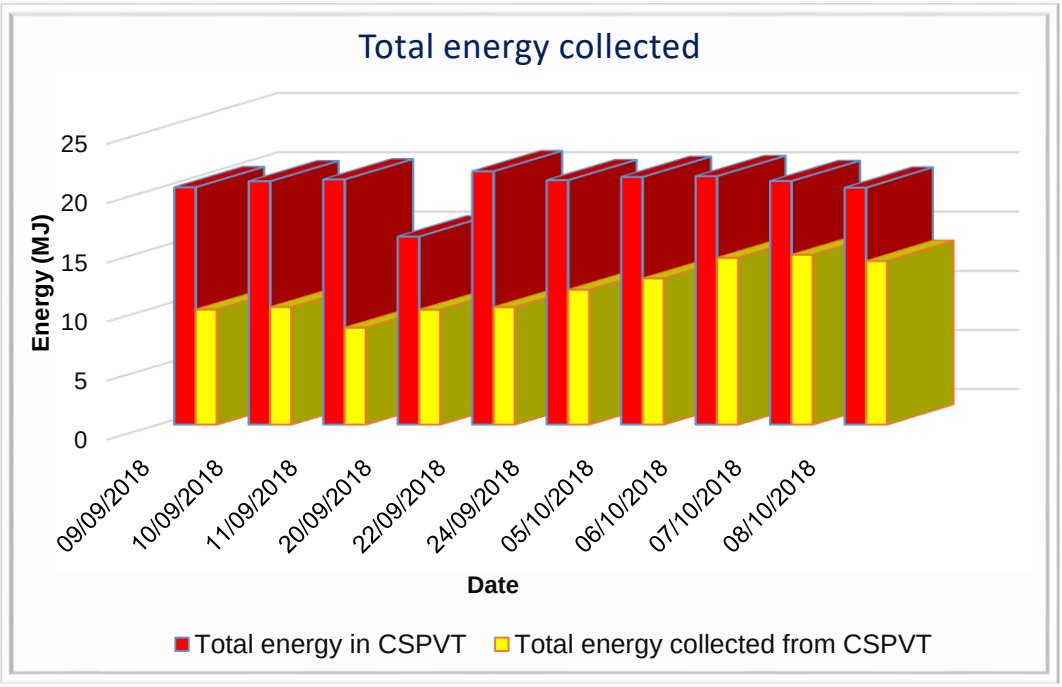

Figure 5-12: Overall performance of the CSPVT

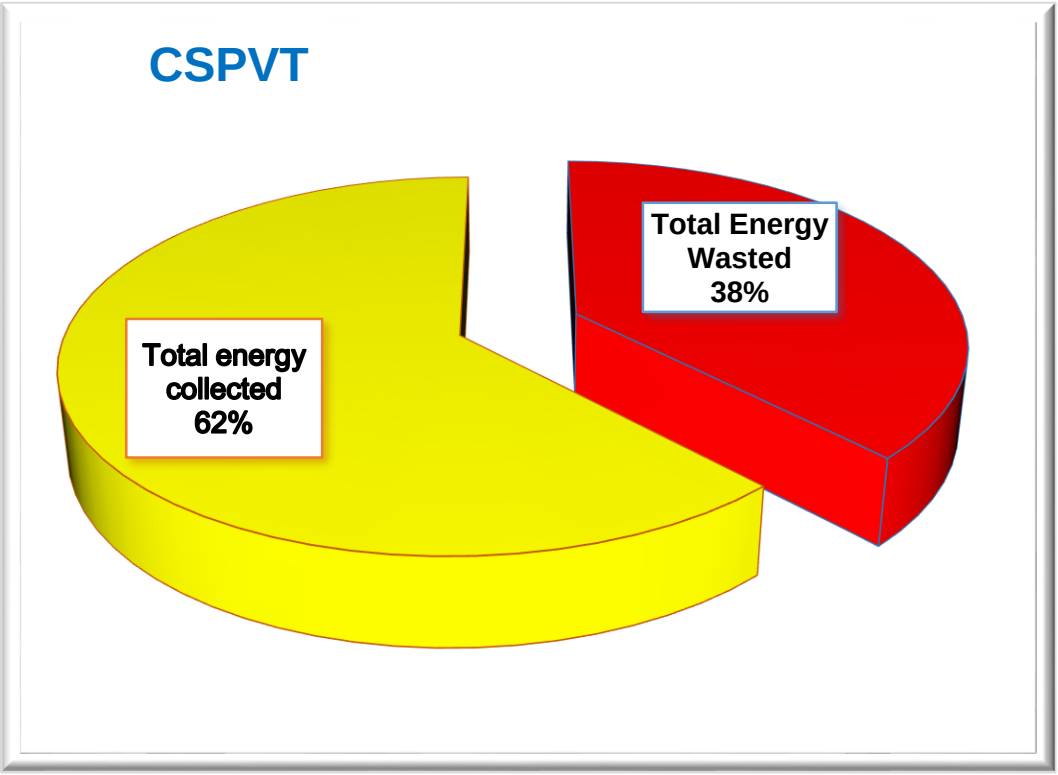

Figure 5-13: Performance of the CSPVT

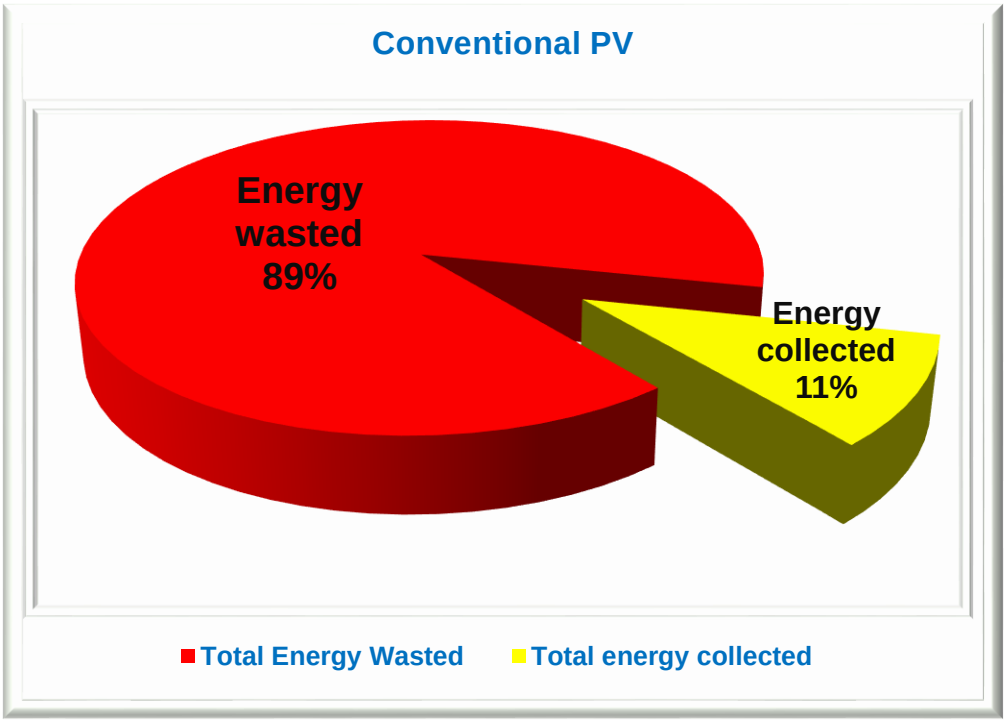

Figure 5-14: Performance of the conventional PV

5.5.3. **Thermal and electrical efficiency analysis**

The electrical performance of the panels is shown from Figures 5.15 to 5.17. For the CSPVT: the figures show the electrical, thermal and total efficiency; for the normal PV system, only the electrical efficiency is shown since there is no heat recovery. By taking a closer look at the graphs, we can deduce that solar panels' efficiency is proportional to solar radiation. As the radiation intensity fluctuates, so does the power of the panel and consequently its efficiency.

The average electrical efficiency of the CSPVT (during the experiments) was 13.17%, while for the PV was 9.63%. The lowest efficiency is noted between 7-9 am and afternoons from 4pm-7pm. The highest efficiency is noted at solar hour or when solar radiation reaches its maximum. However, in some cases this can be contradicted. As was mentioned earlier, PV's electrical efficiencies tend to drop with excessive heat. The more intense the sunshine is, the less likely is the panel to perform at its best due to overheating of the cells.

The electrical efficiency of the CSPVT was higher compared to the conventional PV during days 1 to 10 except for days 3 and 5 (11/09/18; 22/09/18), where its performance was quite similar to the other PV. During that period the CSPVT azimuth angle was constant and facing true north. That step was necessary to check its behaviour and performance when not tracking. Between 7am and 10am the sun's position is more inclined on the east side. Therefore, its electrical yield was lower than that of its counterpart. From 10h30, as the sun moved closer to the north facing the CSPVT perpendicularly, its electrical yield started to increase up until 2pm as displayed in Figure 5-11 (11/09/18) and figure 5-12 (22/09/18). As

the sun moved away from north heading west, again its efficiency began to drop to a value lower than the semi-fixed PV. This loss was caused by the reflective surface as it tends to shade the panel when no tracking is involved.

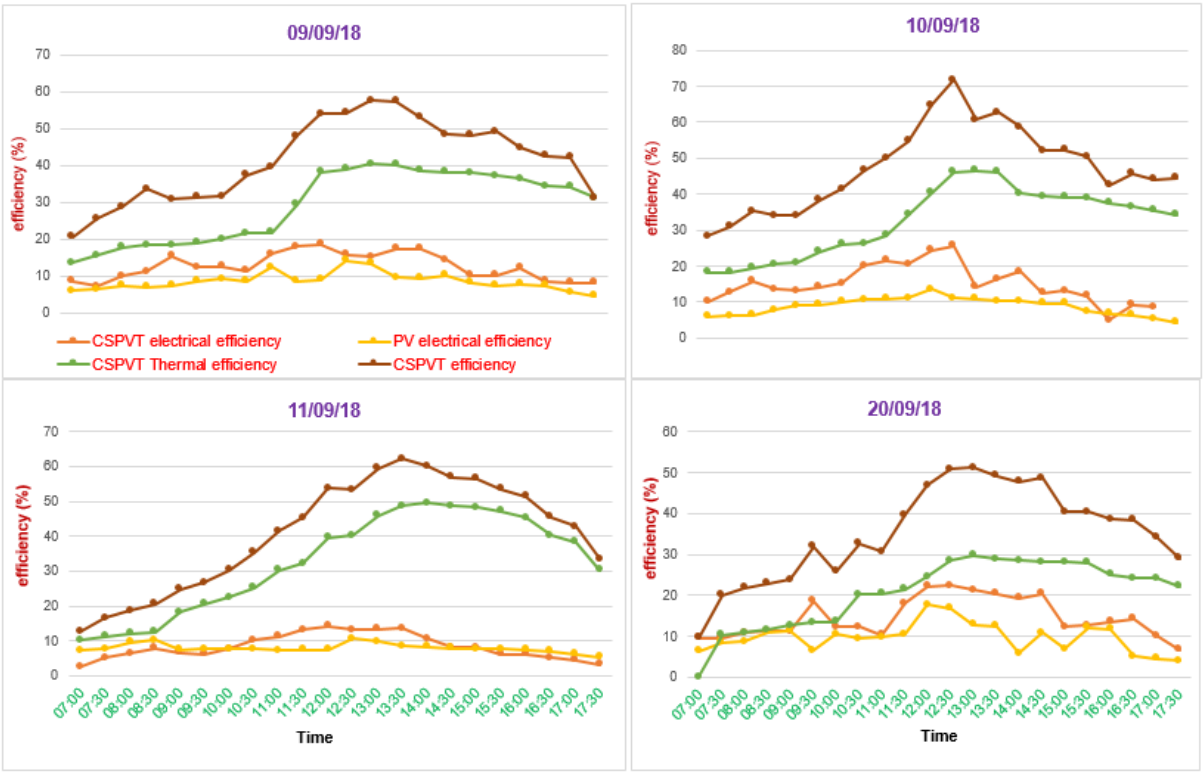

Figure 5-15: Daily graphical plot of the efficiencies recorded

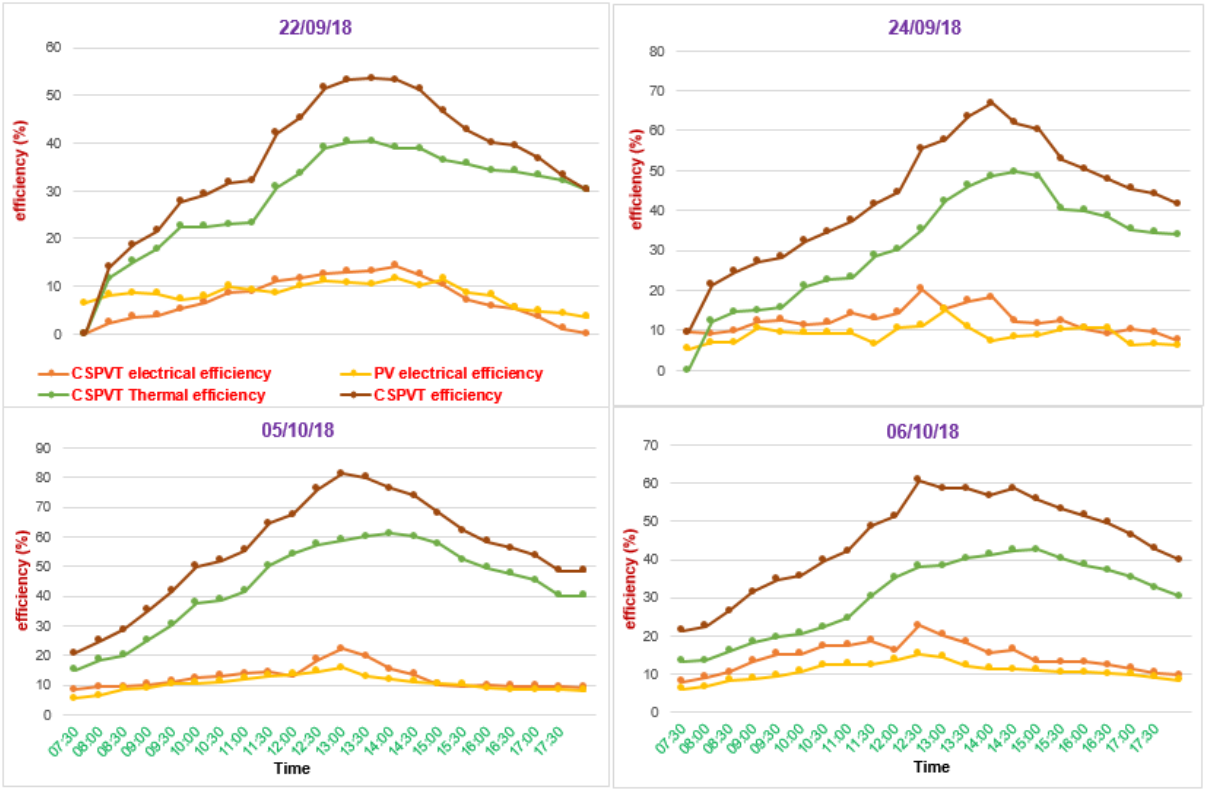

Figure 5-16: Daily graphical plot of the efficiencies recorded

The thermal efficiency curve shows a high potential of heat recovery from PV panels. The thermal efficiency was undoubtedly higher than the electrical efficiency throughout the experiments; ranging from zero to a maximum value of 61.20%. The maximum heat production is obtained between 11 am and 2 pm. Unlike electrical efficiency, thermal efficiency requires high temperature for best results. This can be noted on the 05/10/18 which was the hottest day. Hence the thermal efficiency on that day was higher compared to other days, with values as low as 15% and reaching over 60% efficiency at about 1pm and water temperature of 60°C as shown in figure 4-4.

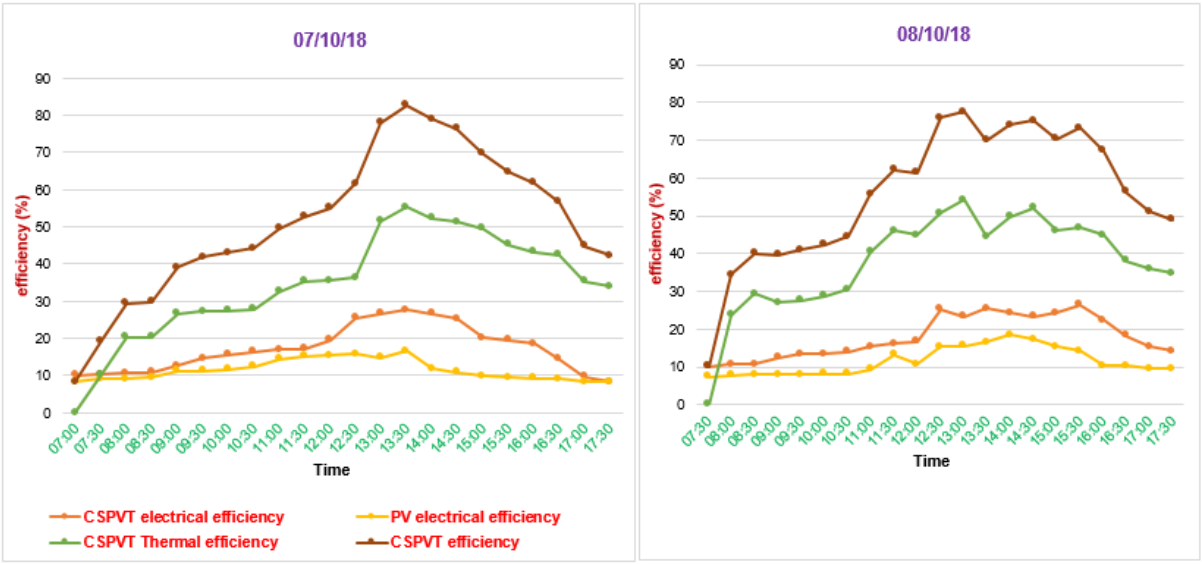

Figure 5-17: Daily graphical plot of the efficiencies computed

Although excessive heat is proved to be bad for the solar panel's efficiency, it is beneficial for thermal energy. For PV/T systems heat is needed so that more energy can be extracted. The thermal efficiency is dependent on the intensity of the solar radiation. Figure 5-18 shows the relationship between the solar radiation and thermal efficiency. Unlike electrical efficiency, thermal efficiency always increases with the increase in radiation and ambient temperature. Depending on the weather, thermal energy is usually low in the morning, then rises as we approach the solar peak hour. After 2 pm it starts to decrease slightly but not as fast as the electrical efficiency.

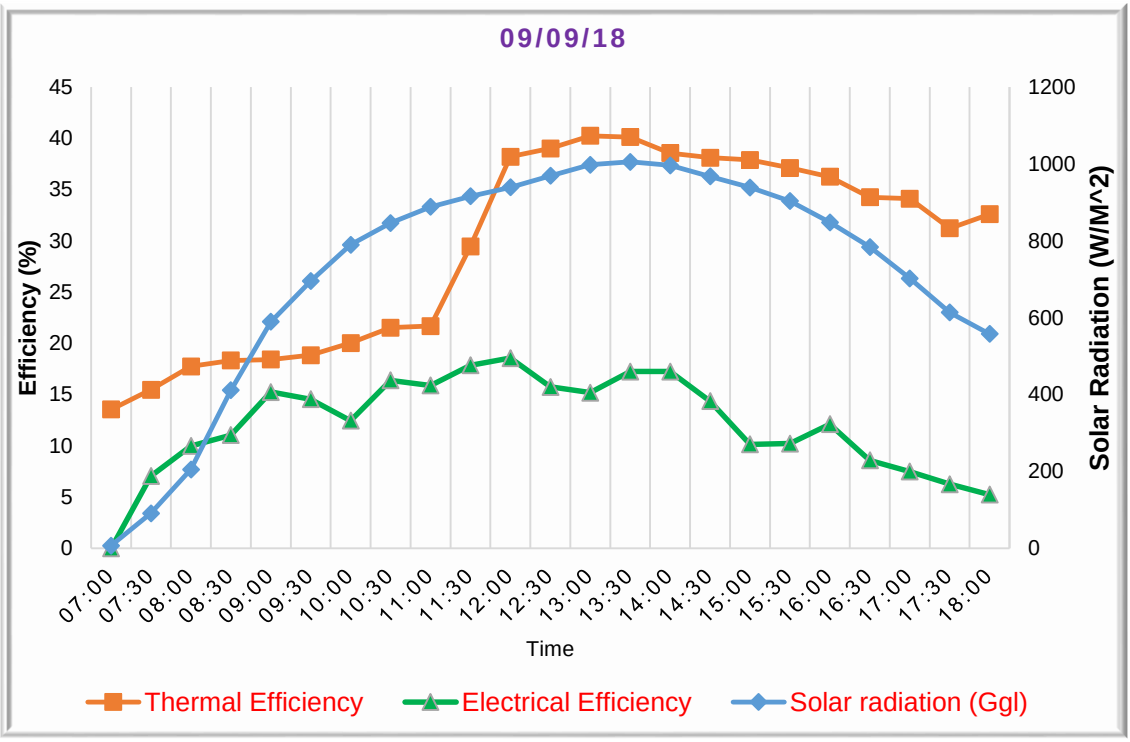

Figure 5-18: Representation of the relationship between solar radiation and thermal efficiency

5.5.4. **Effect of tilt angle, ß**

Section 4.3 indicated that the CSPVT was inclined at an angle of 25º whilst the conventional PV was at 30º slope. One may question this discrepancy. But is important to note that the CSPVT tilt angle was selected by a modification of Kanyarusoke's recommendation in Kanyarusoke et al., (2012). The optimum angle was altered to cater for the parabolic reflector dimensions and aperture angle ensuring the reflector did not shade the panel. Although the angles were not identical, the difference in terms of solar radiation onto the panels was negligible. Figure 5-19 represents the average solar energy reaching a PV module under two different angles, 25º and 30º. It can be seen that both panels get almost the same energy although at different angles.

The CSPVT was designed in such a way that all angles for both the panel and the reflector could be adjusted. However, while running the experiment not all desirable angles were attained. As we adjust the angle of the reflector, so should the panel's. It was noticed that for steeper angles (like 34°) the reflector was shading the panel. Hence, the maximum tilt angle for the CSPVT was 25°. However, this is only true for Cape Town. For other geographical locations the system might work efficiently at different slopes.

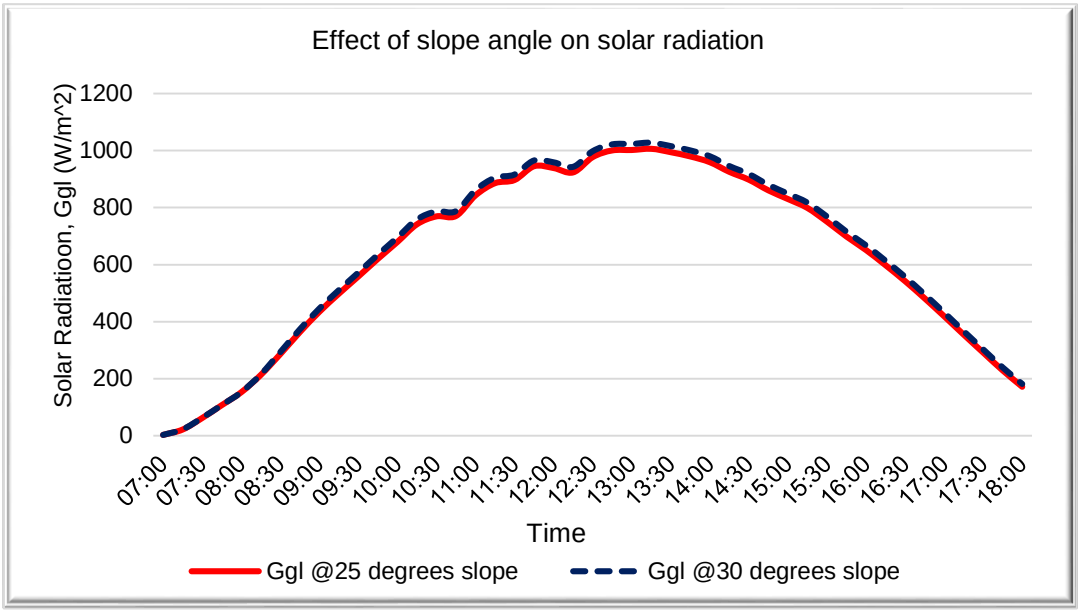

Figure 5-19: Effect of slope angle on solar radiation reaching the PV panel

Figure 5-20 and 5-21, illustrates how the tilt angle affects the solar radiation onto the panel. Different tilt angles were simulated using Matlab to estimate the amount of G_{gl} available on the panel for random days in winter and early days of spring. Solar radiation on panels inclined at 25º, 30º and 34º proves to be the best as it provides the highest radiation on the panel. It is crucial to note that, these values were validated for cape town only and should not be used to estimate the best slope for a different geographical location.

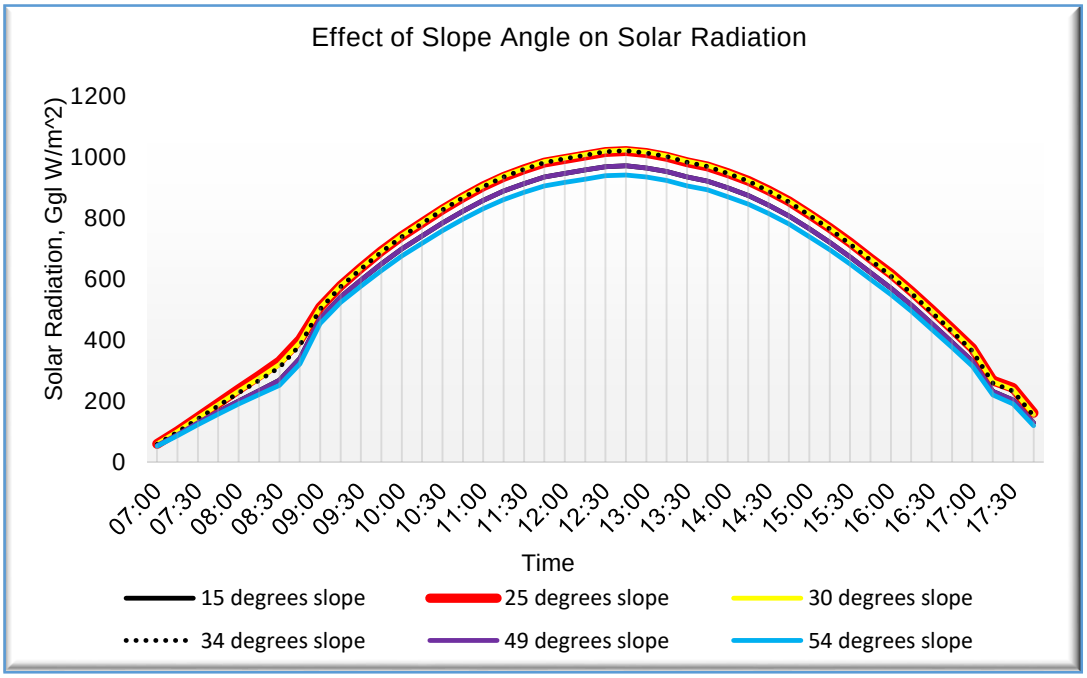

Figure 5-20: Effect of slope angle on solar radiation reaching the PV panel

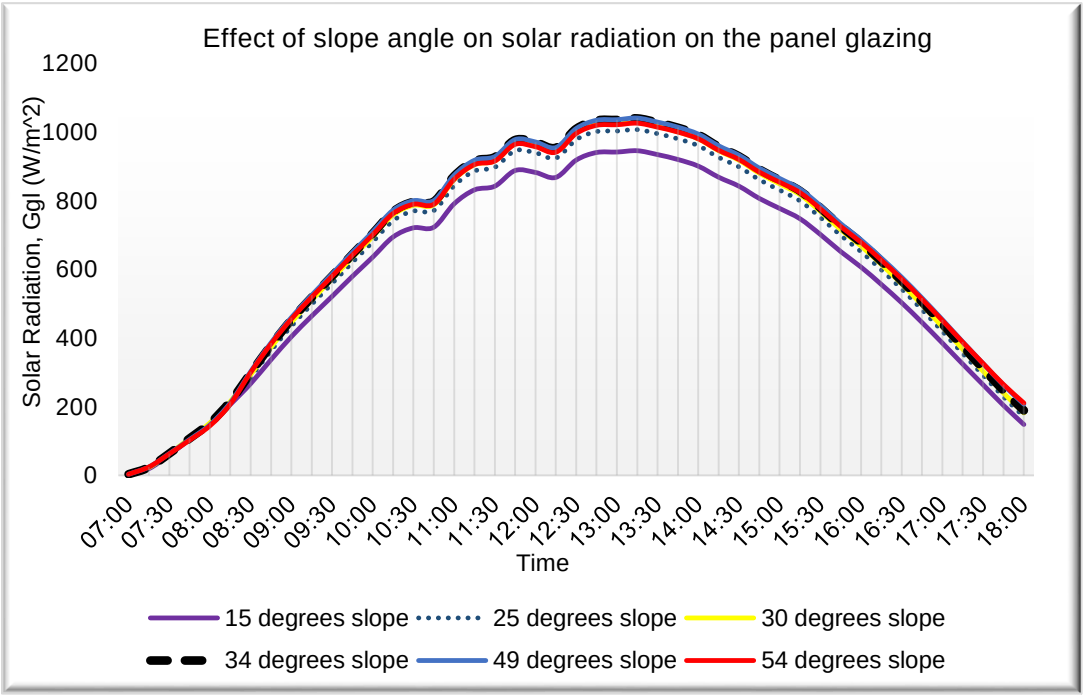

Figure 5-21: Effect of slope angle on solar radiation reaching the PV panel

5.5.5. **Effect of tracking**

As mentioned in chapter 2, tracking helps improve the efficiency of solar panels. That is possible because tracking increases the amount of solar radiation onto the panel as seen from figure 5-22. MATLAB simulations of two PV panels inclined at 25º is shown in the figure 5-23. One panel is tracking while the other one is fixed. It is clear that the one tracking gathers the most radiation. By calculating the average percentage increase from the data label, it will be detected that tracking increased the energy by at least 34.6%. This makes tracking worth it.

However, it is important to choose the best possible tracking method to use. There are many types of tracking, which sometimes may not be efficient in all cases. Figure 5-23 compares two categories of tracking: the seasonal tracking (where the panel changes position three times per day), and the hourly tracking (where the panel moves 15º every hour), which was used for this research. It is clear that tracking hourly is the better method.

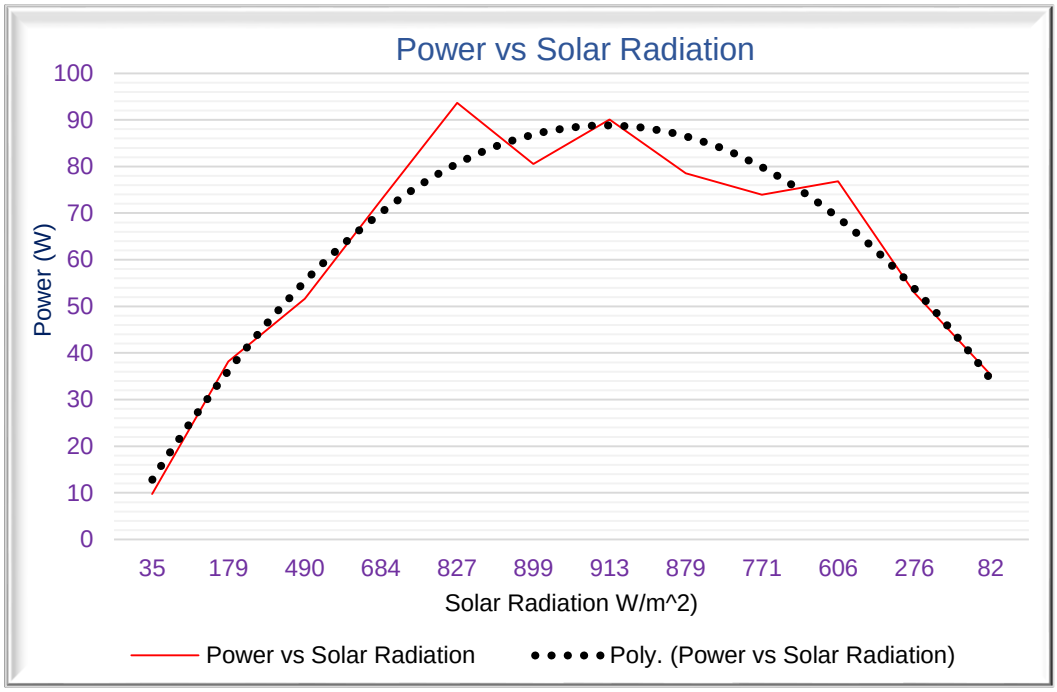

Figure 5-22: Effect of tracking on solar radiation reaching the panel

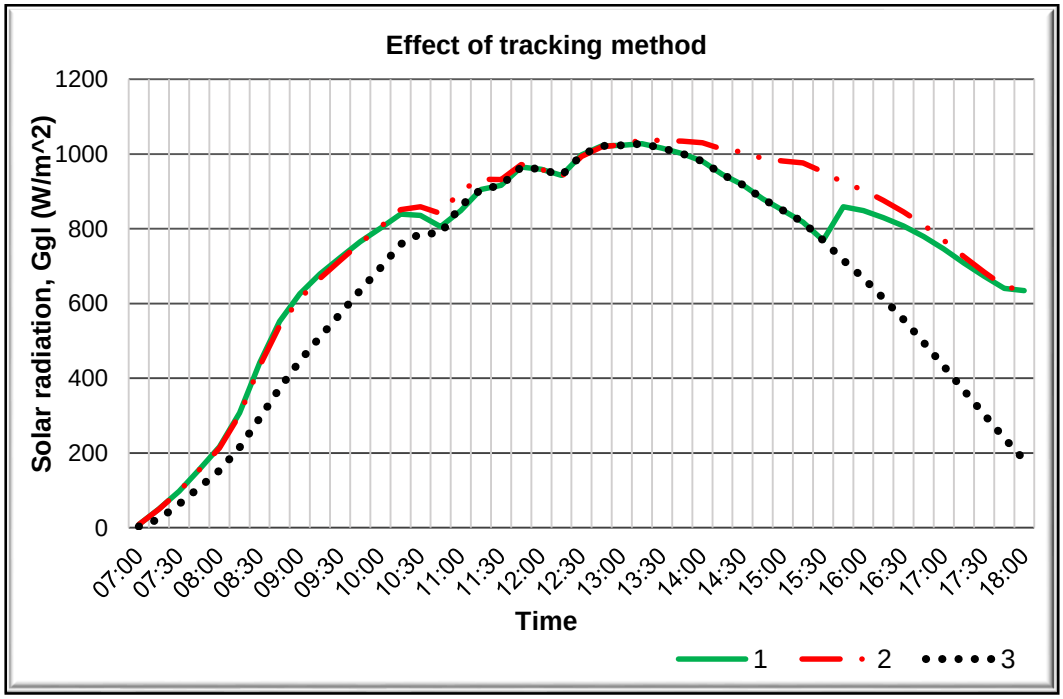

Figure 5-23: Effect of different tracking method on solar radiation. 1: Panel changes position three times daily (East-North-West). 2: Panel tracks hourly making 15° per step. 3: Panel is fixed

In figure 5-24, the electrical yields of a PV panel are presented. Two identical photovoltaic systems were modelled in TRNSYS to analyse the impact of tracking in solar systems. The panel have the same specifications as the one used for current experimental work, the 90Wp mono-crystalline silicon PV. From the same panel, two results were obtained: one when tracking and the other when fixed. Results revealed that tracking increased the efficiency of the same by at least 27%. If tracking can increase the efficiency by 27%, then one may ask: how much is added from cooling alone and concentrating. A study conducted by a Germany

solar industry PlusAmpere GmbH, showed an increase of 20% from concentration only (plusAmpere, 2019). In addition, section 5.1.4, showed that the CSPVT improved the efficiency of the PV by 60.1%. That being known, we can deduce that: if about 27% of the improvement comes from tracking, and 20% from concentration, then about 13% improvement is from cooling.

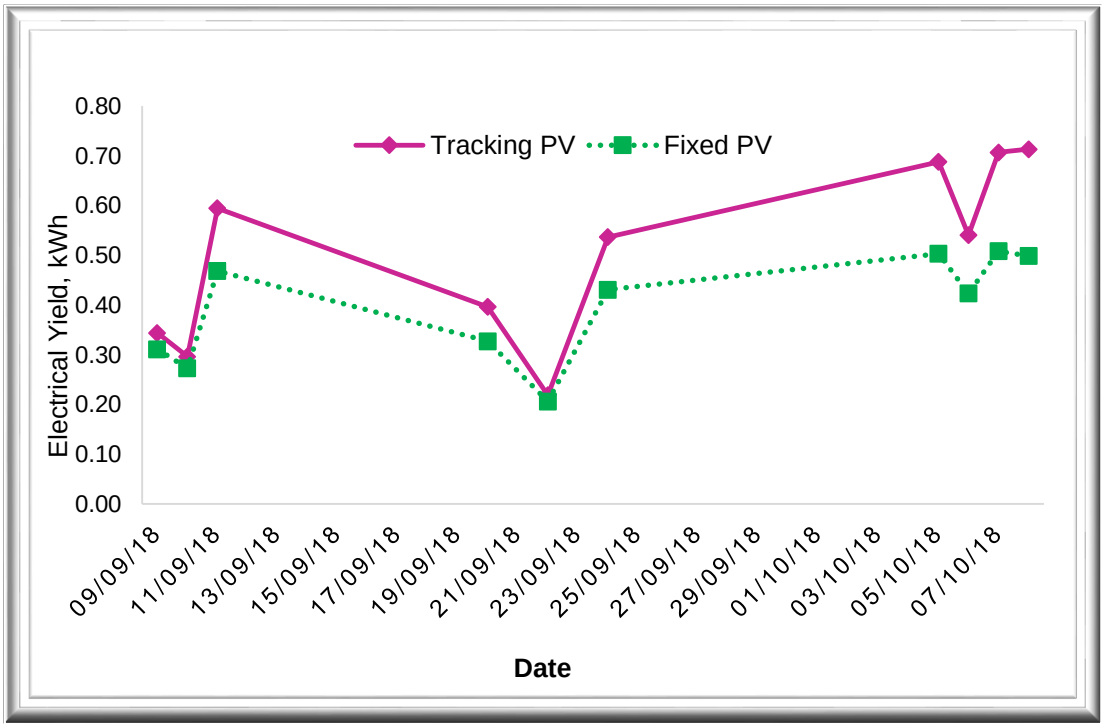

Figure 5-24: TRNSYS model for a tracking and non-tracking PV

5.5.6. **Effect of cooling**

Although we use water (in this research) as a heat recovery fluid, it is important to note that, the water is primarily meant to cool the panel's cells. Therefore, water should not steam up, evaporate or boil. That can be ensured by sizing the water tank bigger than the required or by using controls in case of industrial use.

In figure 5-25 is a representation of the temperature of the panels on 05/10/18. Under normal working conditions, the temperature of the CSPVT is expected to be higher than of the conventional PV due to the concentrating effect. However, because of cooling, its temperature was kept lower than of the conventional PV. When the ambient temperature was between 14ºC and 40.05ºC, the CSPVT temperature reached a maximum value of 46 ºC while the PV reached a max. of 59.8 ºC. This results were obtained with water cooling rate of 0.0015 kg/s. For a system using gravity to circulate the coolant, we cannot expect better results. The CSPVT outperformed in all aspects of this experimental work.

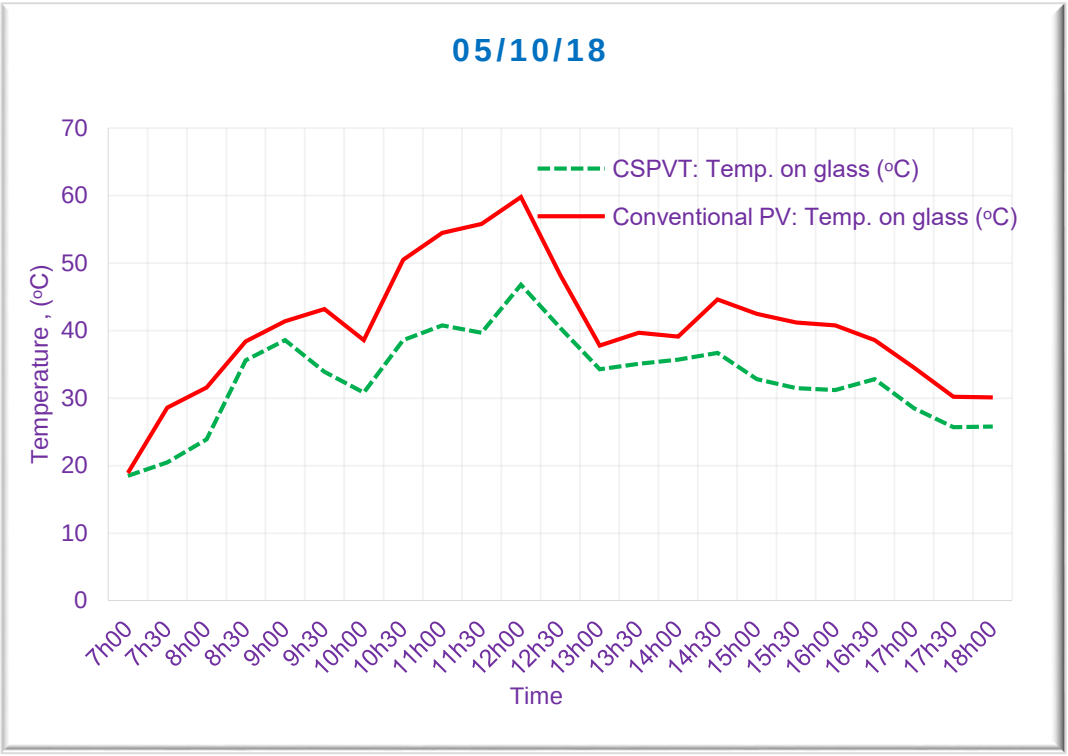

Figure 5-25: Effect of cooling

To estimate the amount of energy gained by cooling alone, TRNSYS simulation was used. Figure 5-26 and 5-27 show screenshots of results from the PV/T system and the PV panel respectively. Yearly results show electrical yield of 275.65 kWh and 248.5 kWh for the PV/T and PV respectively. These figures show an increase of approximately 11%.

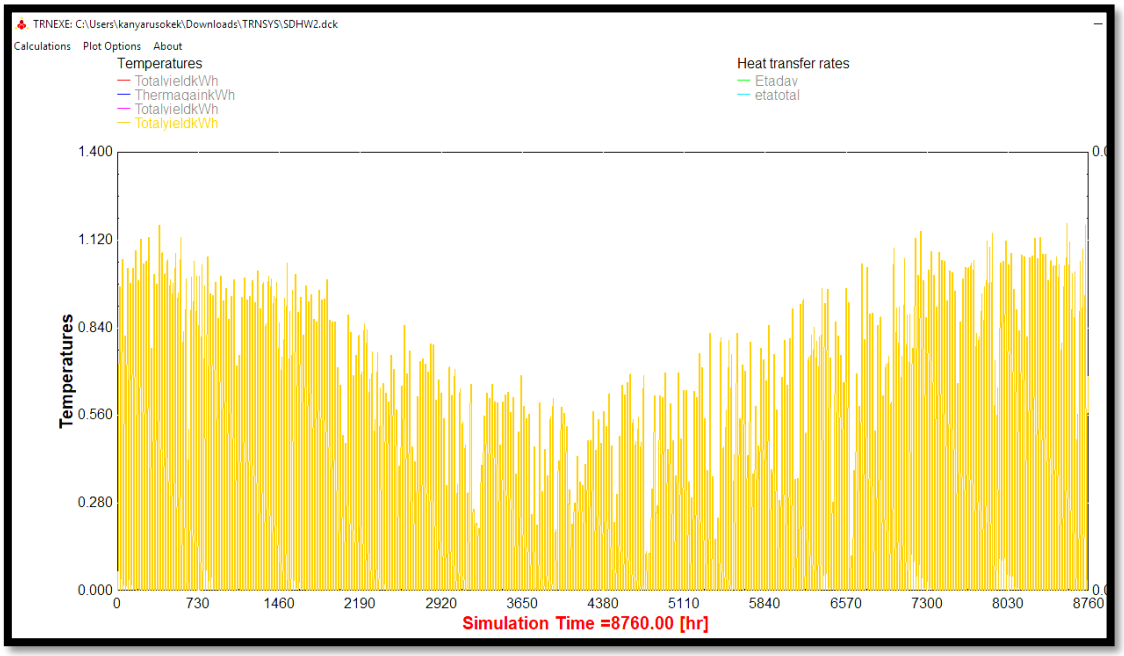

Figure 5-26: Screenshot of TRNSYS model results for a PV/T

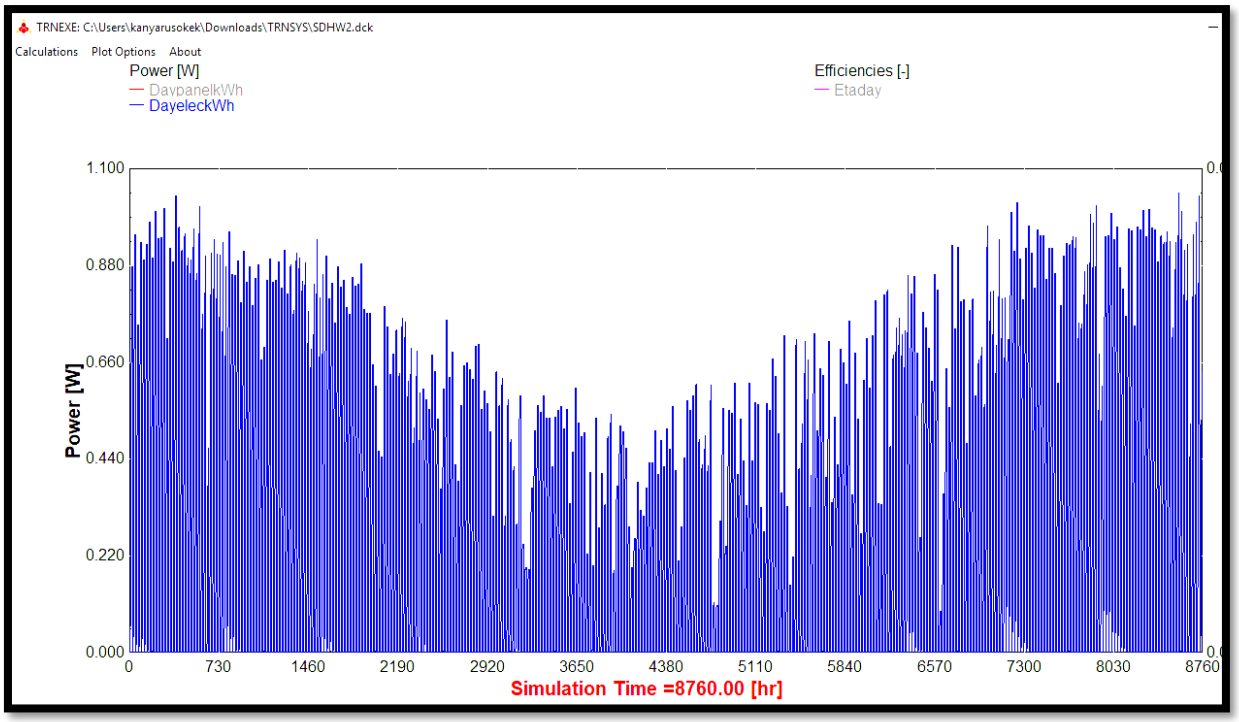

Figure 5-27: Screenshot of TRNSYS model results for a conventional PV

5.5.7. **Effect of weather, temperature**

As known, meteorological parameters do have an impact on the overall performance of PV panels. The weather and temperature do not stay constant throughout and nor does the performance of the panels. As the temperature fluctuates, the efficiency of the PV also does. Every season affects the energy production of solar panels. The CSPVT performs better on bright sunny days. Intermittent clouds and rain make the system ineffective.

It is also crucial to note that, although high temperature is good for the CSPVT, it might cause the cooling water to reach its boiling point, which is something that is not expected to happen. As CSPVT is designed to cool the PV panel and extract dissipated heat. So the cooling water should not reach temperatures above 70 º, else it will no longer cool the panel effectively.

5.5.8. **Effect of solar radiation**

The intensity of solar radiation falling on the panels depends on many factors: season, geographical location and the time. Consequently, solar radiation will have an effect on the output of the panel. The amount of energy generated from PV panels generally increases with the level of solar radiation it receives. Figure 5-28 is an example of how the power output is affected by the solar radiation. The dotted curve is the polynomial trend determined by EXCEL. As the radiation increases, so does the power. However, in some instances it can be noted that the power tends to decrease a bit. That is due to reasons discussed in this report. For example, over-heating of the cells.

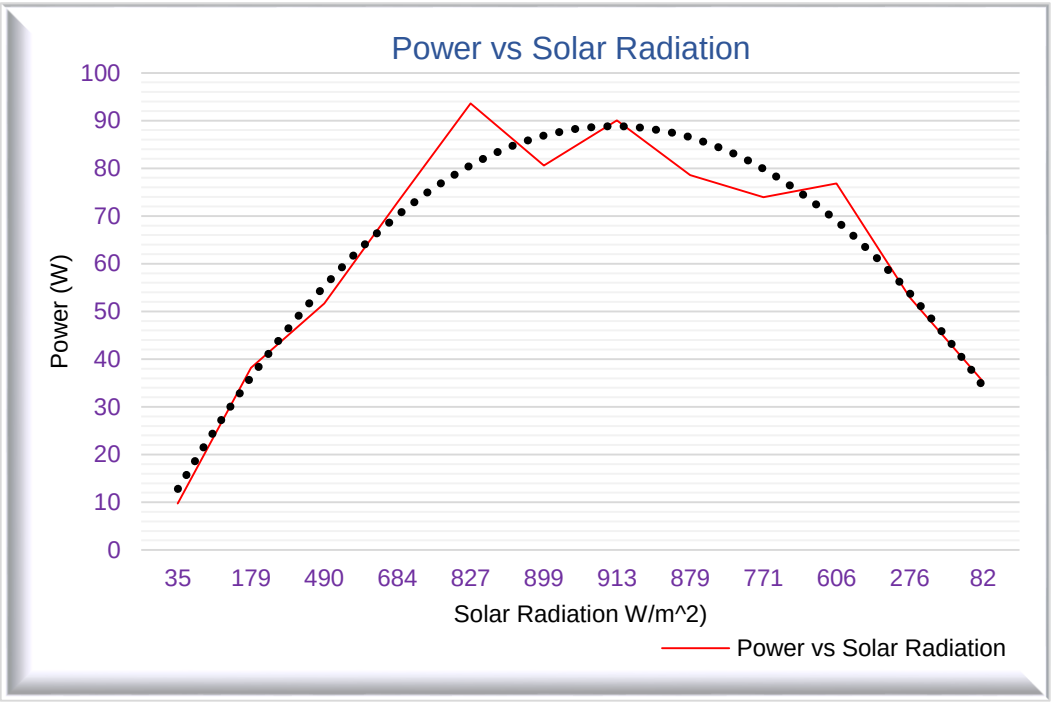

Figure 5-28: Variation of power with solar radiation

5.6. **Validation of actual results using TRNSYS simulation**

Transient system simulation program, shortened TRNSYS, is a simulation system used by engineers and researchers to model solar energy engineering systems. It is commonly used to simulate results for a period of one year. The software was used to validate the experimental performance of the CSPVT model under normal conditions. For more information on how the simulation studio work, please refer to a transient system simulation program volume 1 at (TRNSYS16, 2007).

The results obtained from the simulation are graphically represented in figures 5-29, 5-30 and table 5-1. There, one can see the expected electrical and thermal yield of the CSPVT for the 10 days. The predictable electrical yield was in the range of 0.66 kWh – 1.05 kWh. The thermal energy range was between 2 kWh and 4.12 kWh. The average predicted efficiencies were 18% and 70% for electrical and thermal respectively.

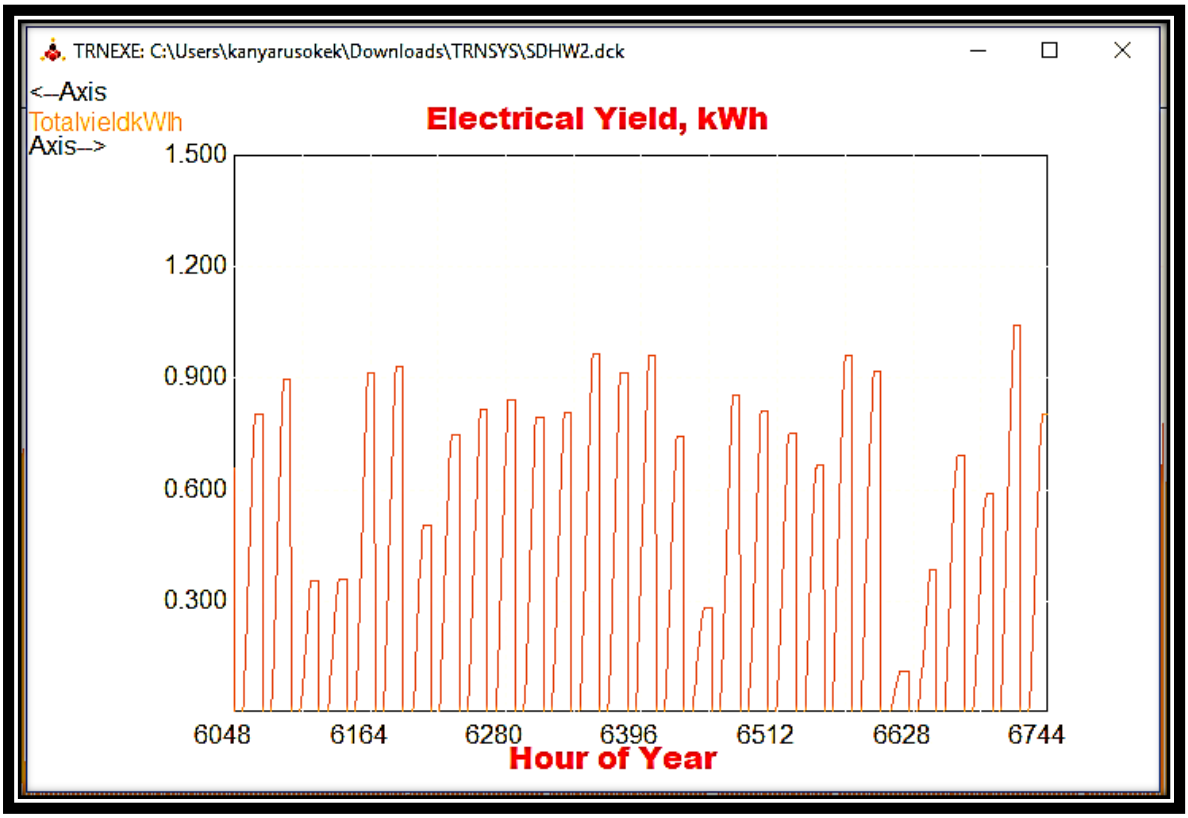

Figure 5-29: TRNSYS model results of the CSPVT

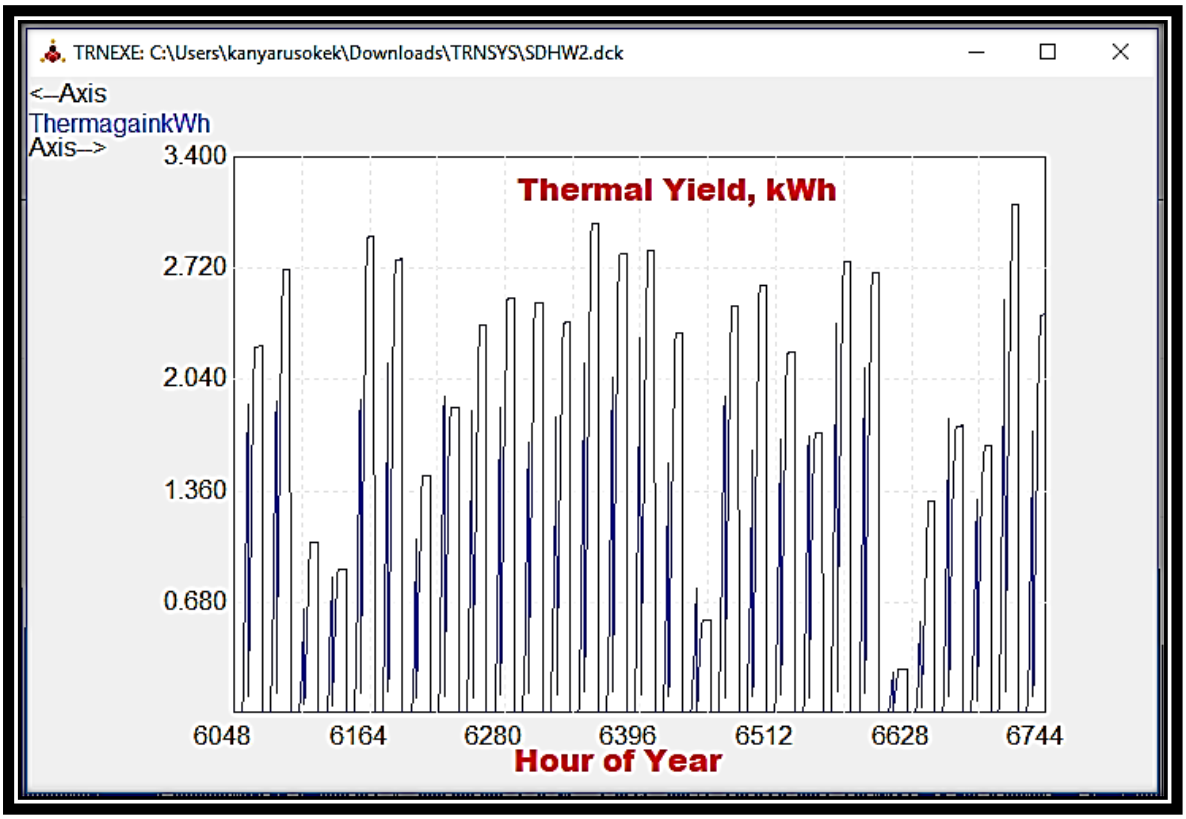

Figure 5-30: TRNSYS model results of the CSPVT

Table 5-1: Typical TRNSYS results

Hour of year	daypanelkWh	dayeleckWh	daythermalkWh	Eta-day	thermal ɳ
6048	3.57	0.66	2.403522182	0.18	0.75
6072	4.50	0.81	2.888282447	0.18	0.68
6096	5.04	0.90	3.392474431	0.18	0.72
6312	4.53	0.80	3.184818818	0.18	0.73
6360	5.58	0.97	3.868819846	0.17	0.71
6408	5.58	0.96	3.729078859	0.17	0.68
6672	3.88	0.69	2.366872643	0.18	0.63
6696	3.21	0.59	2.06926797	0.18	0.70
6720	6.13	1.05	4.118064052	0.17	0.68
6744	4.53	0.80	3.084026969	0.18	0.72

Figures 5-31 and 5-32 compare the experimental and TRNSYS results (theoretical). The experimental results obtained from days 1,2 and 7 (09/09/18; 10/09/18; 5/10/18) were similar to theoretical ones as depicted in figure 5-28, while others differ with a percentage error of 11.3. The thermal energy error between an experimental measured value and a theoretical actual value of the model was about 14%. TRNSYS reports a total of 31.1 kWh (111.98 MJ) of thermal gain. Nevertheless, the actual results show a total of 26.7kWh (96.3 MJ) of extracted heat. In overall, the model predicts 39.34 kWh (141.62 MJ) of energy collected (thermal plus electrical). That is about 82% overall efficiency. Compared to the actual value of 34.8 kWh (125.6 MJ) from the CSPVT prototype. Appendix A3 presents TRNSYS sourced files of the results discussed here.

The discrepancy seen between the two results might have been caused by the following factors:

1. TRNSYS uses a typical meteorological year data to estimate the performance of the model. While the prototype was analysed under real weather conditions of Cape Town, South Africa.

2. TRNSYS assumes no experimental error such as: leakages. The thermal yield can be affected by the quality and accuracy of the PV/T design and manufacturing.

3. TRNSYS uses MPPT which are high performance charge controllers. Due to unavailability, during experiments the MPPT was not used. Hence the results of the model were higher than of the prototype.

4. Construction errors. A more accurate model would give best results.

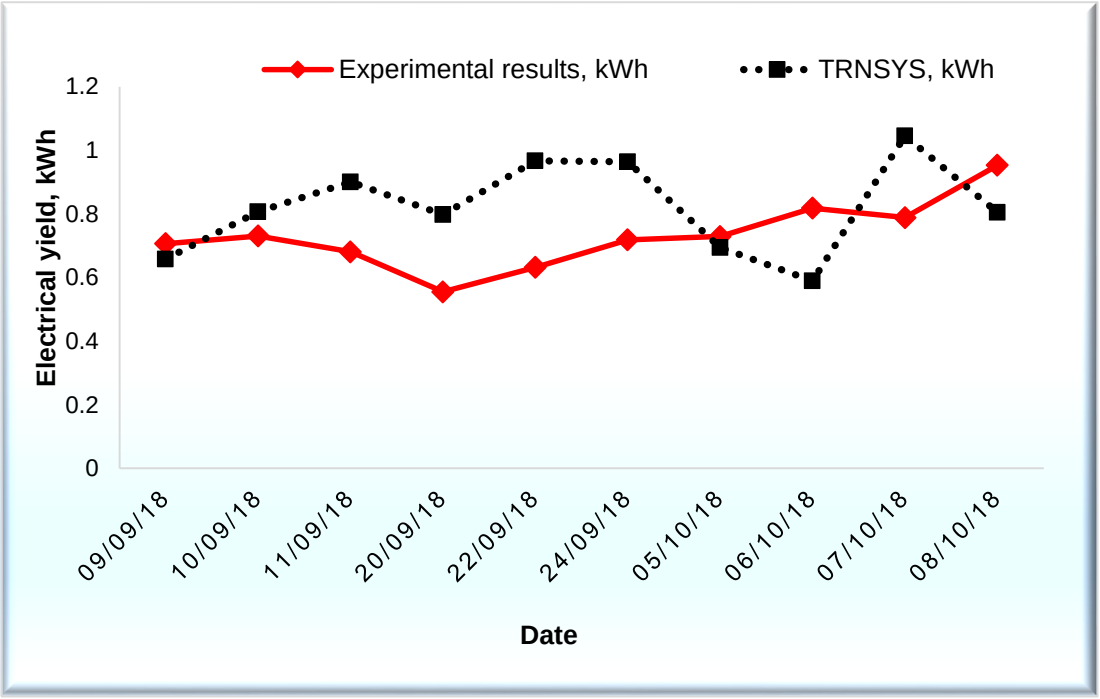

Figure 5-31: TRNSYS and experimental results compared

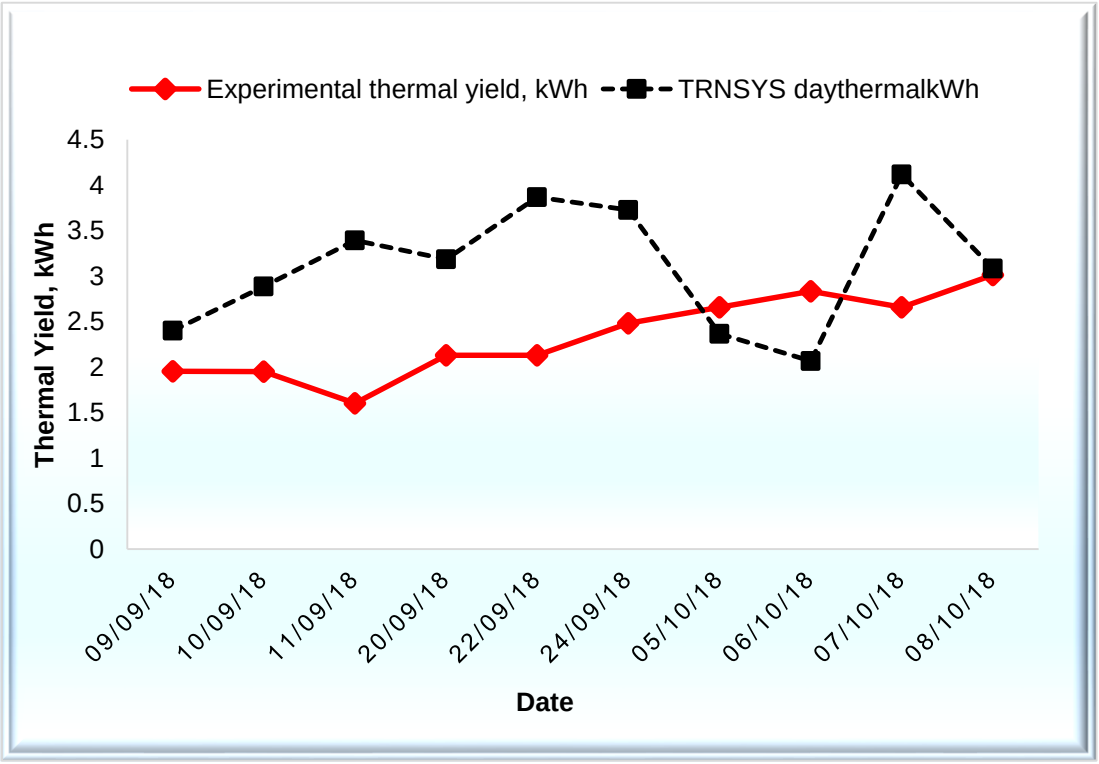

Figure 5-32: TRNSYS and experimental results compared

5.7. **CSPVT potential and economic analysis**

By generating both electricity and thermal energy, concentrated solar photovoltaic thermal system (CSPVT) offer higher overall efficiency compared to PV/T or CPV systems. From the same receiving surface, one can produce both electricity and heat which is not the case with the normal PVs. Under one single system, we were able to concentrate, cool and track. The

heat production was the biggest advantage of this system. The system can be used to heat or pre-heat water for domestic use. CSPVTs can be economically viable depending on the geographical location. Africa being known as a sunny continent, receiving a lot of radiation each year, as depicted in figure 5-33, one can see the big potential of this system. Looking at cost, currently in South Africa, a 100Wp multi-crystalline PV panel costs around $100 (Sustainable.co.za, 2019). According to Kanyarusoke, (2019) 1m^2 solar collector costs about $255. For a single home to have both systems it will require at least $355. This amount can be saved by using a CSPVT or a PVT, which according to costs in this project, means spending $150-$180 for water and electricity generation. There is an additional benefit of space saving.

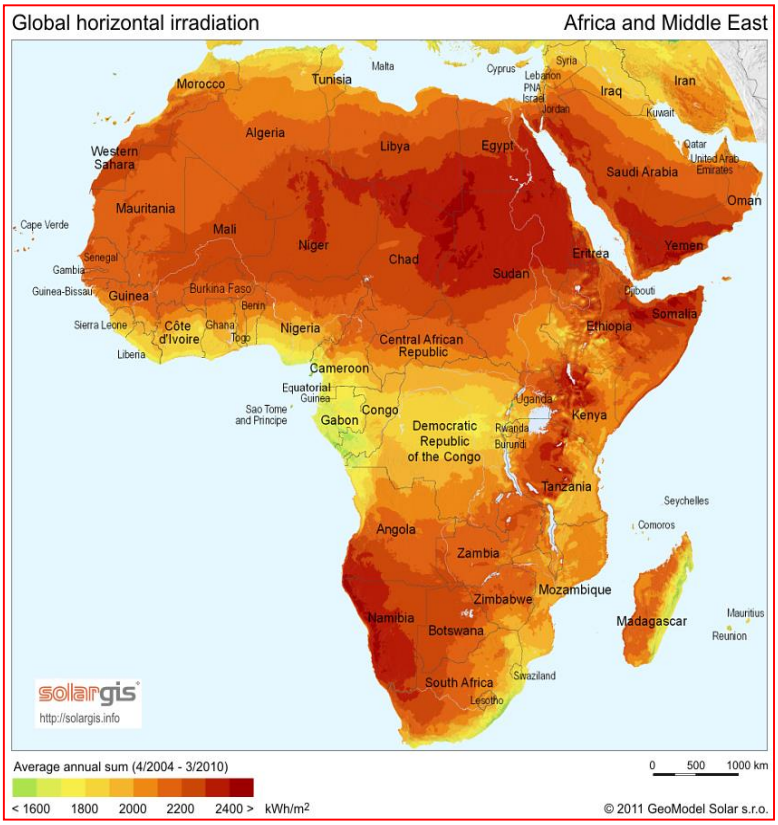

Figure 5-33: Africa solar insulation map

Image source: https://www.hotspotenergy.com/DC-air-conditioner/solar-map-africa-middle-east.php

5.8. **Summary**

Experimental results from the analysis of the CSPVT system have been presented in this chapter. An evaluation between the performance of a normal PV system and the CSPVT has been scrutinised. Results obtained by experiments were validated using TRNSYS simulation engine. It has been shown that the CSPVT has a great potential in terms of increasing energy production from existing PV panels. Their efficiencies are much higher than those of normal PV units. The proceeding chapter concludes this dissertation by highlighting its most important aspects.

CHAPTER SIX
CONCLUSION AND RECOMMEDANTIONS

6.1. **Conclusions**

This research work has introduced a new design, the concentrated solar and photovoltaic thermal cooled system (CSPVT). The system is aimed to improve the energy yield from solar panels and consequently its efficiency. To evaluate the performance of the design, two systems were tested simultaneously: the conventional PV and the CSPVT. By doing so, we could actually analyse how much energy is wasted from the conventional PV panels and how it can be recovered efficiently while improving its output. From the results obtained the following was concluded:

6.1.1. **Application of parabolic reflector**

Reflective surfaces or simply reflectors, can help increase overall efficiency between 14-22%. Good quality concentrators can significantly increase the amount of energy received and converted to useful forms. The more radiation the panel receives, the more the energy that can be generated and collected if additional actions are made on the system. However, reflectors are more efficient on sunny days. During cloudy and rainy days', they are not useful as they are meant to focus beam radiation on the panel. In addition, it is critical to design parabolic concentrated PV adequately, as failure to do so may cause the reflector to shade the panel at some point instead of focusing the energy. CSPVTs require tracking systems to ensure it is receiving beam radiation at all times and that its reflected light always intercepts the panel.

Conversely, it was similarly noticed from the experiments that the application of reflectors does not always increase the efficiency of solar panels. For locations with high solar radiation and temperature, unless additional mechanisms are implemented on the system, the concentrator can actually lead to a decrease of efficiency of the panel, instead of improving it.

6.1.2. **Water cooling system**

Water cooling can improve efficiencies by ≈11%. The results obtained show that the efficiency of the CSPVT decreases with the increase of temperature. Therefore, water cooling should never be neglected. Concentrating reflectors can boost the energy output from the panel by a significant factor when combined with cooling. As seen in chap.5, a lot of thermal energy can be harvested when cooling is used. During hot sunny days it is vital to have a pump in the system to increase the flow rate of water as the heat removal rate of the coolant circulating in the system by gravity may be too low. It is also important to ensure that no internal or external leakages are present in the system. Leakages can decrease the

efficiency of the panel and damage the cells if internal. In addition, a proper insulation system is required on the water pipes and the water reservoir, so that heat loss due to conduction is minimised.
Most importantly, it is crucial to note that, the CSPVT is not meant to boil water. Water going through the system should never reach its boiling point. A proper control system is required to ensure the water temperature never goes beyond 60ºC.

6.1.3. **Solar tracking**

Tracking can increase efficiencies between 30-34%. A solar tracking mechanism is essential for solar systems using reflectors. It helps prevent shading, increases the amount of radiation incident onto the panels, and consequently boosts the useful energy generated by the panels. However, solar tracking can be expensive and for some systems, regular maintenance is required.

6.1.4. **Total energy gain**

Yearly results from TRNSYS show a total energy gain of ± 420,6 % over the conventional PV. The ten days' experimental results show gains of approximately 500%.

6.1.5. **Tilt angle, β**

Tilt angle is crucial for optimum energy output of all solar energy systems. Solar irradiance can be maximized or minimized depending on the azimuth and slope (ß) angles. For tracking systems inclined at an optimum variable angle ß, the irradiance is higher as they face the sun at all times throughout the day.

6.2. **Recommendations**

Throughout this research work a lot was encountered. During and after the design, construction and experimental work several issues were noticed. As a result, the following is recommended for future work and research:

1. When constructing the PV/T, it is recommended to weld the chosen system instead of using a high temperature adhesive as in this project. This would ensure longevity and minimise risks of accidental leakages. For this project, PVC piping rated 140F was used. However, for locations where the system is likely to heat-up the water above the rated temperature, it is recommended to use other type of piping material such has CPVC rated at 200F, although it is not recommended to allow the water in the PVT reach temperatures above 60ºC.

2. Using a pump on the system is highly recommended. The pump will increase water circulation and will prevent the water in the system from over-heating.

3. To reduce cost, the tracking mechanism can be manual, with between 3 and 6 daily step changes instead of 12. This would eliminate the battery power supply system and its associated electronics.

REFERENCES

Akindele, O. & Adejumobi, O. 2017. Domestic Electric Power Generator Usage and Residents Livability Milieu in Ogbomoso, Nigeria. *Environmental Management and Sustainable Development*, 6(1): 91–104.

Alexandru, C. & Pozna, C. 2010. Simulation of a dual-axis solar tracker for improving the performance of a photovoltaic panel. *Proceedings of the Institution of Mechanical Engineers, Part A: Journal of Power and Energy*, 224(6): 797–811. https://www.researchgate.net/publication/235770378_Simulation_of_a_dual-axis_solar_tracker_for_improving_the_performance_of_a_photovoltaic_panel.

Alkhalidi, A. & Hussain Al Dulaimi, N. 2018. *Design of an Off-Grid Solar PV System for a Rural Shelter*. German Jordanian University. https://www.researchgate.net/publication/322738988_Design_of_an_Off-Grid_Solar_PV_System_for_a_Rural_Shelter.

Allan, J. 2015. *The Development and Characterisation of Enhanced Hybrid Solar Photovoltaic Thermal Systems*. Brunel University. https://pdfs.semanticscholar.org/66da/bc0d452cdd99aa84578c3c9391e84962fcab.pdf 21 December 2018.

Andrews, R. 2015. Photovoltaic system performance enhancement : Validated modeling methodologies for the improvement of PV system design by. , (June).

Askari, M., Mirhabibi, M. & Abadi, V. 2015. Types of Solar Cells and Application. *American Journal of Optics and Photonics*, 3(5): 94–113. https://www.researchgate.net/publication/281148723_Types_of_Solar_Cells_and_Application.

Assembe, C.O. 2016. *Integrated solar photovoltaic and thermal system for enhanced energy efficiency*. Cape Peninsula University of Technology. http://etd.cput.ac.za/handle/20.500.11838/2387.

Assembe, O. & Kanyarusoke, K. 2016. Integrated Solar Photovoltaic And Thermal System For Enhanced Energy Efficiency. In *LeNS Conference*. Cape Town: 273–282.

Azarian, R.D., Cuce, E. & Cuce, P.M. 2017. An Overview of Concentrating Photovoltaic Thermal (CPVT) Collectors. *Energy Research Journal*, 8(1): 18. http://thescipub.com/pdf/10.3844/erjsp.2017.11.21 4 June 2018.

Baig, H., Siviter, J., Li, W., Paul, M.C., Montecucco, A., Rolley, M.H., Sweet, T.K.N., Gao, M., Mullen, P.A., Fernandez, E.F., Han, G., Gregory, D.H., Knox, A.R. & Mallick, T. 2018. Conceptual design and performance evaluation of a hybrid concentrating photovoltaic system in preparation for energy. *Energy*, 147: 547–560. https://linkinghub.elsevier.com/retrieve/pii/S0360544217321709 21 December 2018.

Barrett, A. 2017. Solar PV-T systems - what are the pros and cons? | YouGen Blog | YouGen, Renewable Energy Made Easy. *YouGen*. http://www.yougen.co.uk/blog-entry/2833/Solar+PV-T+systems+-

+what+are+the+pros+and+cons%273F/ 16 June 2019.

Bhattarai, S., Oh, J.-H., Euh, S.-H., Kafle, K. & Kim, H. 2012. Simulation and model validation of sheet and tube type photovoltaic thermal solar system and conventional solar collecting system in transient states. *Solar Energy Materials and Solar Cells*, 103: 184–193. http://dx.doi.org/10.1016/j.solmat.2012.04.017 21 December 2018.

Bilal, M., Naeem Arbab, M., Zain Ul Abideen Afridi, M. & Khattak, A. 2016. Increasing the Output Power and Efficiency of Solar Panel by Using Concentrator Photovoltaics (CPV). *International Journal of Engineering Works Kambohwell Publisher Enterprises ISSN*, 3(12): 2409–2770. https://hal.archives-ouvertes.fr/hal-01430790/document 5 June 2018.

Blakers, A., Zin, N., McIntosh, K.R. & Fong, K. 2013. High Efficiency Silicon Solar Cells. *Energy Procedia*, 33: 1. https://www.sciencedirect.com/science/article/pii/S187661021300043X 10 June 2018.

Ceylan, I., Etem Gü Rel B,⇑, A., Ergü, A. & Tabak, A. 2016. Performance analysis of a concentrated photovoltaic and thermal system. *Solar Energy*, 129: 217–223. http://dx.doi.org/10.1016/j.solener.2016.02.010 21 December 2018.

Charfi, W., Chaabane, M., Mhiri, H. & Bournot, P. 2018. Performance evaluation of a solar photovoltaic system. *Energy Reports*, 4: 400–406. https://doi.org/10.1016/j.egyr.2018.06.004.

Chow, T. 2007. *Hybrid solar technology: a way to maximise the use of captured solar radiation*. Delhi. http://www6.cityu.edu.hk/bst/BEET/BEET_files/Research/Hybrid_photovoltaic.pdf 21 December 2018.

Cozzi, L., Chen, O., daly, H. & Koh, A. 2018. Population without access to electricity falls below 1 billion. *IEA*. https://www.iea.org/newsroom/news/2018/october/population-without-access-to-electricity-falls-below-1-billion.html 13 June 2019.

Daneshazarian, R., Cuce, E., Cuce, P.M. & Sher, F. 2018. Concentrating photovoltaic thermal (CPVT) collectors and systems: Theory, performance assessment and applications. *Renewable and Sustainable Energy Reviews*, 81: 473–492. https://linkinghub.elsevier.com/retrieve/pii/S1364032117311619 7 December 2018.

Darling, D. 2016. Archimedes and the burning mirrors. http://www.daviddarling.info/encyclopedia/A/Archimedes_and_the_burning_mirrors.html 3 June 2018.

Das, D., Kalita, P. & Roy, O. 2018. Flat plate hybrid photovoltaic- thermal (PV/T) system: A review on design and development. *Renewable and Sustainable Energy Reviews*, 84: 111–130. https://linkinghub.elsevier.com/retrieve/pii/S1364032118300029 5 December 2018.

Dash, P.K. & Gupta, N.C. 2015. Effect of Temperature on Power Output from

Different Commercially available Photovoltaic Modules. *Journal of Engineering Research and Applications www.ijera.com*, 5(1): 148–151. https://www.ijera.com/papers/Vol5_issue1/Part - 1/R50101148151.pdf 21 December 2018.

Dobrnjac, M., Zivkovic, P. & Babic, V. 2017. The possibility of developing hybrid PV/T solar system. http://iopscience.iop.org/article/10.1088/1757-899X/200/1/012040/pdf 23 November 2018.

Dricus. 2015. Solar Concentrators: what are the different technologies? - Sinovoltaics - Your Solar Supply Network. *24 July*. https://sinovoltaics.com/learning-center/technologies/solar-concentrators-different-technologies/ 21 December 2018.

Duffie, J. & Beckman, W. 2013. *Solar Engineering of Thermal Processes, 4th ed.* 4 Edition. New Jersey: John Wiley & Sons.

Dupeyrat, P., Mé Né Zo, C., Wirth, H. & Rommel, M. 2011. Improvement of PV module optical properties for PV-thermal hybrid collector application. *Solar Energy Materials and Solar Cells*, 95: 2028–2036. https://www.sciencedirect.com/science/article/pii/S0927024811002510 21 December 2018.

EMworks. 2018. Stepper Motor. https://www.emworks.com/application/stepper-motor 22 December 2018.

Farret, F.A. & Simões, M.G. 2006. *Integration of alternative sources of energy*. New Jersey: IEEE Press. https://www.wiley.com/en-us/Integration+of+Alternative+Sources+of+Energy-p-9780471712329 11 June 2018.

Fenner. Section 2: Chain Drives. www.fptgroup.com 18 February 2019.

Green Rhino Energy. 2016. Concentrated Solar Thermal | Technologies. http://www.greenrhinoenergy.com/solar/technologies/cst_technologies.php 11 June 2018.

Handoyo, E.A. & Ichsani, D. 2013. International Conference on Sustainable Energy Engineering and Application The optimal tilt angle of a solar collector. *Physics Procedia*, 32: 166–175. https://www.researchgate.net/publication/256981847_The_Optimal_Tilt_Angle_of_a_Solar_Collector 21 December 2018.

Javed, A. 2014. The Effect of Temperatures on the Silicon Solar Cell. *International Journal of Emerging Technologies in Computational and Applied Sciences (IJETCAS)*, 9: 305–308. https://www.researchgate.net/publication/283644148_The_Effect_of_Temperatures_on_the_Silicon_Solar_Cell.

Kanyarusoke, K. 2019. Problems of engineering entrepreneurship in Africa: A design optimization example in solar thermal engineering. *Engineering Science and Technology, an International Journal*, (xxxx). https://doi.org/10.1016/j.jestch.2019.05.002.

Kanyarusoke, K.E. 2017. NOVEL APPROACHES TO IMPROVING DOMESTIC SOLAR PANEL ENERGY YIELDS IN SUB-SAHARA AFRICA Thesis submitted in fulfilment of the requirements for the degree. http://etd.cput.ac.za/bitstream/handle/20.500.11838/2520/209230681-Kanyarusoke-Kant Eliab-D.Eng-Mechanical-Engineering-Eng-2017.pdf?sequence=1&isAllowed=y 13 June 2018.

Kanyarusoke, K.E., Gryzagoridis, J. & Oliver, G. 2012. Annual Energy Yields Prediction From Manufacturers ' P hotovoltaic Panel Specifications For Sub Sahara Africa. In 1–25.

Kanyarusoke, K.E., Gryzagoridis, J. & Oliver, G. 2016. Re-mapping sub-Sahara Africa for equipment selection to photo electrify energy poor homes. *Applied Energy*, 175: 240–250. http://dx.doi.org/10.1016/j.apenergy.2016.05.021.

Kaya, M. 2013. *Thermal and Electrical Performance Evaluation of PV/T Collectors in UAE*. http://www.diva-portal.org/smash/get/diva2:621183/FULLTEXT01.pdf&sa=U&ei=PIFiU9aOHenP2wXXiIDYDA&ved=0CDcQFjAG&usg=AFQjCNF_XVLENVJ3ucsqOyrE98fGpOys1w 6 December 2018.

Khumalo, K. 2019. Pessimism over Eskom grows | IOL Business Report. *iol*. https://www.iol.co.za/business-report/energy/pessimism-over-eskom-grows-21162627 13 June 2019.

Kramer, S.C., Gritzki, R., Perschk, A., Rösler, M. & Felsmann, C. 2015. Fully parallel, OpenGL-based computation of obstructed area-to-area view factors. *Journal of Building Performance Simulation*, 8(4): 266–281. https://www.researchgate.net/publication/271904452_Fully_parallel_OpenGL-based_computation_of_obstructed_area-to-area_view_factors 3 March 2019.

Kumar, A., Baredar, P. & Qureshi, U. 2015. Historical and recent development of photovoltaic thermal (PVT) technologies. *Renewable and Sustainable Energy Reviews*, 42: 1428–1436. https://ac.els-cdn.com/S1364032114009757/1-s2.0-S1364032114009757-main.pdf?_tid=bf4a560a-5115-45d9-b7fa-2894e6488003&acdnat=1545349696_49c6dac6600b0f8ca8bb5be5a9037f4d 21 December 2018.

Labordena, M. 2018. How sub-Saharan Africa can harness its big electricity opportunities. *June 7, 2018*. https://theconversation.com/how-sub-saharan-africa-can-harness-its-big-electricity-opportunities-97391 20 December 2018.

Lovegrove, K. & Stein, W. eds. 2012. *Concentrating solar power technology*. Cambridge: Woodhead Publishing Limited.

Mailoa, J. P., Bailie, C. D., Johlin, E. C., Hoke, E. T., Akey, A. J., Nguyen, W.H. 2015. A 2-terminal perovskite/silicon multijunction solar cell enabled by a silicon tunnel junction. *Applied Physics Letters*, 106(12): 121105. http://aip.scitation.org/doi/10.1063/1.4914179 9 June 2018.

Manuel, J. 2010. Concentrating Photovoltaic Systems - Can Light Tricks Make Solar Photovoltaics Affordable ? *Popular Mechanics*. https://www.popularmechanics.com/science/energy/a5592/concentrating-solar-pv-power/ 4 June 2018.

Mar, A., Parmar, A., Dave, K., Pithadiya, P.G. & Vasaiya, V.M. 2015. Efficiency Improvement Technologies of Solar PV power plant. *International Journal of Advance Engineering and Research Development*, 2(7): 99–109. http://www.ijaerd.com/papers/finished_papers/Efficiency Improvement Technologies of Solar PV power plant-20993.pdf 4 June 2018.

Matasci, S. 2018. Solar Panel Cost in 2018 | Updated Average Solar Panel Prices by State. *December 2, 2018*. https://news.energysage.com/how-much-does-the-average-solar-panel-installation-cost-in-the-u-s/ 20 December 2018.

Meth, O. 2018. Department of Environmental Affairs has 'secretly' weakened sulphur dioxide (SO2) emission standards for coal-fired power stations - Greenpeace Africa. *Green Peace 14 November 2018*. https://www.greenpeace.org/africa/en/issues/protecttheenvironment/5607/department-of-environmental-affairs-has-secretly-weakened-sulphur-dioxide-so2-emission-standards-for-coal-fired-power-stations/ 1 February 2019.

Mokri, A. & Emziane, M. 2011. Concentrator photovoltaic technologies and market: a critical review. In Masdar. http://www.ep.liu.se/ecp/057/vol11/006/ecp57vol11_006.pdf 21 December 2018.

Muhammad-sukki, F., Ramirez-iniguez, R., Mcmeekin, S.G., Stewart, B.G. & Clive, B. 2001. Solar Concentrators. *US Patent Application Publication 0277494*, (1): 357–436. http://homepages.rpi.edu/~keblip/ENERGYECONOMY/READING/solar_concentrated.pdf.

Nivas, V. marketplace.yet2.com - V-trough solar collector provides both increased electricity and domestic hot water for rural families. http://marketplace.yet2.com/app/list/techpak?id=71332&sid=90&abc=0&page=development 11 June 2018.

Nteka, N.E. & Kanyarusoke, K.E. 2019. Concentrated Solar and Photovoltaic Thermal Cooled System for Domestic Use. In *2019 International Conference on the Domestic Use of Energy (DUE)*. Cape Town: cape peninsula university of technology: 232–237. https://ieeexplore.ieee.org/stamp/stamp.jsp?tp=&arnumber=8734446&tag=1.

Oorjan Cleantech. 2018. Solar Concentrator- Types, Working And Advantages. *Solar education*. https://www.oorjan.com/blog/2018/06/08/solar-concentrator/ 7 December 2018.

Ozgoren, M., Aksoy, M.H., Bakir, C. & Dogan, S. 2013. Experimental Performance Investigation of Photovoltaic/Thermal (PV–T) System. *EPJ Web of Conferences*, 45: 01106. https://cyberleninka.org/article/n/924589.pdf.

Papadopoulos, A., Tsoutsos, T., Frangou, M., Kalaitzakis, K., Stefanakis, N. & Boudouvis, A.G. 2017. Innovative optics for concentrating photovoltaic/thermal (CPVT) systems – the case of the PROTEAS Solar Polygeneration System. *International Journal of Sustainable Energy*, 36(8): 775–786. https://www.tandfonline.com/doi/full/10.1080/14786451.2015.1100195 4 June 2018.

plusAmpere. 2019. INNOVATIVE REFLECTOR SYSTEM - plusAmpere GmbH.

https://www.plusampere.de/english/achievements/innovative-reflector-system/ 1 July 2019.

Ponce-Alcantara, S., Connolly, J.P., Sanchez, G., Miguez, J.M., Hoffmann, V. & Ordas, R. 2014. A statistical analysis of the temperature coefficients of industrial silicon solar cells. *Energy Procedia*, 55: 578–588. http://dx.doi.org/10.1016/j.egypro.2014.08.029.

Ramos, A., Guarracino, I., Mellor, A., Alonso-álvarez, D., Childs, P., Ekins-daukes, N.J. & Markides, C.N. 2017. A.Ramos-Briefing Paper_2017. *Grantham Institute, Briefing paper No 22. Imperial College London*, (22): 1–20. https://www.imperial.ac.uk/media/imperial-college/grantham-institute/public/publications/briefing-papers/2679_Briefing-P-22-Solar-heat_web.pdf.

Rawat, P. & Dhiran, T.S. 2017. Comparative Analysis of Solar Photovoltaic Thermal (PVT) Water and Solar Photovoltaic Thermal (PVT) Air Systems. , (1): 8–12. https://www.researchgate.net/publication/315657756_Comparative_Analysis_of_Solar_Photovoltaic_Thermal_PVT_Water_and_Solar_Photovoltaic_Thermal_PVT_Air_Systems.

Reddy, S.P.M., Venkataramaiah, P. & Reddy, D.V.V. 2014. Selection of Best Materials and Parametric Optimization of Solar Parabolic Collector Using Fuzzy Logic. , 6: 527–536. http://www.scirp.org/journal/epehttp://dx.doi.org/10.4236/epe.2014.614046http://dx.doi.org/10.4236/epe.2014.614046http://creativecommons.org/licenses/by/4.0/ 9 December 2018.

Rosa-Clot, M. & Tina, G.M. 2018. Chapter 2 - Photovoltaic Electricity. In M. Rosa-Clot & G. M. Tina, eds. *Submerged and Floating Photovoltaic Systems*. Academic Press: 13–32. http://www.sciencedirect.com/science/article/pii/B9780128121498000028.

Salameh, Z. 2014. *Renewable Energy System Design*. 1st ed. london: Academic Press. https://www.elsevier.com/books/renewable-energy-system-design/salameh/978-0-12-374991-8.

Sheikh, A. 2018. Solar Concentrators Types & Applications | Electrical Academia. http://electricalacademia.com/renewable-energy/solar-concentrators-types-applications/ 21 December 2018.

Solar Aid. Kerosene and Paraffin Lamps in Africa - SolarAid. *Solar Aid*. https://solar-aid.org/kerosene-paraffin-lamps-africa/ 13 June 2019.

Sonneveld, P.J., Swinkels, G.L.A.M., Van Tuijl, B.A.J., Janssen, H.J.J., Campen, J. & Bot, G.P.A. 2011. Performance of a concentrated photovoltaic energy system with static linear Fresnel lenses. https://www.sciencedirect.com/science/article/pii/S0038092X10003658 21 December 2018.

Sustainable.co.za. 2019. PANEL. *Sustainable.co.za*: 10–12. https://www.sustainable.co.za/solar-power/solar-panels.html.

TESZEUS. Photovoltaic-Thermal Hybrid Solar Collector.

http://www.tessolarwater.com/index_en.html?zeuspv-t.html&2 30 May 2018.

TRNSYS16. 2007. Trnsys 16. , 1. http://sel.me.wisc.edu/trnsys.

Victoria, C. 2017. The History Of Solar Power | Experience. https://www.experience.com/advice/careers/ideas/the-history-of-solar-power/ 20 December 2018.

Zipp, K. 2013. How does a solar tracker work? *April 4, 2013*. https://www.solarpowerworldonline.com/2013/04/how-does-a-solar-tracker-work/ 21 December 2018.

Appendices

A1: Experimental results

Table A1-1: Experimental results for chapter 5

		CSPVT				Conventional PV				Weather data	
	Local Time	Voltage (V)	Current (A)	t° on glass (°C)	t° on back sheet (°C)	Voltage (V)	Current (A)	t° on glass (°C)	t° on back sheet (°C)	T_{amb}(°C)	Wind speed (m/s)
Day 1	7h00	11.67	0.1	5.9	5.6	8.8	0	5.6	5.2	5.541	1.637
	7h30	12.7	0.9	9.1	8.6	10.7	0.1	8.6	8.1	8.5	0.979
	8h00	12.8	1.9	12.5	12.8	11.2	0.5	11.9	11.4	11.76	1.196
	8h30	13.5	2.9	17.7	18.1	12.6	1.8	24.9	24.5	16.61	0.032
	9h00	13.9	3.1	23.1	21.6	12.67	1.9	29.7	29.3	19.79	0.053
	9h30	14.2	3.5	26	24.3	13.3	1.8	33.4	33	22.28	0.6
	10h00	14.5	3.8	25.2	23.5	13.32	3.1	32.4	32	21.59	1.735
	10h30	15.52	3.5	24	20.7	13.5	3.2	28.5	28.1	18.99	0.889
	11h00	15.67	4.2	30.7	25.0	13.67	3.4	36.4	36	24.27	1.103
	11h30	15.8	4.1	33.7	27.5	14.5	3.3	39.9	39.5	26.62	0.534
	12h00	17.34	5.8	34.9	28.5	14.2	4.2	41.4	40.9	27.57	0.558
	12h30	19.47	6.1	26.2	21.4	15.6	4.2	31.1	30.6	20.7	0.663
	13h00	19.7	6.5	27	22.1	15.8	4.3	32.1	31.7	21.38	1.406
	13h30	19.7	6.4	25.4	20.7	16.7	5.1	30.1	29.7	20.08	1.427
	14h00	14.67	5.8	27.3	23.0	15.7	4.7	32.4	32	21.61	0.883
	14h30	13.5	5.8	26.4	22.2	14.3	4.9	31.3	30.9	20.86	1.534
	15h00	13.5	5.4	24.4	20.5	13.9	4.1	28.9	28.5	19.25	2.875
	15h30	12.67	5.2	22.9	19.3	13.5	3.4	27.2	26.8	18.14	3.431
	16h00	12.5	5.4	22.4	18.8	12.5	3.1	26.5	26.1	17.68	3.114
	16h30	12.8	4.5	22.8	19.2	12.3	2.4	27.0	26.6	18	2.612
	17h00	12.85	3.2	20.9	17.6	11.5	1.8	24.8	24.4	16.56	2.602
	17h30	12.85	2.1	20.6	17.3	11.6	1.9	24.4	24	16.25	3.033
	18h00	12.85	1.9	19.3	16.2	11.8	1.7	22.8	22.4	15.23	3.3

		CSPVT				Conventional PV				Weather data	
	Local Time	Voltage (V)	Current (A)	t° on glass (°C)	t° on back sheet (°C)	Voltage (V)	Current (A)	t° on glass (°C)	t° on back sheet (°C)	Tamb(°C)	Wind speed (m/s)
Day 2 10/09/2018	7h00	12	0	9.2	9.2	13.24	0	8.6	8.4	6.569	1.301
	7h30	13.56	0.4	10.6	9.6	13.4	0.2	10.6	10.9	9.66	0.845
	8h00	13.56	1.9	19.5	10.2	13.45	0.8	19.8	19.8	13.91	0.811
	8h30	13.8	2.7	20.2	15.2	13.55	0.9	28.4	28.9	18.67	0.859
	9h00	14.24	3.4	24.6	18.9	13.6	0.7	31.5	31.2	20.51	0
	9h30	15.02	3.9	34.7	22.1	13.25	1.2	34.2	33.1	26.29	0.124
	10h00	19.44	3.8	28.8	22.8	12.88	2.1	33.8	33.1	23.98	1.718
	10h30	18.9	4.5	27.9	22.7	12.87	2.5	32.5	32.3	20.49	1.895
	11h00	19.28	4.7	27.8	23.5	14.25	2.8	36.8	36.2	24.25	2.358
	11h30	19.45	4.8	29.8	24.6	14.82	3.1	34.9	34.5	26.3	2.173
	12h00	19.34	5.7	32.9	24.8	15.2	3.1	36.8	36.4	27.09	2.021
	12h30	19.47	4.9	28.8	22.7	14.7	3.5	30.5	29.5	22.26	2.306
	13h00	19.4	4.2	29.8	22.1	15.8	4.2	38.8	37.9	22.74	1.883
	13h30	19.52	4.8	29.5	22.5	14.67	4.5	32.1	32	22.69	2.31
	14h00	19.34	4.9	29.8	21.5	14.7	4.8	33.9	33.1	21.89	3.125
	14h30	19.25	5.5	28.2	21.7	14.71	4.6	31.5	30.5	21.61	3.364
	15h00	19.25	4.9	27.5	20.2	13.87	5.9	30.8	29.8	20.7	3.508
	15h30	19.55	4.2	25.2	20.1	13.87	5.8	31.2	31	20	3.208
	16h00	13.6	4.7	23.6	24.6	12.54	4.2	26.5	25.6	19.72	3.325
	16h30	12.28	3.6	22.5	19.8	12.4	1.8	29.8	28.5	19.51	3.625
	17h00	12.23	2.4	21.5	19.8	12.36	1.6	26.7	27.5	18.66	3.033
	17h30	12	2.2	23.5	19.7	12.34	1.2	24.8	24.8	18.77	3.225
	18h00	12	1.8	23.5	19.4	12.1	0.8	26.4	26.5	18.08	1.687

Table A1-2: Experimental results for chapter 5

	CSPVT					Conventional PV				Weather data	
	Local Time	Voltage (V)	Current (A)	t° on glass (°C)	t° on back sheet (°C)	Voltage (V)	Current (A)	t° on glass (°C)	t° on back sheet (°C)	T_{amb}(°C)	Wind speed (m/s)
Day 3 11/09/2018	7h00	12.34	0	9.2	8.6	8.5	0	9.1	9.1	8.54	1.481
	7h30	12.57	0.4	15.8	13.5	12.2	0.8	16.5	16.8	12.94	2.875
	8h00	12.62	1.2	21.3	15.4	12.5	1.2	19.8	19.8	15.34	2.181
	8h30	12.5	1.9	24.5	16.8	12.6	1.7	20.1	20.2	17.97	3.042
	9h00	12.52	3.9	26.4	16.8	12.6	2.6	25	25	19.39	3.758
	9h30	12.9	4.3	27	17.6	12.6	2.7	27.2	27.7	23.17	2.839
	10h00	13.2	4.6	25.6	17.8	12.6	3.1	32.5	28.3	24.58	3.575
	10h30	14.35	4.7	27.5	18.6	12.6	3.8	33.2	29.3	23.64	3.467
	11h00	14.65	4.8	29.1	19.4	13.5	3.8	38.9	37.9	27.28	3.675
	11h30	15.9	5.5	31.7	19.8	12.72	4.1	39.8	37.8	28.58	4.392
	12h00	15.4	5.8	33.8	21.5	12.75	4.3	40.1	39.4	29.47	3.5
	12h30	15.89	6.4	28.9	24.4	12.75	5.1	33.6	32.8	23.95	4.558
	13h00	15.8	5.6	28.6	24.4	12.8	5.6	30.4	29.8	21.8	4.675
	13h30	15.7	5.4	27.6	25	12.8	4.8	30.1	31.4	21.13	4.517
	14h00	15.9	5.2	27.8	21.2	12.8	4.7	30.1	29.8	21.68	4.033
	14h30	15.84	5.9	28.9	21.2	12.8	4.9	30	30.1	21.36	3.558
	15h00	17.34	5.1	28.8	20.4	12.8	4.5	30.5	30.4	21.39	3.433
	15h30	16.58	4.9	24.6	20.6	12.8	3.9	30.2	30.5	20.81	3.717
	16h00	16.54	3.8	21.4	22.3	12.7	2.8	28.5	28.6	19.24	3.7
	16h30	15.23	3.5	22.1	20.1	11.8	2.7	28.4	28.3	18.81	4
	17h00	15.48	2.8	19.9	18.5	11.4	1.9	27.6	26.8	17.31	4.092
	17h30	13.5	2.5	18.3	19.5	11.4	1.7	22.36	22.1	16.35	4.767
	18h00	11.4	1.8	18.2	19.4	11.4	1.7	21.5	21.6	15.84	3.858

	CSPVT					Conventional PV				Weather data	
	Local Time	Voltage (V)	Current (A)	t° on glass (°C)	t° on back sheet (°C)	Voltage (V)	Current (A)	t° on glass (°C)	t° on back sheet (°C)	T_{amb}(°C)	Wind speed m/s
Day 4 20/09/2018	7h00	12.34	0	6.1	4.8	12.3	0	7.2	7.2	5.057	0.594
	7h30	13.5	1.8	12.3	5.8	12.3	0.5	15.6	15.2	11.34	0.291
	8h00	13.24	2.3	15.6	6.8	12.4	0.9	20.5	20.4	14.49	0.738
	8h30	13.8	2.7	17.8	7.4	12.5	1.2	22.3	22.5	15.49	1.061
	9h00	14.2	3.3	20.2	8.9	13.5	2.5	28.9	28.7	20.52	0.346
	9h30	16.2	3.4	24.8	10.8	14.7	2.5	31.3	37.2	23.29	0.281
	10h00	15.2	4.6	27.8	17.8	12.65	2.5	36.5	36.4	25.04	0.269
	10h30	14.3	5.5	28.5	19.8	12.65	3.8	31.4	35.3	23.69	1.011
	11h00	15.33	5.7	30.5	22.3	12.7	3.1	37.5	38.5	25	1.228
	11h30	15.42	6.4	22.6	18.7	13.1	2.8	24.9	25.2	18.72	0.704
	12h00	15.5	1.4	32.3	19.5	13.1	1.9	39.7	39.2	26.62	1.127
	12h30	15.34	6.2	20.3	19.6	12.6	3.8	26.5	24.8	18.1	1.017
	13h00	15.3	6.6	23.7	20.5	12.9	4.2	30.1	25.8	21.29	1.522
	13h30	15.1	6.2	23.7	20.4	12.5	6.3	24.3	24.2	18.59	1.196
	14h00	13.2	1.5	23.8	20.3	12.4	1.6	25.6	25.2	19.29	1.232
	14h30	13.8	5.2	23.5	20.2	12.3	4.5	24.5	24.2	16.96	3.333
	15h00	13.8	1.5	22.5	17.8	12.2	1.5	23.9	23.8	16.7	2.931
	15h30	12.5	1.8	21.2	17.5	11.3	1.4	23.6	23.5	16.52	2.954
	16h00	12.5	1.9	19.8	17.3	11.32	1.4	23.9	23.9	16.7	2.823
	16h30	13.2	2.1	18.7	15.4	12.3	1.6	22.5	23.1	15.72	2.991
	17h00	12.68	1.4	15.6	15.4	11.32	1.3	21.5	21.6	14.78	2.458
	17h30	12.5	1.7	15.8	14.6	11.4	1.6	21.4	21.5	14.34	2.592
	18h00	11.5	1.6	15.8	14.5	11.3	1.6	21.4	20.8	14.08	2.517

Table A1-3: Experimental results for chapter 5

	CSPVT					Conventional PV				Weather data	
	Local Time	Voltage (V)	Current (A)	t° on glass (°C)	t° on back sheet (°C)	Voltage (V)	Current (A)	t° on glass (°C)	t° on back sheet (°C)	T_{amb}(°C)	Wind speed m/s
Day 5 22/09/2018	7h00	12	0.1	12.3	11.8	11.4	0.1	12.3	12.2	11.45	3.092
	7h30	12.5	1.7	15.2	14.6	11.3	0.9	14.6	13.5	14.32	2.525
	8h00	13.25	1.9	19	14.6	11.2	1.5	20.5	20.2	18.07	1.246
	8h30	13.55	2.1	19.8	14.5	11.2	2.2	20.6	20.8	18.33	2.297
	9h00	13.62	3.2	21.6	14.8	11.6	2.8	21.4	20.8	20	3.283
	9h30	13.7	4.1	23.4	18.9	12.2	4.3	29.7	28.3	21.66	3.221
	10h00	14.36	4.7	23	16.9	12.5	4.5	30.8	30.2	21.25	3.364
	10h30	14.83	4.6	24.8	18. 3	12.8	5.1	29.8	27.2	22.99	3.148
	11h00	16.98	5.4	26	20.3	12.9	5.3	32.7	29.9	23.86	3.3
	11h30	16.7	5.4	27.4	20.5	12.8	5.2	38.3	37.1	25.15	2.852
	12h00	15.62	7.1	27.8	24.5	12.9	5.6	37.5	36.8	25.48	2.673
	12h30	15.8	6.7	23.2	22.3	12.9	4.8	31.5	30.9	21.26	3.192
	13h00	14.6	4.5	22.3	20.5	12.9	4.9	29.8	29.8	20.42	4.275
	13h30	15.3	4.6	22.4	20.5	12.8	4.5	31.4	31.3	20.53	3.95
	14h00	14.8	5.8	22	20.5	12.7	5.1	27.4	28.2	20.15	4.417
	14h30	15	4.9	21.3	20.6	12.5	4.5	26.4	29.2	19.5	5.208
	15h00	15.4	4.9	20.6	17.8	12.5	4.6	29.2	25.4	18.91	5.1
	15h30	12.62	3.9	19.9	17.8	12.4	4.1	30.3	31.4	18.26	5.783
	16h00	13.2	3.7	19.6	17.8	12.4	3.9	28.3	28.2	17.95	5.558
	16h30	13.28	2.5	19.4	17.8	12.2	2.3	25.6	25.1	17.82	6.092
	17h00	12.37	1.8	19.0	15.8	12.2	1.8	24.2	23.5	17.45	5.633
	17h30	12.5	1.5	17.8	22.3	12.2	1.5	22.8	22.2	16.27	6.008
	18h00	12	0.9	12.3	20.5	11.2	0.8	21.6	20.8	15.58	6.675

	CSPVT					Conventional PV				Weather data	
	Local Time	Voltage (V)	Current (A)	t° on glass (°C)	t° on back sheet (°C)	Voltage (V)	Current (A)	t° on glass (°C)	t° on back sheet (°C)	T_{amb}(°C)	Wind speed m/s
Day 6 24/09/2018	7h00	12.34	0.3	11.6	10.5	10.8	0.1	13.5	13.4	10.68	0.463
	7h30	13.4	1.8	16.5	13.5	11.7	0.5	20.5	20.1	14.79	0.146
	8h00	13.43	2.8	22.5	20.2	11.6	0.8	28.6	28.4	20.88	0.373
	8h30	13.52	3	25.6	23.2	11.7	1.2	33.5	32.1	22.86	0.268
	9h00	13.8	3.3	30.5	23.2	12.5	1.9	38.4	37.5	27.44	0.287
	9h30	19.2	4.8	33.5	25.2	12.7	2.3	41.5	40.2	29.37	0.207
	10h00	15.29	4.7	34.5	26.9	12.3	2.7	41.3	39.5	29	0.297
	10h30	13.89	5.9	33.5	29.4	12.4	3.2	42.5	41.8	31.52	0.689
	11h00	16.5	5.8	38.5	24.5	12.3	4.7	50.8	49.7	32.78	0.583
	11h30	15.7	6.5	37.8	28.7	12.3	5.3	41.4	40.4	32.63	1.123
	12h00	17.78	6.9	37.2	29.9	12.9	5.5	46.6	45.6	31.87	1.563
	12h30	17.89	5.8	30.5	27.7	12.9	5.6	39.5	38.8	26.3	1.513
	13h00	15.49	6.5	32.5	27.5	12.9	5.8	41.8	55.4	26.34	1.525
	13h30	15.68	5.4	30.8	27.2	12.9	5.7	38.5	45.5	25.65	2.381
	14h00	15.4	4.9	31.6	27.1	12.8	5.5	40.6	40.3	26.08	1.63
	14h30	14.67	4.9	33.5	25.3	12.6	5.1	35.6	33.6	25.11	3.139
	15h00	16.5	4.5	31.5	23.8	12.6	4.7	32.2	31.5	24.36	2.908
	15h30	13.8	4.6	28.7	21.7	12.4	3.7	32.3	31.1	22.08	3.467
	16h00	12.53	3.5	26.8	20.9	12.4	3.5	32.5	29.9	21.01	3.042
	16h30	12.5	2.9	25.2	20.1	11.33	2.7	32.5	27.5	20.64	3.156
	17h00	12.3	1.9	23.3	19.2	11.2	2.3	25.8	25.6	19.87	3.131
	17h30	12.3	1.9	20.4	19.2	11.2	1.3	20.4	20.5	17.96	3.764
	18h00	12	1.9	19.5	19.1	11.2	1.3	20.8	20.5	16.69	3.196

Table A1-4: Experimental results for chapter 5

	CSPVT					Conventional PV				Weather data	
	Local Time	Voltage (V)	Current (A)	t° on glass (°C)	t° on back sheet (°C)	Voltage (V)	Current (A)	t° on glass (°C)	t° on back sheet (°C)	T_{amb}(°C)	Wind speed m/s
Day 7 05/10/2018	7h00	12.45	0.8	18.5	14.5	9.8	0.6	18.9	17.5	14.04	0.135
	7h30	12.7	0.4	20.5	15.2	10.3	0.9	28.6	28.2	18.52	0
	8h00	13.63	2.8	23.9	15.6	10.6	2.6	31.6	30.8	19.88	0.063
	8h30	13.5	3.4	35.6	20.5	12.2	3.6	38.4	37.5	28	0.146
	9h00	12.6	4.1	38.6	30.2	12.3	4.1	41.4	41.9	29.84	0.496
	9h30	13.1	4.5	33.9	29.5	12.5	4.5	43.2	43	29.33	1.382
	10h00	14	5.2	30.8	26.5	12.5	5.3	38.6	38.1	27.17	1.248
	10h30	14.4	4.7	38.6	35.6	12.5	4.9	50.5	50	34.62	0.754
	11h00	16.8	5.6	40.8	37.8	12.7	5.4	54.5	53.2	37.55	0.781
	11h30	15.3	5.9	39.7	36.5	12.7	5.4	55.8	53.2	37.83	1.081
	12h00	16.8	6.5	46.8	38.5	12.7	5.4	59.8	58.1	40.05	0.484
	12h30	16.58	6.4	40.4	35.8	12.7	4.8	48.2	47.6	35.52	0.522
	13h00	15.8	4.7	34.3	29.8	12.7	5.2	37.8	37.5	30.76	3.692
	13h30	15.4	4.5	35.1	30.8	12.7	5.4	39.7	39.7	29.83	2.721
	14h00	15.4	4.8	35.7	30.5	12.7	5.3	39.1	38.5	28.89	2.989
	14h30	15.4	4.8	36.7	30.4	12.7	5.1	44.6	43.5	28.7	2.875
	15h00	15.4	4.8	32.8	28.5	12.7	5.3	42.5	40.6	28.34	2.573
	15h30	12.88	5.9	31.5	27.5	12.7	4.8	41.2	41.3	28.58	2.789
	16h00	12.8	6.4	31.2	25.8	12.6	4.9	40.8	39.8	28.91	2.029
	16h30	12.8	4.6	32.8	24.5	12.5	4.6	38.6	38.2	29.84	2.975
	17h00	12.6	4.2	28.5	23.9	12.5	3.9	34.5	32.3	24.07	3.092
	17h30	12.6	3.4	25.7	23.7	12.5	3.3	30.2	30.1	23.06	2.137
	18h00	12.6	2.8	25.8	23.5	12.5	2.3	30.1	30	23.47	1.424

	CSPVT					Conventional PV				Weather data	
	Local Time	Voltage (V)	Current (A)	t° on glass (°C)	t° on back sheet (°C)	Voltage (V)	Current (A)	t° on glass (°C)	t° on back sheet (°C)	T_{amb}(°C)	Wind speed m/s
Day 8 06/10/2018	7h00	12.4	0.5	17	17.2	8.8	0.4	17.8	17.6	16.8	1.612
	7h30	11.5	2.8	20.7	18.6	10.7	2.6	21.7	21.4	20.52	1.597
	8h00	13.45	2.8	21.8	18.9	11.2	2.5	22.8	22.6	21.61	1.94
	8h30	13.7	2.9	24.5	18.7	12.6	2.6	24.3	24.0	22.28	2.771
	9h00	14.89	3.3	27.9	19.5	12.67	2.9	27.6	27.4	25.34	2.692
	9h30	15	3.8	28.7	20.1	13.3	3.2	31.3	31.0	26.08	3.617
	10h00	18.4	4.2	27.2	24.3	12.32	3.6	29.7	29.5	24.75	5.908
	10h30	18.67	4.5	32.7	26.3	13.5	3.8	37.2	36.9	28.83	4.214
	11h00	18.67	4.4	33.7	26.5	13.67	3.8	36.8	36.6	27.89	5.017
	11h30	19.28	4.6	35.9	26.8	14.5	3.9	38.4	38.1	29.07	5.117
	12h00	19.45	6.8	37.2	27.9	14.2	4	40.9	40.6	30.98	4.025
	12h30	19.47	6.9	34	28	15.6	3.6	37.4	37.1	28.33	4.35
	13h00	19.5	4.2	33.1	28.2	15.8	3.6	38.1	37.9	27.62	4.992
	13h30	19.52	6.45	34.1	28.4	16.7	3.9	39.2	38.9	28.38	3.506
	14h00	19.34	5.2	34.4	28.4	15.7	4.2	37.8	37.5	28.63	3.964
	14h30	19.25	5.6	34.5	28.6	14.3	4.5	37.9	37.7	28.74	5.1
	15h00	19.3	5.2	34.4	29	13.9	4.8	38.2	37.9	28.69	4.9
	15h30	19.55	4.4	30.8	29.1	13.5	4.4	34.5	34.3	28.52	4.55
	16h00	13.6	4.2	30.8	29.2	12.5	3.2	34.5	34.2	28.5	3.754
	16h30	12.28	4	32.4	29.1	12.3	2.8	36.3	36.1	30.01	2.756
	17h00	12.3	3.8	29.9	29	11.5	2.3	33.4	33.2	27.64	5.083
	17h30	12.5	2.5	29.7	28.7	11.5	1.8	33.3	33.0	27.5	3.433
	18h00	12.5	2	28.5	28.7	11.5	1.5	31.9	31.6	26.36	3.708

Table A1-5: Experimental results for chapter 5

	CSPVT					Conventional PV				Weather data	
	Local Time	Voltage (V)	Current (A)	t° on glass (°C)	t° on back sheet (°C)	Voltage (V)	Current (A)	t° on glass (°C)	t° on back sheet (°C)	T_{amb}(°C)	Wind speed m/s
Day 9 07/10/2018	7h00	11.64	0.9	17.5	16.5	10.6	0.9	18	18	17.99	0
	7h30	14.1	2.1	19.6	18.3	11.1	1.3	26.2	26.2	23.56	0
	8h00	13.4	2.3	19.8	19.4	11.2	2.5	30.2	30.4	27.21	0.238
	8h30	12.8	3.1	28.1	19.5	11.3	2.9	35.1	36.1	29.93	0.446
	9h00	12.6	3.5	27.5	20.1	12.4	3.5	39.4	37.6	30.67	1.181
	9h30	12.6	5.1	29.9	20.3	12.5	4	39.2	39.8	30.9	1.296
	10h00	12.8	5.4	29.7	20.5	12.6	4.3	41.1	40.9	30.66	2.047
	10h30	13.1	5.9	31.8	20.4	12.7	4.9	36.1	36.8	31.91	3.133
	11h00	15.2	6.1	33.6	20.8	12.8	5.1	39.2	39.8	32.25	3.393
	11h30	14.5	6.5	35.5	21.1	12.8	5.1	40.7	40.5	32.5	3.783
	12h00	16.48	6.9	34.9	21.3	12.8	5.3	44.6	43.1	33	3.442
	12h30	15.5	7.2	34.6	23.5	12.8	5.2	41.6	38.5	30.61	3.389
	13h00	15.5	7.7	36.5	28.6	12.7	5.2	42.3	42	31.1	3.208
	13h30	13.9	6.5	38.1	28.8	12.7	4.5	42.1	39.8	31.16	3.375
	14h00	13.75	6.8	37.1	29.5	12.8	3.9	42.8	42.1	31.52	3.187
	14h30	14.8	6.5	40.7	29.8	12.8	4.9	43.3	43	31.63	2.875
	15h00	14.3	5.8	39.2	30.2	12.8	4.8	40.5	40.6	31.59	2.683
	15h30	14.3	6.4	38.5	30	12.7	4.7	40.6	39.8	31.97	2.823
	16h00	12.6	4.2	35.2	31	12.7	4.5	42.3	39	30.94	2.55
	16h30	12.5	5.1	33.5	30.9	12.7	4.1	43.5	41.7	32.13	1.961
	17h00	12.5	3.2	33.4	30.4	11.8	3.3	38.5	37.6	29.32	2.387
	17h30	12.6	2.9	33.4	28.4	11.8	2.3	33.4	33.2	27.95	2.198
	18h00	12.6	2.3	30.5	29.1	11.8	1.7	30.5	30.6	24.9	2.358

	CSPVT					Conventional PV				Weather data	
	Local Time	Voltage (V)	Current (A)	t° on glass (°C)	t° on back sheet (°C)	Voltage (V)	Current (A)	t° on glass (°C)	t° on back sheet (°C)	T_{amb}(°C)	Wind speed m/s
Day 10 08/10/2018	7h00	13.5	0.6	18.9	17.8	10.6	0.7	19.1	18.5	17.39	1.772
	7h30	13.25	1.8	22.6	19.2	10.9	1.1	20.8	20.2	18.88	3.842
	8h00	14.65	2.5	23.4	19.2	10.9	1.3	26.5	25.9	20.92	3.542
	8h30	16.59	2.7	28.5	20.5	11.2	2.2	28.9	28.3	22.32	3.725
	9h00	16.58	3.2	32.6	24.6	11.2	2.3	38.4	37.8	26.51	3.167
	9h30	16.4	4.5	37.9	25.6	12.6	2.8	38.2	37.6	26.76	4.667
	10h00	17.34	4.6	38.4	27.5	12.6	2.9	39.6	39.0	27.07	5.05
	10h30	19.68	5.5	39.7	31.2	12.5	3.2	43.5	42.9	30.84	3.892
	11h00	19.56	6.8	40.6	33	12.5	3.8	50.9	50.3	32.74	3.767
	11h30	19.56	6.8	40.3	33.1	12.5	3.9	57.8	57.2	33.99	3.333
	12h00	19.64	7.8	42.2	33.1	12.6	4.2	58.5	57.9	35.86	2.939
	12h30	15.48	7.2	40.7	33.5	12.6	4.4	56.2	55.6	33.53	2.629
	13h00	19.1	7.4	42.1	34.2	12.6	4.5	60.3	59.7	35.4	1.737
	13h30	19.25	7.2	42.8	34.1	12.7	4.6	53.7	53.1	35.67	1.421
	14h00	19.35	5.5	38.5	34.5	12.7	4.8	50.1	49.5	30.3	2.472
	14h30	18.9	5.8	36.4	27.9	12.8	4.9	38.6	38.0	27.82	3.514
	15h00	19.5	5.5	34.1	27.9	12.7	5.2	37.5	36.9	26.6	2.733
	15h30	16.235	6.1	34.5	27.5	12.8	4.6	38.1	37.5	27.89	1.333
	16h00	12.5	6.8	36.7	27.4	12.6	4.3	34.1	33.5	28.76	1.918
	16h30	12.3	4.8	39.8	29.4	12.6	3.9	40.3	39.7	30.54	0.979
	17h00	13.1	4.2	32.8	29.8	12.3	3.2	39.2	38.6	29.79	1.258
	17h30	13.2	2.9	31.4	29.8	12.2	2.3	39.5	38.9	29.57	1.121
	18h00	13.5	0.6	28.5	29.4	12.1	1.9	25.1	24.5	17.39	1.772

A2: Sample data logger results

Table A2-1: Sample data logger results for section 5.1.1 and 5.2

TOA5	CR1000 SlrW Avg	SlrMJ Tot	CR1000.Std.25 SlrW_2_Avg Avg (diffuse radiation)	CPU:CR1000 CPUT, Cape Town Oct14.CR1 SlrMJ_2_Tot	SlrW_3_Avg	SlrkJ_Tot	PanelT_Avg		
TIMESTAMP	W/m^2	MJ/m^2	W/m^2	MJ/m^2	W/m^2	kJ/m^2	degrees	WS_ms_Avg	WS_ms_Max
09/09/18 06:00	0	0	0	0	0	0	5.841	0.127	0.95
09/09/18 06:15	0	0	0	0	0	0	5.726	0	0
09/09/18 06:30	0	0	0	0	0	0	5.842	0.438	1.7
09/09/18 06:45	0.406	3.66E-05	0.156	1.40E-05	0	0	5.634	1.014	2.45
09/09/18 07:00	4.541	0.000409	2.001	0.0001801	2.205	0.1984696	5.541	1.637	3.2
09/09/18 07:15	19.47	0.001753	13.69	0.0012325	15.84	1.425783	6.217	1.624	3.2
09/09/18 07:30	62.81	0.005653	54.34	0.0048909	54.16	4.874325	8.5	0.979	1.7
09/09/18 07:45	105.8	0.009523	94.3	0.0084907	98.6	8.87248	10.24	1.391	2.45
09/09/18 08:00	144.1	0.01297	124.9	0.0112442	140.7	12.66443	11.76	1.196	2.45
09/09/18 08:15	190.8	0.017171	140.4	0.0126322	188.9	16.99719	13.45	0.971	1.7
09/09/18 08:30	226.7	0.020407	83.4	0.0075066	226.6	20.39113	16.61	0.032	0.95
09/09/18 08:45	280.6	0.025252	39.37	0.0035435	280.6	25.25188	19.73	0	0
09/09/18 09:00	336.8	0.030309	29.36	0.0026423	337.1	30.3393	19.79	0.053	0.95
09/09/18 09:15	388.4	0.03496	26.81	0.0024127	388.5	34.96326	23.22	0.154	1.7
09/09/18 09:30	437.3	0.039358	25.43	0.0022888	437.7	39.39299	22.28	0.6	2.45
09/09/18 09:45	487.2	0.04385	26.38	0.0023744	488.1	43.92758	21.87	1.278	2.45
09/09/18 10:00	535.6	0.048202	27.2	0.0024482	536.5	48.28113	21.59	1.735	3.2
09/09/18 10:15	585.9	0.052728	26.63	0.0023967	586.9	52.82062	21.33	1.18	3.2
09/09/18 10:30	606.7	0.0546	27.98	0.0025184	610.4	54.93828	18.99	0.889	2.45
09/09/18 10:45	608.7	0.054783	28.71	0.0025843	612.7	55.14017	24.66	0.535	1.7
09/09/18 11:00	668.9	0.060198	30.44	0.0027394	671.2	60.40675	24.27	1.103	2.45
09/09/18 11:15	707	0.063631	27.6	0.0024837	706.1	63.5462	27.09	0.6	2.45
09/09/18 11:30	716.7	0.064501	26.16	0.0023545	715.6	64.4053	26.62	0.534	2.45
09/09/18 11:45	753.6	0.067824	26.37	0.0023735	754.8	67.92925	27.02	0.731	1.7
09/09/18 12:00	745	0.067052	25.91	0.0023318	750.2	67.51646	27.57	0.558	1.7
09/09/18 12:15	729.7	0.065676	25.17	0.002265	738.2	66.44148	23.19	0.764	2.45
09/09/18 12:30	769.7	0.06927	27.06	0.002435	781.2	70.30759	20.7	0.663	1.7
09/09/18 12:45	784.8	0.070631	27.66	0.0024895	800	72.02267	20.92	1.356	3.95
09/09/18 13:00	783.1	0.070476	26.45	0.0023806	801	72.04795	21.38	1.406	3.2
09/09/18 13:15	786.2	0.070755	26.09	0.0023477	804	72.34277	20.97	1.369	3.2
09/09/18 13:30	776.6	0.069896	26	0.00234	794.1	71.47001	20.08	1.427	3.2
09/09/18 13:45	763.9	0.06875	26.57	0.0023911	781.6	70.3477	20.62	1.337	3.95
09/09/18 14:00	749	0.067408	27.58	0.002482	764.7	68.8206	21.61	0.883	2.45
09/09/18 14:15	723	0.065071	28.53	0.002568	736.8	66.31559	21.5	0.76	1.7
09/09/18 14:30	699.1	0.062923	29.36	0.0026426	713.8	64.24304	20.86	1.534	3.95
09/09/18 14:45	668.7	0.060181	29.28	0.0026355	682.8	61.45541	19.79	1.717	3.95
09/09/18 15:00	643.8	0.057944	28.36	0.0025523	657.1	59.14187	19.25	2.875	5.45
09/09/18 15:15	619.4	0.055747	26.02	0.0023418	630.5	56.74635	18.95	2.873	5.45
09/09/18 15:30	580.4	0.052232	24.96	0.0022464	590.6	53.15088	18.14	3.431	6.2
09/09/18 15:45	539.4	0.048542	23.97	0.0021576	547.2	49.25078	18.01	2.846	5.45
09/09/18 16:00	501.2	0.045109	22.96	0.0020664	507.6	45.68655	17.68	3.114	6.2
09/09/18 16:15	459.1	0.04132	21.92	0.0019727	463.2	41.68616	17.64	3.231	5.45
09/09/18 16:30	414.9	0.037341	20.38	0.0018339	416.6	37.4949	18	2.612	4.7
09/09/18 16:45	366.5	0.032989	17.58	0.0015818	366.4	32.97418	16.87	2.625	4.7
09/09/18 17:00	316.2	0.028457	15.9	0.0014307	314.1	28.27098	16.56	2.602	5.45
09/09/18 17:15	264.5	0.023803	14.6	0.0013138	260.7	23.46581	16.24	2.629	4.7
09/09/18 17:30	213.4	0.019208	13.72	0.0012345	208.2	18.74182	16.25	3.033	5.45
09/09/18 17:45	163	0.014671	11.98	0.0010779	155.6	14.0061	15.57	3.1	5.45
09/09/18 18:00	110.7	0.009964	10.08	0.0009074	105.6	9.499641	15.23	3.3	5.45
09/09/18 18:15	23.57	0.002122	7.504	0.0006754	60.75	5.467859	14.71	3.308	5.45
09/09/18 18:30	19.98	0.001798	4.915	0.0004424	24.14	2.172307	14.19	2.708	5.45
09/09/18 18:45	6.511	0.000586	1.762	0.0001586	3.136	0.2822368	13.66	2.122	3.95

A3: TRNSYS files for Cape Town

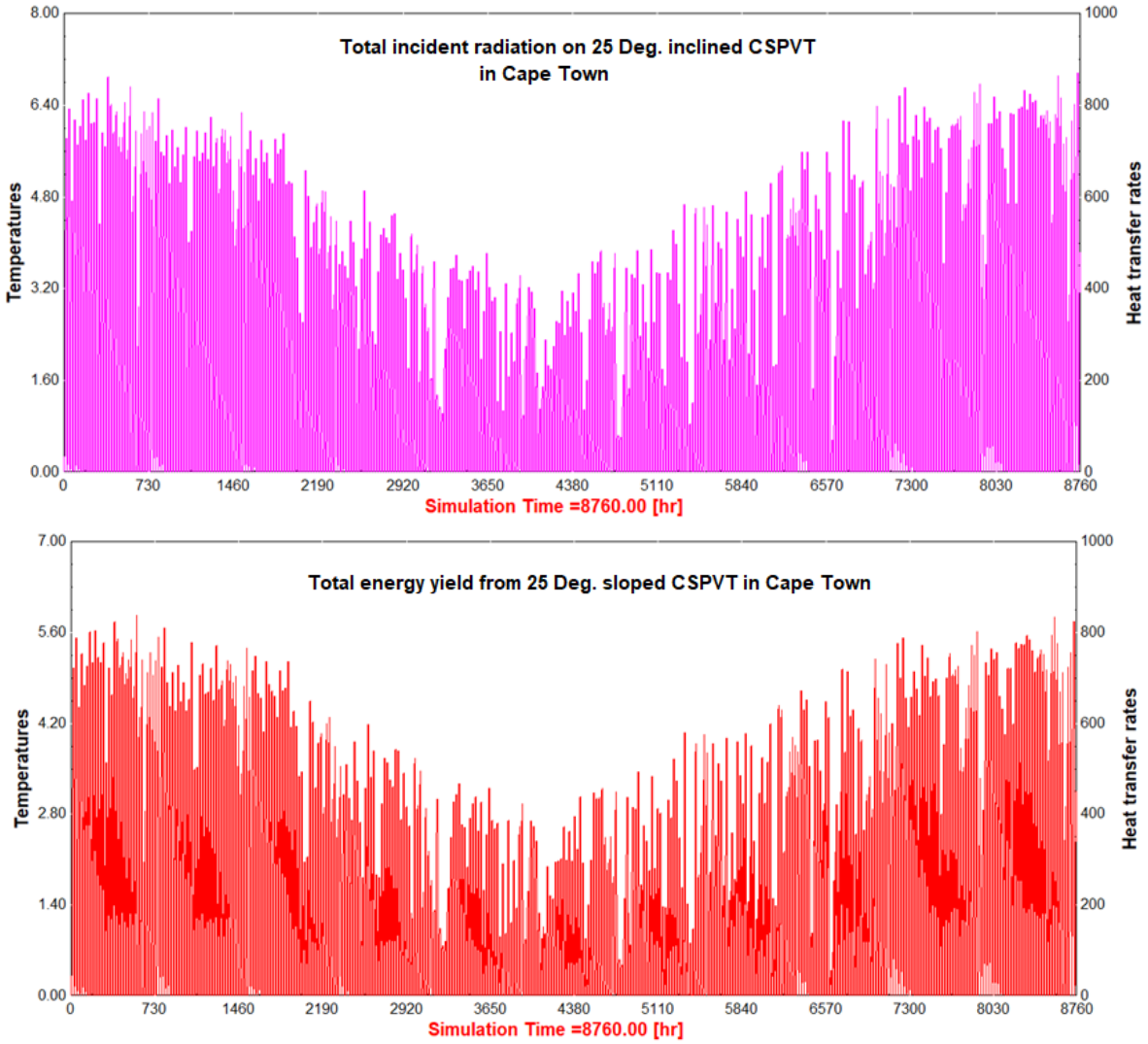

Figure A3-1: Sample data logger results for section 5.6

A4: Arduino programming code used

```
 //

#include <Stepper.h>
int hours = 0;
int timer = millis();
int counter = 0;
int day = 0;
const int stepsPerRevolution = 400;  // change this to fit the number of steps per revolution
// for your motor

// initialize the stepper library on pins 6 through 7:
Stepper myStepper(stepsPerRevolution, 6, 7);

void setup() {
  // set the speed at 500 rpm:
  myStepper.setSpeed(500);
  // initialize the serial port:
  Serial.begin(9400);
}
//timer = millis();
void loop() {
      //Serial.print("timer: ");
    //Serial.print(timer);
    //Serial.print("\n");
   if(counter >= 12){
    delay(1000*3600);
    for(int i=0;i<12;i++){
          myStepper.step(stepsPerRevolution);
          myStepper.step(stepsPerRevolution);
          myStepper.step(stepsPerRevolution);
          myStepper.step(stepsPerRevolution);
          myStepper.step(stepsPerRevolution);
          myStepper.step(stepsPerRevolution);
          myStepper.step(stepsPerRevolution);
    }
    counter =0;
    day = 1;
   }else{
    if(day == 0){
    delay(1000*3600);
  // step one revolution  in one direction:

    timer = millis();

    //while(abs((millis()-timer)<163){
    //Serial.println("clockwise");
    myStepper.step(-stepsPerRevolution);
    myStepper.step(-stepsPerRevolution);
    myStepper.step(-stepsPerRevolution);
    myStepper.step(-stepsPerRevolution);
```

```
    myStepper.step(-stepsPerRevolution);
    myStepper.step(-stepsPerRevolution);
    myStepper.step(-stepsPerRevolution);

    counter ++;


    //myStepper.step(-stepsPerRevolution);
    //myStepper.step(-stepsPerRevolution);
    //myStepper.step(-stepsPerRevolution);
    //delay(1);
    //}

   // timer = millis();
   }else{
    delay(12000*3600);
    day = 0;
   }
    }
}
```

A5: Matlab programing code used to compute G_{gl} and G_{in}

```
Ren=[];
rhog=0.20;% Ground reflectivity; can be varied depending on conditions
geog=[-33.932 -18 68.5 -15];
L=geog(1); Long=geog(2); h=geog(3);
Longt=geog(4);MJdayh=zeros(40,1);MJdayn=zeros(40,1);
k=sum(Ren(:,1)>0);%This gives the day's results (Ren)from the data logger
and the number of daylight readings, k.
n=Ren(:,1);time=Ren(:,2);Gh=Ren(:,4); Gd=Ren(:,3); Ta=Ren(:,5);
vw=Ren(:,6); gama=Ren(:,7); beta1=Ren(:,8); anglesky=Ren(:,9);
anglegrd=Ren(:,10); %equivalent incidence angles for diffuse radiation


dayminutes=15*k;t=time-0.5*dayminutes;
delta=23.45*sin(2*pi*(284+n)/365); %declination angle in degrees
Bdeg=360*(n-1)/365; %Spencer's correction angle due to variable earth
orbital speed
G0=1367*(1.000110+0.034221*cos(pi*Bdeg/180)+0.001280*sin(pi*Bdeg/180)+0.000
719*cos(pi*Bdeg/90)+0.000077*sin(pi*Bdeg/90)); %Extraterrestrial radiation
in kW/m2
E=229.2*(0.000075+0.001868*cos(pi*Bdeg/180)-0.032077*sin(pi*Bdeg/180)-
0.014615*cos(pi*Bdeg/90)-0.04089*sin(pi*Bdeg/90)); %Equation of time in
min. due to earth orbit perturbations

alpha=max(0,asind(cos(pi*L/180)*cos(pi*delta/180).*cos(pi*t/720)+sin(pi*L/1
80)*sin(pi*delta/180)));% Defines solar altitude
z=90-alpha;cosine=cos(pi*z/180)+(z==90)*0.001;%This avoids dividing by zero
at z=90deg.
mair=(exp(-0.0001184*h))./((cosine+0.50572*(96.07995-z.*(z<96.07995)).^(-
1.6364))); %This gives the apparent air mass accounting for altitude as
well

Gbh=Gh-Gd; Gbn=Gbh./cosine; %This avoids a situation of cosine = 0
e=1+Gbn./(Gd.*(1+5.535*10^(-6).*z.^3));% This is the Perez clearness
parameter at a given time
del=mair.*Gd./G0; %This is the Perez brightness parameter at a given time;
if e<1.065, f=[-0.008 0.588 -0.062; -0.060 0.072 -0.022];
elseif e<1.230, f=[0.130 0.683 -0.151; -0.019 0.066 -0.029];
elseif e<1.500, f=[0.330 0.487 -0.221; 0.055 -0.064 -0.026];
elseif e<1.950, f=[0.568 0.187 -0.295; 0.109 -0.152 0.014];
elseif e<2.800, f=[0.873 -0.392 -0.362; 0.226 -0.462 0.001];
elseif e<4.500, f= [1.132 -1.237 -0.412; 0.288 -0.823 0.056];
elseif e<6.200, f=[1.060 -1.600 -0.359; 0.264 -1.127 0.131];
else f=[0.678 -0.327 -0.250; 0.156 -1.377 0.251];
end; % These are the Perez brightness coefficients for an anisotropic sky
F1=max(0,(f(1)+del*f(1,2)+z*pi*f(1,3)/180));
F2=f(2)+del*f(2,2)+z*pi*f(2,3)/180;
gamas=sign(t).*abs(acosd((cosine*sin(pi*L/180)-
sin(pi*delta/180))./(sin(pi*z/180)*cos(pi*L/180))))+(t==0)*180;
iangle=acosd((cosine.*cos(pi*beta1/180)+sin(pi*z/180).*sin(pi*beta1/180).*c
os(pi*(gamas-gama)/180)));
% incidence angle in terms of solar azimuth, gamas, panel azimuth, gama and
inclination angle beta1 for a tracking panel.
a=max(0,cos(pi*iangle/180)); b=max(cos(pi*85/180),cosine);%a and b define
effects of cone circumsolar
%incidence angles on inclined panel and horizontal plane respectively.
Rb=(cosd(iangle).*(iangle<90))./cosine;
```

```
Gpanel=max(Gbh.*Rb+Gd.*(1-
F1)*0.5.*(1+cos(pi*beta1/180))+Gd.*F1.*a./b+Gd.*F2.*sin(pi*beta1/180)+Gh*rh
og*0.5.*(1-cos(pi*beta1/180)),0);
Gbpanel=Gbh.*Rb;
Gdskypanel= Gd.*(1-
F1)*0.5.*(1+cos(pi*beta1/180))+Gd.*F1.*a./b+Gd.*F2.*sin(pi*beta1/180);
Gdgrdpanel=Gh*rhog*0.5.*(1-cos(pi*beta1/180));
npolycarb=1.6; %refractive index
Kpolycarb=42.6; xpolycarb=0.003;
rangle=asind(sin(pi*iangle/180)/npolycarb); %refraction angle
R1=sin(pi*(iangle-rangle)/180)./sin(pi*(iangle+rangle)/180+0.001);
rper=R1;%the 0.001 degrees added to avoid dividing by zero
R2=tan(pi*(iangle-rangle)/180)./tan(pi*(iangle+rangle)/180+0.001);
rpar=R2;
taur=0.5*((1-rpar)./(1+rpar)+(1-rper)./(1+rper));
taua=exp(-2*Kpolycarb*xpolycarb./cos(pi*rangle/180+0.001));%The 2 in the
eponent is for double glazing
tau=taua.*taur;%Effective transmissivity on beam radiation
Gbinside=Gbpanel.*tau;
rskyangle=asind(sin(pi*anglesky/180)/npolycarb); %refraction angle

R1sky=sin(pi*(anglesky-
rskyangle)/180)./sin(pi*(anglesky+rskyangle)/180+0.001);
rskyper=R1sky;%the 0.001 degrees added to avoid dividing by zero
R2sky=tan(pi*(anglesky-
rskyangle)/180)./tan(pi*(anglesky+rskyangle)/180+0.001);
rskypar=R2sky;
%RESUME HERE

taursky=0.5*((1-rskypar)./(1+rskypar)+(1-rskyper)./(1+rskyper));
tauasky=exp(-Kpolycarb*xpolycarb./cos(pi*rskyangle/180+0.001));
tausky=tauasky.*taursky;%transmissivity for diffuse sky radiation
Gskyinside=Gdskypanel.*tausky;
%Evaluating ground radiation entering purifier

rgrdangle=asind(sin(pi*anglegrd/180)/npolycarb); %refraction angle

R1grd=sin(pi*(anglegrd-
rgrdangle)/180)./sin(pi*(anglegrd+rgrdangle)/180+0.001);
rgrdper=R1grd;%the 0.001 degrees added to avoid dividing by zero
R2grd=tan(pi*(anglegrd-
rgrdangle)/180)./tan(pi*(anglegrd+rgrdangle)/180+0.001);
rgrdpar=R2grd;



%RESUME HERE

taurgrd=0.5*((1-rgrdpar)./(1+rgrdpar)+(1-rgrdper)./(1+rgrdper));
tauagrd=exp(-Kpolycarb*xpolycarb./cos(pi*rgrdangle/180+0.001));
taugrd=tauagrd.*taurgrd;%transmissivity for diffuse sky radiation
Ggrdinside=Gdgrdpanel.*taugrd;


Ginside=Gbinside+Gskyinside+Ggrdinside;
Inside= [Gbinside Gskyinside Ggrdinside Ginside];
```

A6: Detailed rig structure and CSPVT diagram

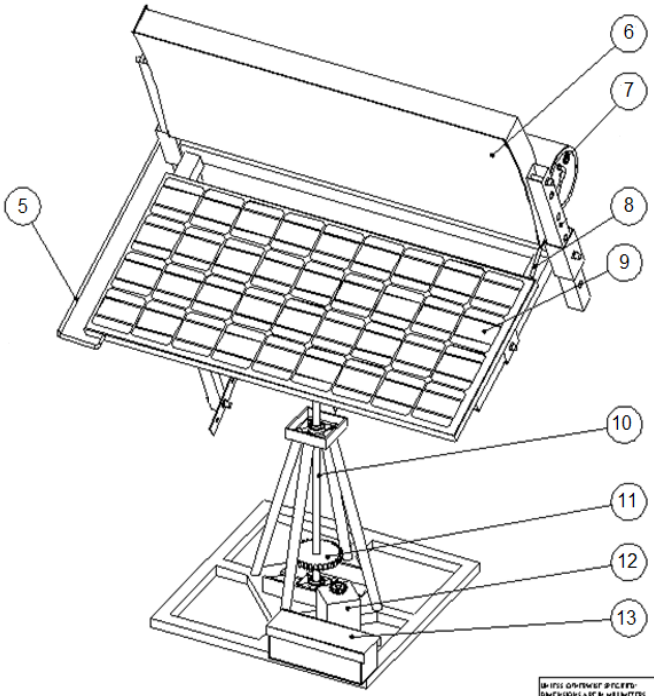

5: Cold water inlet pipe
6: Reflector
7: Hot water thermometer
8: Hot water outlet pipe
9: PV panel
10: Shaft
11: Sprocket
12: Motor cover
13: Electronics box

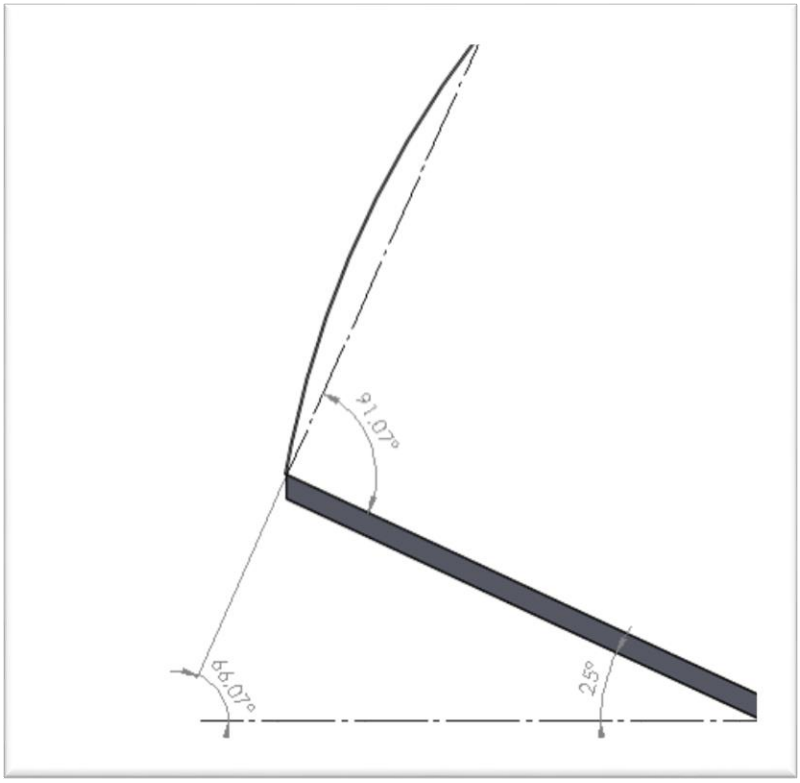

A7: Tank assembly and components

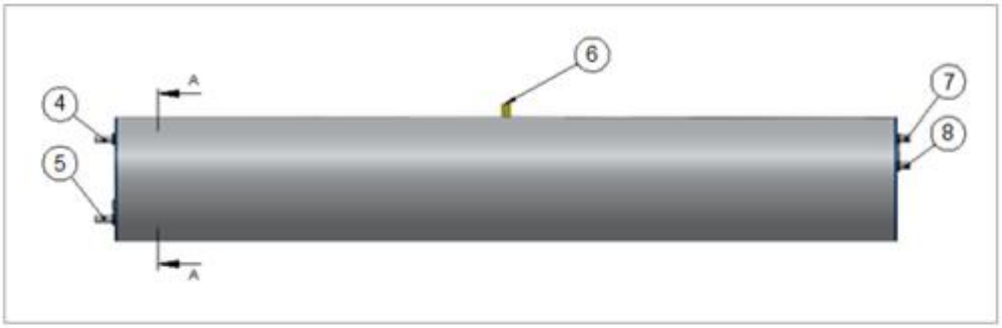

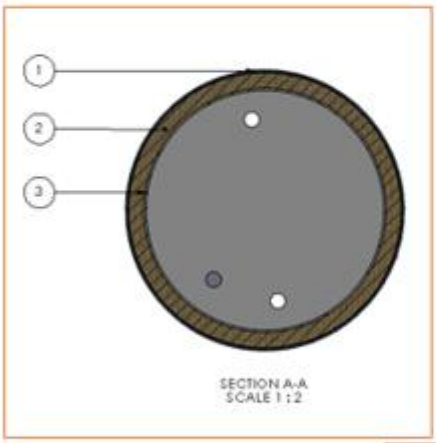

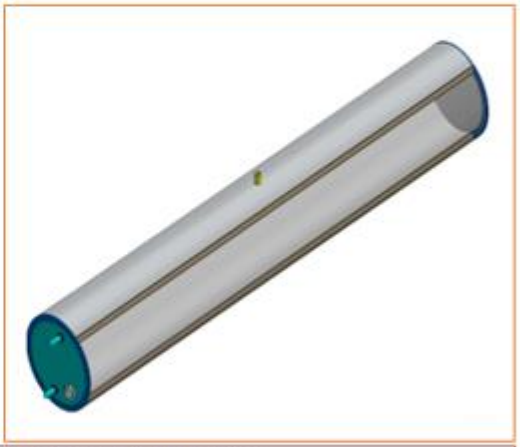

1: 1 mm tick Aluminium sheet
2: 15 mm tick insulation
3: Tank
4: Cold water inlet from the municipality/reservoir
5: Cold water outlet to the PV panel
6: Vent
7: Hot water inlet from the panel
8: Hot water Thermometer

A8: Photos of the experiments

A9: Solar tracker Video

Solar Tracker Video